

MSIS

3

MICHIGAN STATE UNIVERSITY LIBRARIES



3 1293 01566 0784



This is to certify that the
dissertation entitled
A Study of Structure in Supersaturated Aqueous
Sucrose Solutions Using Fluorescence Spectroscopy
presented by
Reena Chakraborty
has been accepted towards fulfillment
of the requirements for
Ph.D. degree in Chemical Engineering

Qui O. England
Major professor

Date 6/11/96

**PLACE IN RETURN BOX to remove this checkout from your record.
TO AVOID FINES return on or before date due.**

DATE DUE DATE DUE DATE DUE		
MAR 10 2002 ∞	_____	_____
DEC 14 2003 ∞	_____	_____
_____	_____	_____
_____	_____	_____
_____	_____	_____
_____	_____	_____
_____	_____	_____

MSU is An Affirmative Action/Equal Opportunity Institution

c:\crl\datedue.pm3-p.1

**A STUDY OF STRUCTURE IN SUPERSATURATED AQUEOUS SUCROSE
SOLUTIONS USING FLUORESCENCE SPECTROSCOPY**

By

Reena Chakraborty

A DISSERTATION

**Submitted to
Michigan State University
in partial fulfillment of the requirements
for the degree of**

DOCTOR OF PHILOSOPHY

Department of Chemical Engineering

1996

ABSTRACT

A STUDY OF STRUCTURE IN SUPERSATURATED AQUEOUS SUCROSE SOLUTIONS USING FLUORESCENCE SPECTROSCOPY

By

Reena Chakraborty

The fluorescence of 8-hydroxy-1,3,6-pyrenetrisulfonate (pyranine), a trace extrinsic probe, was measured in aqueous sucrose, glucose, lactose and fructose solutions. The peak intensity ratio (PIR), the emission intensity of pyranine at 440 nm to that at 515 nm, shows a strong concentration dependence in supersaturated solution. The PIR represents the ratio of solvation to bulk water per molecule of solute, and determines concentration and activity simultaneously. Non-solvation water in aqueous sucrose solutions, designated bulk water, exhibits one proton exchange rate. In other sugar solutions, it exhibits more exchange rates, depending upon the strength of the hydrogen bonds formed by the solvation water with the various moieties of the solute molecules. Steady state and time resolved fluorescence spectroscopy in supersaturated aqueous sucrose solutions indicate differences in structure and mobility of both bulk and solvation water compared to undersaturated solutions.

Solvent distribution near growing and dissolving sucrose crystals was investigated using laser optical fluorescence microscopy. The ratio of integrated half-peak intensities (IIR) of pyranine in sucrose solutions from 370 nm to 445 nm and 485 nm to 507 nm exhibits a strong concentration dependence. Solvent microphase distribution in regions of solution, $0.4 \mu\text{m} \times 0.4 \mu\text{m}$, indicated an isotropic distribution of pyranine in both excited states. Interfacial solution structure differs from bulk structure. A strong crystal-size dependence was observed in the extent of the concentration boundary layer; supersaturation dependence was not observed.

Solvatons, molecules of sugar and their solvation water, are convenient structural descriptors in non-dilute solution: in undersaturated solution, bulk-water solvates solvatons; in supersaturated solution, the solvatons solvate bulk-water. Saturation is akin to phase-inversion. The self-diffusion coefficient, D_{self} , is a ratio of the surface area of a sphere with radius, R (the distance between identical solvation environments for a solvaton), and the time, τ , required to traverse R ; the viscosity coefficient, μ , as the ratio of the force of resistance, F_r , experienced by the solvaton in traversing R , to D_{self} . Near saturation, R decreases, τ increases, and F_r becomes very large, explaining precipitous drops in D_{self} and order of magnitude increases in μ , reported in literature.

To my parents,
Dr. Bijoy Kumar Chakraborty
&
Mrs. Radha Rani Chakraborty
who believe in me,
and supported and encouraged
my educational pursuits.

ACKNOWLEDGEMENTS

Dr. Kris A. Berglund is thanked for serving as my graduate advisor. Dr. Daina M. Briedis, Dr. Carl T. Lira, and Dr. George E. Leroi are thanked for serving on my graduate committee and providing encouragement.

Dr. Donald K. Anderson is thanked for many terms of financial support. Many terms were spent working for and with Dr. Martin C. Hawley and Dr. Krishnamurthy Jayaraman, who are thanked for helping me appreciate process engineering design and optimization as much as they do. Thanks also to Dr. Wei E. Kuan, Dr. William T. Sledd, Dr. Mary Winter, and Mrs. Elizabeth D. Phillips of the Math Department at Michigan State University who allowed me to learn how to teach Intermediate Algebra to freshmen during the 2 semesters it took to dot the i's and cross the t's.

I looked to many friends for perspective, encouragement, and support. Chief among them Afalah Radford, Maria Tjani, Shobha Ramanand, Susan Jones, Margaret Green, Elizabeth Davenport, Suvarna Padhalkar, V. Subba Rao, Anil Menon, Joel Dulebohn, my sister Hena, and brother-in-law Kalyan Pyada. Thanks to the Berglund Group, and Mike Bly, Ramkumar Subhramanian and the Pictionary Gang for perspective and good company. Special thanks go to Tricia Moore and the folks at I-5, Carl and Barbera Bourdelais and the folks at TBT, and Paul Hoelderle and all my friends at FPC. Thanks also to Dr. Robert E. Buxbaum and Mrs. Gail C. Buxbaum. Laura G. Berry is thanked for demonstrating the power of the ACAS, positive thinking, and friendship. Hobbes, Leo, and Axel and the late Calvin, Maurice and Portia, are thanked for many hours of fine, furry, four-legged companionship.

TABLE OF CONTENTS

Chapter One: Introduction	1
1.1 Crystal Growth from Solution	1
1.2 Supersaturated Solutions are Difficult to Investigate	2
1.3 Consequences of Limited Experimental Techniques: Limited Information Regarding Solution Structure	3
1.4 A Broad Overview of this Work	4
1.4.1 The Subject of Investigation	4
1.4.2 The Experimental Approach	5
1.4.3 Objectives	6
1.4.4 An Overview of the Chapters	7
1.5 References	9
Chapter Two: Literature Review	10
2.1 Background	10
2.2 Crystal Growth from Solution	13
2.2.1 The Requirements for Crystal Growth from Solution	13
2.2.2 Crystal Growth Kinetics.....	13
2.2.3 Nucleation.....	14
2.2.4 The BCF Theory of Crystal Growth.....	15
2.2.4.1.....	17
2.2.5 Evidence for Non-Cluster Dependent Growth Mechanisms	18
2.3 Solution Structure	19

2.3.1 The relevance of structure to crystallization research	19
2.3.2 Ideal Solution and the classical treatment of solution structure	21
2.3.3 Other Concepts of Solution Structure.....	26
2.3.4 Non-Continuum Descriptions of Solvation and Structure.....	30
2.4 Techniques commonly used to measure concentration in supersaturated solutions.....	32
2.4.1 Spectroscopic Sensing Techniques.....	33
2.5 References	36
Chapter Three: The use of pyranine as a trace fluorescent probe to study structure in aqueous sucrose solutions.....	40
3.1 Background	40
3.2 Photochemical Techniques using Trace Fluorescent Probes	44
3.3 Materials and Methods:	48
3.4 Results and Analysis	50
3.5 Conclusions	57
3.6 Acknowledgements.....	57
3.7 Literature Cited.....	57
Chapter Four: Steady State Fluorescence Spectroscopy of Pyranine as a Trace Extrinsic Probe to Study Structure in Aqueous Sugar Solutions	62
4.1 Background	62
4.2 NMR.....	64
4.3 Raman Spectroscopy.....	65
4.4 X-ray Diffraction	66
4.5 Diffusion and Viscosity Measurements.....	66
4.6 Correlation of Macroscopic and Microscopic transport properties.....	67
4.7 Photochemical Techniques using Extrinsic Trace Fluorescent Probes	69
4.8 Materials and Methods	71

4.9 Results and Analysis	73
4.10 Conclusions.....	79
4.11 Acknowledgements	80
4.12 References	81
Chapter Five: The PIR as a measure of deviation from Ideal Solution Behavior	98
5.1 Background	98
5.2 Materials and Methods	100
5.3 Results	101
5.4 Analysis.....	101
5.5 Discussion	104
5.6 Conclusions	105
5.7 Notation.....	106
5.8 References	106
Chapter Six: The Study of Structure in Saturated and Supersaturated Sucrose Solutions using Steady State and Time Resolved Fluorescence Spectroscopy	113
6.1 Background	113
6.2 Experimental Methods	117
6.2.1 Fluorescent probes:	117
6.2.2 Preparation of Solutions.....	118
6.3 Results and Discussion	119
6.3.1 Steady State Fluorescence Spectra and UV Absorption	119
6.3.2 Time resolved Fluorescent Lifetimes	120
6.3.3 Time Resolved Fluorescence Anisotropy	121
6.4 Structural Characteristics of Sucrose Solutions from Transport Properties.....	128
6.5 Self-Diffusion and Structure	133
6.6 Conclusions	135

6.7 References.....	137
Chapter Seven: Solvent Imaging Studies of Supersaturated Sucrose Solutions in the Absence of Crystals and of the Near Interfacial Region of Growing and Dissolving Sucrose Crystals.....	150
7.1 Background	150
7.2 Materials and Methods	151
7.3 Results	153
7.4 Discussion.....	156
7.5 Crystal Growth.....	158
7.6 Conclusion	160
7.7 Acknowledgements.....	160
7.8 References.....	161
Chapter Eight: Summary, Conclusions, & Recommendations for Further Work	171
8.1 Summary	171
8.1.1 Issues Related To Solution Structure	171
8.1.2 SRO and LRO in The Aqueous Sucrose System.....	173
8.1.3 Bulk Water and Solvation Water as indicators of SRO	178
8.1.4 Other effects on structure and LRO	181
8.1.5 Issues related to structure near growing sucrose crystals.	184
8.2 Conclusions	186
8.3 Recommendations for Further Work.....	187

LIST OF FIGURES

Chapter Three

Figure 3.1. Chemical structure of pyranine or 8-hydroxy-1, 3, 6-pyrenetrisulfonate.....45

Figure 3.2. Emission equilibrium of pyranine. The equilibrium between the protonated form (absorbs at 350 nm and emits at 440 nm when excited at 342 nm) and the deprotonated form (absorbs at 405 nm and emits at 511 nm when excited at 342 nm) is determined by ability of the microenvironment of the hydroxyl group to participate in proton transfer.....46

Figure 3.3. The emission spectra of pure water and sugar solutions of 20, 40, 60, and 70 wt.% sucrose doped with 100 ppm (1.9×10^{-4} M) pyranine at 20 degrees C. Emission maxima occur at 440 nm. and 511 nm. An isosbestic point is observed, represented by the pointer at 485 nm.....50

Figure 3.4. Graph of PIR (peak intensity ratio) vs. wt% sucrose in solution at 20 degrees C using 100 ppm (1.9×10^{-4} M) pyranine. The PIR is defined as the ratio of peak intensities at 440 nm and 511 nm. The arrow represents concentration at saturation.....53

Figure 3.5. Total, bulk and solvation water (number of molecules of water per molecule of sucrose) vs. wt% sucrose in aqueous solution with 100 ppm (1.9×10^{-4} M) pyranine at 20 degrees C. The values on the graph are obtained from the analysis presented in Tables 1 and 2. The vertical line represents saturation.....55

Figure 3.6. Graph of total water, bulk water and solvation water per molecule of sucrose in aqueous solutions doped with 100 ppm (1.9×10^{-4} M). pyranine at 20 degrees C versus the degree of supersaturation, DS. The DS is given by the difference between the solution concentration and the saturation concentration at 20 degrees C divided by the saturation concentration at 20 degrees C.....56

Chapter Four

Figure 4.1. Chemical structure of pyranine or 8-hydroxy-1, 3, 6-pyrenetrisulfonate.....84

Figure 4.2. Emission equilibrium of pyranine. The equilibrium between the protonated form (absorbs at 350 nm and emits at 440 nm when excited at 342 nm) and the deprotonated form (absorbs at 405 nm and emits at 511 nm when excited at 342 nm) is determined by ability of the microenvironment of the hydroxyl group to participate in proton transfer.....85

Figure 4.3. The emission spectra of pure water and sugar solutions of 20, 40, 60, and 70 wt.% sucrose doped with 100 ppm (1.9×10^{-4} M) pyranine at 20 degrees C. Emission maxima occur at 440 nm. and 511 nm. An isosbestic point is observed, represented by the pointer at 485 nm.....86

Figure 4.4. Graph of PIR (peak intensity ratio) vs. wt% sucrose in solution at 20 degrees C using 100 ppm (1.9×10^{-4} M) pyranine. The PIR is defined as the ratio of peak intensities at 440 nm and 511 nm. The arrow represents concentration at saturation.....87

Figure 4.5. Graph of PIR (peak intensity ratio) vs. wt% glucose in solution at 20 degrees C using 100 ppm (1.9×10^{-4} M) pyranine. The PIR is defined as the ratio of peak intensities at 440 nm and 511 nm. The dashed line represents concentration at saturation.....88

Figure 4.6. Graph of PIR (peak intensity ratio) vs. wt% fructose in solution at 20 degrees C using 100 ppm (1.9×10^{-4} M) pyranine. The PIR is defined as the ratio of peak intensities at 440 nm and 511 nm. The arrow represents concentration at saturation.....89

Figure 4.7. Graph of PIR (peak intensity ratio) vs. wt% lactose in solution at 20 degrees C using 100 ppm (1.9×10^{-4} M) pyranine. The PIR is defined as the ratio of peak intensities at 440 nm and 511 nm. The dashed line represents concentration at saturation.....90

Figure 4.8. Total, bulk and solvation water (number of molecules of water per molecule of sucrose) vs. wt% sucrose in aqueous solution with 100 ppm (1.9×10^{-4} M) pyranine at 20 degrees C. The values on the graph are obtained from an analysis using a two state model for water. The vertical line represents saturation.....91

Figure 4.9. Graph of bulk water and solvation water per molecule of sucrose in aqueous solutions doped with 100 ppm (1.9×10^{-4} M). pyranine at 20 degrees C versus the degree of supersaturation, DS. The DS is given by the difference between the solution concentration and the saturation concentration at 20 degrees C divided by the saturation concentration at 20 degrees C.....92

Figure 4.10. Total, bulk and solvation water (number of molecules of water per molecule of glucose) vs. wt% glucose in aqueous solution with 100 ppm (1.9×10^{-4} M) pyranine at 20 degrees C. The values on the graph are obtained from an analysis using a two state model for water. The vertical line represents saturation.....93

Figure 4.11. Total, bulk, and solvation water (per molecule of fructose) as a function of % fructose in solution. Data obtained for aqueous fructose at 293 K doped with 100 ppm pyranine.....94

Figure 4.12. Total, bulk and solvation water (number of molecules of water per molecule of lactose) vs. wt% lactose in aqueous solution with 100 ppm (1.9×10^{-4} M) pyranine at 20 degrees C. The values on the graph are obtained from an analysis using a two state model for water. The vertical line represents saturation.....95

Figure 4.13. Bulk water, solvation water, and non-bulk-non-solvation water (number of molecules of water per molecule of glucose) vs. wt% glucose in aqueous solution with 100 ppm (1.9×10^{-4} M) pyranine at 20 degrees C. The values on the graph are obtained from an analysis using a three state model for water. The vertical line represents saturation.....96

Figure 4.14. Bulk water, solvation water, and non-bulk-non-solvation water (number of molecules of water per molecule of lactose) vs. wt% lactose in aqueous solution with 100 ppm (1.9×10^{-4} M) pyranine at 20 degrees C. The values on the graph are obtained from an analysis using a three state model for water. The vertical line represents saturation.....97

Chapter Five

Figure 5.1. The emission spectra of pure water and sugar solutions of 20, 40, 60, and 70 wt.% sucrose doped with 100 ppm (1.9×10^{-4} M) pyranine at 20 degrees C. Emission maxima occur at 440 nm. and 511 nm. An isosbestic point is observed, represented by the pointer at 485 nm.....108

Figure 5.2. Chemical structure of pyranine or 8-hydroxy-1, 3, 6-pyrenetrisulfonate.....109

Figure 5.3. Emission equilibrium of pyranine. The equilibrium between the protonated form (absorbs at 350 nm and emits at 440 nm when excited at 342 nm) and the deprotonated form (absorbs at 405 nm and emits at 511 nm when excited at 342 nm) is determined by ability of the microenvironment of the hydroxyl group to participate in proton transfer.....110

Figure 5.4. Graph of $x_w \ln \gamma_w$ versus \ln PIR for aqueous sucrose solutions at 293 K.....111

Figure 5.5 Graph of $x_w \ln \gamma_w$ versus \ln Bulk water/Solvation Water (CA or Chemically Associated water) for aqueous glucose solutions at 293 K.....112

Chapter Six

Figure 6.1. Structure of PBA (left) and pyranine (right).....138

Figure 6.2. UV-vis spectra of 10 ppm pyranine in aqueous sucrose solutions of various concentrations at 293 K.....139

Figure 6.3. Fluorescent lifetimes of PBA in sucrose solutions observed at 380 nm and 293 K as a function of sucrose concentration. Squares (\square) represent the long lifetime component and triangles (Δ) represent the short lifetime component.....140

Figure 6.4. Ratio of the intensities of the long lifetime component to the short lifetime component of PBA at 380 nm.....141

Figure 6.5. Fluorescent lifetimes of PBA in sucrose solutions observed at 400 nm and 293 K as a function of sucrose concentration. Squares (\square) represent the long lifetime component and triangles (Δ) represent the short lifetime component.....142

Figure 6.6 Ratio of the intensities of the long lifetime component to the short lifetime component of PBA at 400 nm.....143

Figure 6.7 Fluorescent lifetimes of pyranine in sucrose solutions at 293 K. Squares (□) represent the emission at 440 nm and triangles (Δ) represent the the emission at 511 nm. Error bars indicate the standard deviation of the measurements.....144

Figure 6.8 Kinetic diagram for the two-state excited state proton transfer of pyranine....145

Figure 6.9 Dependence of the rotational correlation time of PBA on sucrose concentration. Squares (□) represent the rotational correlation time for the long lifetime component and triangles (Δ) represent the rotational correlation time for the short lifetime component..146

Figure 6.10 Dependence of the rotational correlation time of PBA on viscosity. Squares (□) represent the rotational correlation time for the long lifetime component and triangles (Δ) represent the rotational correlation time for the short lifetime component.....147

Figure 6.11 Dependence of the rotational correlation time of pyranine on sucrose concentration. Squares (□) represent the rotational correlation time observed at 440 nm and triangles (Δ) represent the rotational correlation time observed at 511 nm.....148

Figure 6.12 Dependence of the rotational correlation time of pyranine on viscosity. Squares (□) represent the rotational correlation time observed at 440 nm and triangles (Δ) represent the rotational correlation time observed at 511 nm. Error bars indicate the standard deviation of the measurements.....149

Chapter Seven

Figure 7.1. Dual detector images for aqueous sucrose solutions of 60, 74 and 76 wt.% at 293 K. Detector 1 images the half peak intensity of pyranine from 485 nm to 507 nm. Detector 2 images the half peak intensity of pyranine from 445 nm to 370 nm. One pixel represents an area of solution $0.4 \mu\text{m} \times 0.4 \mu\text{m}$162

Figure 7.2. A plot of IIR (integrated emission intensity) of pyranine vs sucrose concentration (wt.% sucrose) at 293 K. Color values represent concentration in weight percent sucrose.....163

Figure 7.3 Dual detector (a) and concentration ratio mode (b) images of a sucrose crystal growing in 68 wt.% solution.....164

Figure 7.4 Dual detector (a and c) and concentration ratio mode (b and d) images of several different sucrose crystals growing in 71 wt.% solution.....165

Figure 7.5 Concentration ratio mode images of several different sucrose crystals growing in 71 wt.% solution.....165

Figure 7.6 Dual detector (a) and concentration ratio mode (b) images of a sucrose crystal growing in 76 wt.% solution.....166

Figure 7.7. Samples of line scans in concentration ratio mode taken in the interfacial region of growing sucrose crystals at 293 K. The big dip in concentration indicates the interface of the crystal.....167

Figure 7.8 A sample of a line scan taken near the interface of a dissolving sucrose crystal in 60 wt% sucrose solution at 293 K. The big dip in concentration indicates the interface of the crystal.....168

Figure 7.9 Dual detector images of a sucrose crystal in 74 wt. % solution at 293 K taken using confocal microscopy in 0.4 μm vertical steps, and 0.2 μm x 0.2. μm horizontal resolution. Instrument settings for this data differ from those of the rest of the data in this work.....169

Figure 7.10. Concentration ratio images of the sucrose crystal imaged in Figure 7.8... .170

Chapter Eight

Figure 8.1 Conceptual diagram of structure in dilute aqueous sucrose solution.....187

Figure 8.2. A conceptual representation of structure in concentrated aqueous sucrose solutions.....188

Figure 8.3. A conceptual representation of structure in saturated aqueous sucrose solutions.....189

Figure 8.4. A conceptual representation of structure in supersaturated aqueous sucrose solutions.....190

Figure 8.5 Structure in the aqueous glucose system.....191

Figure 8.6 Structure in the aqueous fructose system.....192

Figure 8.7 Summary of structure in aqueous citric acid systems.....193

Figure 8.8 Regimes of solution structure in aqueous sucrose solutions.....194

Chapter One

Introduction

Crystallization is one of the most widely used unit operations in the chemical process industry (1). Many processes utilize crystallization from solution as a means to purify, produce, or recover solid material. Cost-effective control of industrial processes related to the production of electronic and optical materials, coatings, and the large scale production of various chemicals including food and food additives, dyes, fertilizers, pharmaceuticals, and fine chemicals is one of the primary objectives of engineering research in separations. This is particularly true of research related to crystallization from solutions. Control schemes for crystallization processes developed and described in literature are derived from the population balance analysis of Randolph and Larson (2-4). The crystal size distribution for a crystallizer can be determined from population balance analysis given the mode of operation, crystallization kinetics, and operating variables of temperature and supersaturation. The relation between the major variables of interest is described using process control analogy. The main challenges to applying such a scheme in a universal manner to provide on-line control of crystallization from solutions, are continuous, rapid, and accurate determination of local supersaturation, and in situ determination of particle size and morphology.

1.1 Crystal Growth from Solution

Crystal growth from solution differs inherently from vapor or melt crystallization due to the presence of significant quantities of at least one non-crystallizing species: the solvent. The effect of solvent composition on the

morphology, habit, growth rate, and crystal size distribution in crystallization from the solution phase has been well documented. Researchers in the field generally agree that there is a cause and effect relationship involved regarding the solvent and its effects on the crystallizing system.

The consensus ends in agreement that a causal relationship between solvent and crystal properties in solution phase crystallization exists. The nature of such a relationship is a subject of speculation. Even so, experimental evidence suggests the solvent affects the crystallization at a microscopic level (involving one or several units of solvated solute molecules and several molecules of solvent) regardless of how it affects the crystallization on larger scales of order.

1.2 Supersaturated Solutions are Difficult to Investigate

Experimental investigation of supersaturated solutions on any scale of order is difficult. Supersaturated solutions are not in a state of equilibrium, rather in what Ostwald first termed as a "metastable state" (5). As a result, localized changes in temperature, concentration, pressure, fluid velocity, viscosity, the presence of foreign particles, or the application of a sudden impact may each individually, or in combination, cause a local or global instability to the system. The end result is often localized or catastrophic (global) nucleation (i.e., not limited to a small region of solution). Reproducing experimental conditions on a reliable basis is challenging. Rapid and accurate determination of local and/or global solution concentration in saturated and supersaturated solutions is difficult. These factors have hindered the experimental study of structure of and phenomena in supersaturated solutions. Consequently, there are few experimental studies related to structure and property determination in supersaturated solutions, and fewer still in nucleating or crystallizing systems. Most structure and property determination related

studies have limited their focus to investigating the role of the solute in structure and property relations.

1.3 Consequences of Limited Experimental Techniques: Limited Information Regarding Solution Structure

The lack of experimental techniques for accurate determination of local supersaturation and changes in local supersaturation has severely limited the ability to measure and quantify interfacial properties during nucleation and crystal growth. Consequently a clear and unambiguous determination of the role of each of the solute and solvent in crystallization from the solution phase has not been determined and remains a subject of a great deal of speculation. This lack of information also affects the extent to which control can be exerted over a crystallization operation in which a solute crystallizes from a mixture of solute and solvent.

The role of solvent structure and properties and the relationship between solute and solvent species in supersaturated solutions has not been a subject of research interest. As a result, the spatial distribution of solvent and solute molecules in supersaturated solutions is poorly understood; additionally, the functional roles each plays in the process of supersaturation, nucleation, and crystal growth is unknown.

Another consequence of this lack of information is that there is no reliable way to account for the solvent or its role in nucleation and crystal growth models. All theories of crystal growth stem, historically, from the study and modelling of vapor or melt phase separations. Such processes do not involve a solvent that has a different molecular structure from that of the solute. Models of such processes thus neglect the presence of a solvent which is chemically distinct from the crystallizing species and are unable to describe how it affects the crystal growth process. These models describe the behavior of vapor and melt phase systems well. Where a solvent differing in molecular structure from the solute is

present, as in crystallization from the solution phase, such models break down because the parameters (which may be insufficient) lose their original physical significance and fail to completely describe the behavior of the system.

An understanding of solvent and the role it plays in determination of structure and transport in supersaturated solution is necessary to explain several phenomena related to crystal growth and nucleation from the solution phase. Unexplained issues related to such phenomena include the origin of secondary nuclei, the growth of crystals from nuclei, the tendency of certain substances, e.g., citric acid, not to nucleate from solutions even at very high supersaturations, and epitaxial growth and polymorphism of nuclei as observed in systems e.g., aqueous anhydrous glucose/glucose monohydrate.

1.4 A Broad Overview of this Work

1.4.1 The Subject of Investigation

As a first step towards extending the understanding of the role of solvent and solute in the structure and properties of supersaturated solutions and their roles in nucleation and crystal growth it is useful to focus on how to accurately measure the one most critical property in such phenomena: concentration in supersaturated solution and small changes in concentration in supersaturated solution. Once it is possible to determine solution concentration in supersaturated solution it is useful to analyze the experimental data to obtain information related to the spatial distribution of the solute and solvent in supersaturated solution. This information can then be related to other information relating to the distribution of solute and solvent in solution and corroborated using another experimental method. Finally it is useful to extend this technique to the determination of local solution concentrations in solution on a time averaged basis both with and without the presence of a crystal interface to determine whether such an approach has the ability to

provide any information regarding the local distribution and role of solvent and solute on a time and space averaged basis..

This study is limited to the development of an experimental technique to determine concentrations in supersaturated solutions of sucrose in water, to determine if such a technique can provide information related to the spatial relationship between solvent and solute in supersaturated solutions, and to relate such information to the body of information available regarding the spatial relationship of solvent and solute in supersaturated solutions of sucrose in water. Supporting experimental evidence in supersaturated solutions of aqueous glucose, fructose, and lactose are presented when appropriate. Sucrose, and each of the other sugars in this study, is a commercial sugar. Solution properties in dilute solution, and crystallization data for each are readily available. Water is a well studied and modelled solvent; its structure and behavior are fairly well known and documented.

1.4.2 The Experimental Approach

The experimental approach to this study has been to find a technique that allows the detection of small changes in the local (microscopic) solvent concentration (in the vicinity of a solute or other probe molecule) in supersaturated solutions where there is relatively little solvent as compared to dilute solutions. Such a technique can then be used to determine a standard calibration curve of sorts for concentration vs some solution property in concentrated saturated and supersaturated solutions. In this way a bulk averaged value of local supersaturation readings can be determined. The second phase of this study relates to trying to determine truly local concentrations based on the findings of the first phase.

The focus of this work is to examine the basis for developing means to monitor supersaturation *in situ* in a manner sensitive to small changes in solute and/or solvent concentration, even in supersaturated solution. Once such means are identified the object is to test some of their limitations. The last step is to attempt to extend such techniques to

monitoring concentrations in the near interface region of growing crystals. At each step an effort is made to correlate the information to understanding the spatial and functional distribution of solute and solvent molecules in solution in order to shed further light on the structure of supersaturated solutions. The determination of how and if the structure observed affects the nucleation or growth processes is not attempted. Instead the object is just to develop the means to observe such structure.

The usefulness of steady state fluorescence spectroscopy of extrinsic fluorescent probe molecules as an experimental technique to determine supersaturation is first demonstrated. The technique is then used in conjunction with fluorescence imaging to investigate local concentrations in the absence of growing crystals. Finally, fluorescence imaging is used to investigate concentration fields near the interface of growing sucrose crystals.

1.4.3 Objectives

The primary objectives of this study are

1. to develop an experimental procedure that allows one to determine the concentration of a saturated or supersaturated sucrose solution either directly i.e., by measurement of a solution property and correlating changes in this solution property to solution concentration or indirectly i.e, by correlating changes in the quantifiable behavior of an extrinsic probe to corresponding changes in solution concentration in saturated and supersaturated sucrose solutions. The procedure or technique must be sensitive to, and capable of differentiating, small differences in solution concentration in supersaturated solutions.
2. to demonstrate that such a technique may be applied, or modified so as to apply, to measurement of concentration in supersaturated solutions of other sugars such as glucose and/or fructose,

3. to briefly examine the ability of this technique to provide information related to the microscopic structure of supersaturated sucrose solutions by relating the analysis of experimental data to related experimental data published in literature, and to published studies of molecular dynamics of aqueous sugar solutions as well,
4. to investigate the extent to which this information is corroborated by time resolved fluorescence spectroscopy which provides somewhat different information on different space and time scales, and
5. to extend and modify this technique via two-dimensional microscopic imaging so as to be able to determine time averaged local concentrations along a two dimensional cross-sectional plane of supersaturated sucrose solution.

1.4.4 An Overview of the Chapters

A discussion of research in the field of solution phase crystallization is presented. Literature related to structure and property determination in solutions is also reviewed in Chapter Two. Concepts are defined in terms of their use throughout this work.

The next few chapters cover the research as it was done and published in chronological order, including details of materials and methods, data acquisition and analysis, and results. The first paper, Chapter Three, deals with detection of small changes in supersaturation rapidly, accurately, and in a manner suitable for use in on-line analysis and control using any means possible. For this purpose spectroscopic techniques like Raman, FTIR, and NMR were initially considered. NMR studies reported in literature indicated the possibility of microheterogeneities in the system (6), but these techniques are slow and inherently not suitable for meeting the objectives of this investigation. Fluorescence techniques are commonly used in the study of microstructure in microheterogeneous systems (7). There are several treatises delineating the procedure and techniques available and the various kinds of information that can be extracted about the

molecule and its environment (e.g., 8-11). Similar techniques had already been used to analyze water content in a variety of systems such as gels, sols, and sol-gels (12-18). It was decided to use the extrinsic fluorescent probe, pyranine or 8-hydroxy-1,3,6-pyrenetrisulfonate (18,19). The object of performing emission experiments on sucrose solutions doped with pyranine was to correlate changes in the emission behavior of pyranine to changes in solution concentration and to find an experimentally observed or derived quantity that is very sensitive to small changes in solute and/or solvent concentration in saturated or supersaturated solutions.

Fluorescent molecules in excited states are extremely sensitive to their solvation environment. It is possible to relate the changes in observed emission behavior to structural changes in the microscopic solvation environment of the molecular probe (7, 18). The goal was to use this information to correlate changes in the solvation environment of the molecular probe to corresponding changes in the microphase distribution of the solute and solvent molecules in solution. This work is introduced in Chapter Three and extended in Chapter Four.

The next step involved investigating other sugar solutions with pyranine to determine if the behavior observed was limited to sucrose or a more general trend among sugars. The goal was to modify the experimental procedure, or data analysis, or both, to enable supersaturation sensing and structural analysis. This is detailed in a second paper, presented in Chapter Four. Chapter Five deals with the subject of simultaneous activity and concentration measurement in a third paper.

Once information about the functional microphase distribution of the solute and solvent was available it was then a goal to experimentally verify the validity of the assumptions used to arrive at this conclusion. These assumptions pertained to the assumption of a homogeneous distribution of the extrinsic probe molecule in solution and the isotropy and homogeneity of the distribution suggested by analysis of the steady state

data. This was accomplished using time resolved fluorescence spectroscopy. This is the subject of the fourth paper, Chapter 6.

Scanning fluorescence imaging was used to investigate the distribution of solvent molecules near the interface of growing sucrose crystals. This work is presented in the fifth and final paper, Chapter 7.

The final chapter includes recommendations for future study. A summary of this work and conclusions are also presented in Chapter 8.

1.5 References

1. Jancic S.J. and E.J. de Jong eds., Industrial Crystallization '84, Elsevier, Amsterdam, (1984)
2. Randolph A. D. and M. A. Larson, Theory of Particulate Processes, Academic Press, New York, NY (1971)
3. Randolph A. D. , *Can. J. Chem. Engg.*, **42**, 280, (1964).
4. Larson M.A. and A. D. Randolph , *Chem. Engg. Progress Symp. Ser.*, **65**(95), 1, (1969).
5. Ostwald W., *Z. Phys. Chem.*, **22**, 289-330, (1897)
6. Richardson S. J. and M. P. Steinberg, in Water Activity: Theory and Applications to Food, L. B. Rockland and L. R. Beauchat eds., Marcel Dekker Inc., New York, 235, (1987).
7. Kalyanasundaram K., Photochemistry in Microheterogeneous Systems, Academic Press Inc., (1987).
8. Turro N. J., Modern Molecular Photochemistry, Benjamin Press, New York, NY, (1978).
9. Lackowicz J. R., Principles of Fluorescence Spectroscopy, Plenum Press, New York, NY, (1984).
10. O'Connor D. V. and D. Phillips, Time Correlated Single Photon Counting, Academic Press, Orlando, FL, (1984)
11. Demas J. N., Excited State Lifetime Measurements, Academic Press, New York, NY, (1983)
12. Clement, N.R. and M. Gould, *Biochemistry*, **20**, 1534 (1981).
13. Kano, K. and J.H. Fendler, *Biochim. Biophys. Acta*, **509**, 289 (1978).
14. Kondo, H., I. Miwa and J. Sunamoto, *J. Phys. Chem.*, **86**, 4826 (1982).
15. Bardez, E., B.T. Gouguillon, E. Keh and B. Valeur, *J. Phys. Chem.*, **88**, 1909, (1984).
16. Pines, E. and D. Huppert, *J. Phys. Chem.*, **87**, 4471 (1984).
17. Kaufman, V.R., D. Avnir, E. Pines-Rojanski and D. Huppert, *J. Non-Crystalline Solids*, **99**, 397 (1988).
18. Pouxviel, J.C., B. Dunn and J.I. Zink, *J. Phys. Chem.*, **93**, 2134 (1989).
19. Kondo, H., I. Miwa and J. Sunamoto, *J. Phys. Chem.*, **86**, 4826 (1982).

Chapter Two

Literature Review

2.1 Background

Crystallization from solution is a unit operation of considerable importance in the food, pharmaceuticals, and fine chemical industries (1). It is a separation technique that yields high purity materials. Crystallization involves the transfer of mass from a vapor, melt, or solution containing the material to be crystallized, onto a solid phase containing nuclei, seeds or crystals of the same substance. This study is limited to aqueous sucrose solutions; therefore, the discussion that follows will be limited to solution phase crystallization. Mass transfer takes place against an interfacial concentration gradient. When the solute loses its water (or solvent) of solvation, the interfacial region becomes more solvent rich than the bulk solution; this gives rise to a concentration gradient. Mass transfer of solute to crystal, and solvent to bulk solution, continues until the concentration of the bulk solution approaches the saturation concentration.

A solution is defined as a mixture of two or more substances. The average particle size in a solution is smaller than 10^{-7} m (2). It can be considered homogeneous on macroscopic scales of volume e.g., a cubic centimeter. Inhomogeneities cannot be usually be detected by such methods as light scattering. That substance which is present in the largest molar quantity is the solvent. Any substance present in a smaller molar quantity is a solute.

A solution of a solute at a given temperature and pressure is said to be saturated if solute added to the system at that temperature and pressure, after being allowed to equilibrate, exists as a separate pure phase in equilibrium with the solution. The solubility of a substance in a particular solvent at a given temperature and pressure, or saturation concentration at the same temperature and pressure, is determined by the chemical nature of

the solute and solvent and their interactions. Only those substances which exist in the form of a crystalline solid at a given temperature and pressure may be crystallized from their solutions at those temperatures and pressures.

A solution of a solute which contains more solute than a saturated solution at the same temperature and pressure is said to be supersaturated. If crystalline solute is added to its supersaturated solution at constant temperature and pressure, and allowed to equilibrate, the solution will tend to eventually attain saturation concentration with respect to the solute, and the solute present in solution in excess of its saturation concentration will tend to deposit on the crystalline solute. Thus the crystals will grow.

Increase in mass is an absolute measure of crystal growth (3). Crystal growth is often described by an increase in characteristic length, for purposes of analysis. Different measures of characteristic length are in use, such as Volume of the crystal/Surface area of the crystal. Characteristic length is not a very important parameter in this study, and thus it will not be discussed in further detail. Characteristic length is a parameter of major importance while describing the growth kinetics, and crystal size distribution for a crystallization process of interest. Randolph (4) together with Larson (5) developed the population balance technique to predict the crystal size distribution in a system of given operating system configuration, process parameters and growth kinetics. Such techniques provide the analytical basis for on-line control of industrial crystallizations i.e., control of the crystal size distribution or CSD. This work will not be discussed in any detail because it is not relevant to this study. It is mentioned because there are significant practical difficulties in applying population balance based analyses to control real crystallization processes. Presently it is not possible to monitor solute and solvent concentration in supersaturated solution both globally and locally on a continuous on-line basis. Consequently, it is not possible to monitor CSD and the morphological quality of crystals during growth and nucleation in a batch process, in a continuous yet non-intrusive manner. Accurate and reliable information related to two key variables:

a. a characteristic length "l" and

b. the supersaturation "s"

is difficult to obtain, particularly on a local basis, e.g., in the neighborhood of the crystal solution interface of a particular site on a growing crystal. The issue of monitoring supersaturation both in the presence and absence of growing crystals is complicated by a limited understanding of the phenomena of supersaturation on a structural and energetic basis, and conflicting ideas and data relating to solution structure and transport. The concept of supersaturation is easy enough to define in the sense of procedure or phenomena. Supersaturation is fairly easy to detect on a macroscopic scale; but, it is difficult to quantitatively relate the saturation temperature, pressure, concentration, and solution structure to chemical, physical, or transport properties of the solute and solvent (6).

This work investigates the issue of measuring supersaturation in solution using spectroscopy, both on a global and local basis for the aqueous sucrose system under common industrial operating conditions. In this work global refers to the entire system, and local refers to less than 10 microns in all directions. The term structure is used in this work to refer to the spatial distribution of molecules in solution. Microstructure refers to structure on the scale of 200 nanometers or less.

Sucrose was chosen as a substance suitable for investigation because its properties and behavior are well known and also because it is a commodity of industrial significance. Its properties have been tabulated and discussed in many articles. The reader is referred to Kirk and Othmer's Encyclopedia of Chemical Technology (7) where a summary of properties of sucrose and several excellent references may be found. Those studies, in which properties which bear a direct relation to this work are determined, will be discussed where appropriate.

Various spectroscopic methods were initially considered for measuring concentration in supersaturated solution because they are capable of detecting phenomena

on a truly local basis. These methods record events on a molecular or sub-molecular space scales, or on the time scales which correspond to such events. Further, interpreting data obtained from such methods is fairly straightforward. There exists a vast and rich literature that deals with various molecular spectroscopies, and spectroscopic analysis. Such literature will be referred to as needed.

A limited amount of experimental data related to phenomena on such space and time scales exists in literature. Of the systems for which some data exists, the aqueous sucrose system is one of the best studied. The choice of the aqueous sucrose system was made in the hope that any data obtained from this study could be compared with reference to published results and add to the total understanding of the crystallization of sucrose from aqueous sucrose solutions. A review of the literature pertinent to this study follows.

2.2 Crystal Growth from Solution

2.2.1 The Requirements for Crystal Growth from Solution

It is generally accepted that for crystal growth from solution to occur, the solution must be supersaturated and there must exist a nucleus of greater than critical size. The nature of the critical size of a nucleus is presently unknown. For growth at the interface of a pre-existing nucleus to occur, the solute must get to the interface, release all solvent not associated with the crystalline structure, assume an orientation favorable to the lattice structure, and become incorporated into the lattice, not necessarily in that order (6, 8, 9).

2.2.2 Crystal Growth Kinetics

The rate of crystal growth is a function of the supersaturation of a solution. Growth rate dispersion has been observed for a population of crystals in many systems. Berglund showed that the growth rate of sucrose crystals is more or less

constant for every crystal, but that a dispersion in growth rates is often observed within a population i.e., some crystals grow faster than others (10). Shiau showed for the fructose water system that growth rate dispersion itself depends on supersaturation (11). Closely related to growth kinetics is nucleation kinetics which is also a function of supersaturation.

2.2.3 Nucleation

Nucleation is a phenomenon by means of which a new crystal is formed. Primary nucleation occurs in the absence of any pre-existing crystals. It may be homogeneous or due to the presence of ordered solute molecules, or heterogeneous i.e., due to the presence of dust or other particulate matter foreign to the system. Secondary nucleation occurs due to the presence of growing crystals (13). It may occur due to the shearing off of crystal dust on the crystal surface of uncured crystals (initial breeding (13)), or due to collisions of crystals with each other, the impeller, or vessel walls (collision breeding (14)), or due to sliding contact on solid interfaces (contact nucleation). Most crystals produced in industrial crystallization from solutions are a result of secondary nucleation (15). Secondary nucleation has an important effect on the crystal size distribution, growth kinetics, and product crystal quality.

The origin and growth mechanism of secondary nuclei are areas of current research effort. There are two explanations for origin of secondary nuclei that are prevalent in literature. One theory, developed by Mullin and Leci (16) and McCabe and Clontz (17), is that the nuclei are produced as a result of coalescence of solvent-exclusive pre-crystalline clusters of sub-critical size which are thought to exist in the boundary layer at the crystal-solution interface. The other theory is that nuclei of critical size are produced due to breakage of micro-dendritic outgrowths on the crystal surface

are sheared off by the fluid surrounding it (18), or that pre-crystalline clusters of critical size are sheared away from the layer of solution adjacent to the crystal face (19).

The conventional analysis of growth incorporates two types of resistances. One arises from volume diffusion or the resistance that a solvaton (a molecule of solute and the solvent most associated with it (20)) experiences when it is transported from the bulk solution to the interface. This resistance is probably very important in systems that contain significant amounts of non-solvation and non-bulk solvent in supersaturated solution. This volume or bulk diffusion resistance was first proposed in the crystal growth theories of Volmer, Brandes, and Stranski. A detailed description of these theories may be found in *Crystal Growth* by H.E. Buckley (21).

The other resistance is thought to be experienced by a partially solvated solute growth unit as it traverses from a point on the crystal surface to a "kink-site" so that growth can proceed via propagation of a dislocation. Burton, Frank and Cabrera (22, 23) first proposed this mechanism to explain crystal growth from vapors onto real crystals with surface defects and other imperfections, and then later extended the analysis to growth of real (imperfect) crystals from solutions (hence referred to as the BCF theory).

Nuclei being real rather than perfect crystals, are thought to grow by propagation of growth defects like growth spirals. Some sites on the crystal surface are thought to be more likely to result in growth than others, in particular an edge of a surface dislocation or other defect. These sites are called kink sites.

2.2.4 The BCF Theory of Crystal Growth

There are many theories of crystal growth from solution. The BCF theory is perhaps most widely accepted. The BCF theory proposes that growth units are present in the solution or boundary layer surrounding a crystal. Such a growth unit is thought

to diffuse from the bulk solution to the crystal surface, be adsorbed on the surface so that it is only mobile in two dimensions, and then diffuse to the kink site.

The BCF theory proposes that the dependence of growth rate on supersaturation follows an Arrhenius type functionality with a clearly defined exponential coefficient. The exponential exponent represents the primary mechanism of growth resistance, i.e., limit 1 for volume diffusion and 2 for surface integration. Surface integration, is the resistance experienced by a growth unit trying to incorporate itself on the surface of the crystal. Such a growth unit is thought to be limited to two dimensional mobility, that is, capable of diffusion in two directions. Volume diffusion, is the resistance experienced by a growth unit in diffusing from bulk solution to the surface of the crystal.

The BCF analysis was originally intended to explain crystal growth from vapor phase or melts. In the case of growth from the vapor phase the growth unit was clearly defined as a single molecule of solute; in the case of melts it was convenient to define the growth unit as one or more molecules of crystallizing substance. The BCF theory, extended to crystallization from solutions, is understandably vague regarding several key issues, among them the structure and composition of the growth unit, the role of the solvent in crystal growth, at what point desolvation occurs, and what happens to the desolvated solvent. Over the years, particularly with the work of Strickland-Constable (12, 14, 18) and also that of Clontz and McCabe (17), there has been a tendency to think of a growth unit as a solvent exclusive pre-crystalline cluster of anywhere between 10's and hundreds of thousands of solute molecules comprising organized structures smaller than critical nuclei. It has been suggested that such clusters exist in saturated and supersaturated solutions(24, 25, 26). It has also been suggested that perhaps the presence of a nucleus or a growing crystal stabilizes such aggregates and that these may be the source of secondary nuclei. There is no conclusive experimental evidence which proves that this is the case.

2.2.4.1 Assumptions related to Solution Structure Implied By the BCF theory

Although it is not clearly evident, the BCF theory pre-supposes that the supersaturated solution is dilute in terms of absolute molar ratio of solute to solvent, and hence the resistances proposed explain those instances where growth is transport limited. In fact, transport limitations are proposed to be the only mechanisms of growth resistance. What happens when an abundant supply of solvated solute is immediately available at the crystal-solution interface, for example, is not considered.

The mechanism of surface integration assumes that there is very poor chemical affinity between the solute and the solvent which allows the growth unit to remain desolvated even though the solute is exposed to solvent many times during that time interval. It further presupposes that the chemical affinity between the solute molecules isn't very great either, because in order for a defect to propagate, and crystal growth to occur, the growth unit must diffuse over an existing solute lattice to a kink site (favorable for growth). Surface integration requires a partially solvated partially bonded solute molecule to "travel" across the crystal surface making and breaking bonds in one dimension. The BCF theory thus implies that solute once (even partially) de-solvated, is likely to stay that way for lengths of time on the scale of a diffusion process. Such time-scales are at least an order of magnitude larger than lengths of time associated with solvation-desolvation processes. Surface integration has appeared in various forms in the growth models proposed by Gilmer (27), Chernov (28), Bennema (29) and others. There is no conclusive and direct experimental evidence available in support of surface integration.

The BCF theory is limited by the fact that only two mechanisms of resistance to crystal growth are proposed. In fact, there is experimental evidence that suggests resistance to crystal growth may be due to other mechanisms in certain systems; for

example, in the secondary nucleation kinetics studies of fructose (30), lactose (31) and ammonium dihydrogen phosphate (32).

2.2.5 Evidence for Non-Cluster Dependent Growth Mechanisms

There is evidence in literature which suggests a molecular growth mechanism for the crystallization of certain organic compounds, among them sucrose. The reader is referred to the work of Addadi and Lahav with amino acids (34-43) and Dunning and Albon (44) and Smythe (45, 46) with sucrose. In the case of amino acids systems studied were such that the absolute molar ratio of solute to solvent is low, even in a supersaturated solution where the solute concentration is double that at saturation. The solubility behavior of the chosen impurities was similar. Addadi and Lahav required concentrations of several hundred grams per liter of the impurity to notice clear morphological changes in crystal habit (growth inhibition without morphological changes may be possible at much smaller impurity concentrations). Impurity concentration in the crystals obtained was normally on the order of several thousandths of a mole percent. Crystal growth was always accomplished via seeding, suggestive of the possibility that homogeneous nucleation is unlikely even at such high degrees of supersaturation possibly because the likelihood of two (or more) solute molecules desolvating and bonding to start the sequence of events leading to nucleation is small. Addadi and Lahav have at all times suggested a molecular mechanism of growth and inhibition and have not once alluded to clustering as an explanation of growth. Thus it is possible, and even likely, that tailor made impurities act on a per molecule basis, suggesting that growth is a sequence of molecular events. It is therefore possible that systems which are affected by tailor made impurities experience crystal growth via a molecule by molecule accretion process rather than by accretion of solvent exclusive clusters.

2.3 Solution Structure

2.3.1 The relevance of structure to crystallization research

The study of structure in supersaturated solution derives its justification as a direct result of three groups of experimental studies: studies of the inability of certain substances to nucleate even at very high supersaturations from their solutions, studies in epitaxial growth where the parent crystal is observed to support the growth of a non-identical crystalline phase, and studies of polymorphism as a result of secondary nucleation wherein contact of parent crystals resulted in the observation of more than one crystalline form of nuclei in solution. Epitaxy refers to packing of the atoms or molecules of a crystal and relative distances between atoms or molecules; morphology, and habit both refer to external differences. Morphology refers to the basic classification of the crystal eg; mono-clinic, or orthorhombic, habit refers to relative extents of different faces given a particular morphology.

Tamman (47) and later Mullin and Leci (16 a.) demonstrated that certain substances, for instance citric acid in aqueous solutions, formed glass-like amorphous solids at high supersaturations which did not nucleate. Mullin and Leci (16 b.) concluded that the ability or inability of a solution to nucleate must somehow depend upon the structure of the supersaturated solution. They reasoned that the molecular structure of citric acid favors intermolecular hydrogen bonding and association. Chains or clusters of solute molecules in supersaturated (and even concentrated but undersaturated) solutions were proposed as precursors to nuclei. This proposition will henceforth be referred to as the cluster hypothesis. Subsequently, Mullin and Leci studied the desupersaturation of citric acid solutions, and applied the cluster hypothesis to explain how and why nucleation did or did not occur from supersaturated solutions.

It is important to note that Mullin and Leci, did not take a conclusive view as to the size of the clusters nor did they rule out the possibility of solvent inclusive clusters. In subsequent studies (none of which were conducted by Mullin or Leci), however, the term "precrystalline clusters" has come to imply solventless solute clusters of 10 to 10,000 molecules.

In the study of contact nucleation of saccharides, Elankovan and Berglund (48, 49) and later Cerreta and Berglund (50, 51) showed that under certain conditions the contact of a parent crystal of a particular form and composition yielded some nuclei of a structure and composition different from that of the parent crystal in addition to nuclei that were of the same structure and composition of the parent crystal. Cerreta observed that under certain conditions the parent crystal supported growth of the non-identical nuclei while under other conditions it would not. As a result, he concluded that neither the attrition theory (small pieces of crystal which break off the surface of the parent crystal by attrition serve as nuclei or precursors to nuclei) nor the cluster theory of origin of secondary nuclei provided satisfactory answers as to the origin and mechanism of this phenomena, and that there was probably a third mechanism responsible.

In each instance the researchers conducted careful global or macroscopic measurements of temperature, pressure and concentration, and were able to determine the supersaturation of the solution. They had enough information to determine macroscopic transport properties from correlations. Yet in each instance, the researchers were of the opinion that a direct cause-effect relationship exists between the local or global structure of the solution (not the macroscopic or global transport properties) and the phenomena they observed. They were unable to define this relationship because adequate information related to solution structure was not available to them. They did not, in general, have any comments regarding what scale or scales of structure were of significance to the phenomena they were studying.

2.3.2 Ideal Solution and the classical treatment of solution structure

The classical or continuum view of a solution is stated by Smith and Van Ness in the third edition of Introduction to Chemical Engineering Thermodynamics (52) thus: "Actually, the components of a solution are intimately intermixed and cannot have private properties of their own. Nevertheless they may be assigned properties on some arbitrary but universal basis, and (the partial molar property), *defines* how a solution property is apportioned among the components of a solution." The partial molar volume of the i^{th} component of a mixture wherein the number of moles of all other components are fixed, at a specified temperature and pressure, is defined as the partial derivative of solution volume with respect to the number of moles of i . A solution in which the partial molar volumes of the components are equal to their pure component volumes is said to be an ideal solution. The fugacity of a component is a property of that component with the units of pressure, such that in the limit of zero pressure the ratio of fugacity to pressure has the value of unity, and the following equation defines fugacity:

$$dG_i = RT d \ln f_i .$$

Where the subscript i denotes the i^{th} component and:

G = Gibbs Free Energy, Joules

R = Gas Constant, 8.314 Joules / mole °K

T = Absolute Temperature, °K

The fugacity of a component in solution is defined by a similar relationship with the partial molar Gibbs Free Energy, subject to the same condition with respect to pressure. The fugacity is thus a property analogous to pressure, and its magnitude is a measure of deviation from ideal gas behavior. The ratio of the fugacity of the i^{th} component in solution to the fugacity of that component in some reference state is the activity, a_i .

The activity is an exponential function of the difference in the partial molar Gibbs Free Energy and the pure component Gibbs Free Energy of a reference state, at a given temperature and pressure. The activity is the most frequent choice as a measure of deviation from ideal solution behavior because it is directly related to the difference in the partial molar Gibbs Free Energy and the pure component Gibbs Free Energy of some reference state. In the particular case of sugar water systems this is of considerable practical significance because the correlation between shelf life, texture, biological stability of foods, and water activity, a_w , is well documented. Several comprehensive reviews of the influence of water on chemical reactions in food are available(53-57). The measurement of a_w , in concentrated and metastable aqueous solutions of sugars is also an area of active interest (58). Official Methods of Analysis of the AOAC (1984) 32.004-32.009 details analytical methods for determination of a_w . Hair hygrometers, electronic hygrometers, and isopiestic methods are commonly used. Electronic hygrometers work on the principle that that changes in conductance, resistivity, impedance, resistance, or capacitance of a thin film or an aqueous solution of a hygroscopic substance can be correlated to corresponding changes in a_w (59). Rugged, stable, rapid and precise techniques for evaluation of a_w are required. There is a need for techniques that can rapidly, accurately, and simultaneously measure solute concentration and water activity.

An excess property is the difference between an actual property and a property that would be calculated at the same temperature, pressure and molar composition for an ideal solution. The molar excess Gibbs Free Energy, G^E , is related to the activity thus:

$G^E/RT = \sum (x_i \ln (\tilde{a}_i / x_i))$. The quantity in the inner brackets is the activity coefficient for component i , γ_i , described by:

$\gamma_i = (\tilde{a}_i / x_i)$. The activity coefficient is also a widely used measure of deviation from ideal solution behavior. The work of Kozak et. al. succeeded in relating structural

effects of interactions between pairs of molecules to the activity coefficient; however, there is no protocol to differentiate and account for site specific differences in interactions between parts of molecules. Understanding such differences in interactions may be a key element in understanding the relation between structure and other solution phase phenomena.

It follows from this discussion that fugacity, activity, and activity coefficients are all measures of the extent to which a solution deviates from the behavior of an ideal solution. Each of these are in fact arbitrary quantities, none of these may be related to an actual spatial or temporal quantity, and all of these are in fact based on the kinetic theory of ideal gases as a model, and are measures of how much a real solution deviates from a solution of ideal gases. None of these can be directly measured and each of these assume that the solution is a continuous and microscopically homogeneous phase. Further the kinetic theory of gases, assumes that the molecules of gas are hard spheres, with mass but no intermolecular forces of attraction.

Models of "real gases" deal with the consequence of the molecules having a finite condensation volume and intermolecular forces of attraction. Yet molecules are still treated as spheres and differences in relaxation and exchange rates among the different moieties within a molecule are not taken into account, nor are differences in function among molecules of the same species within a mixture. Such models do not account for the fact that some fraction of molecules of a given species, particularly the solvent in a solution, may be engaged in solvation of solute at any given time while others may be engaged in pure component like behavior at the same time. Even the most advanced treatments of solution thermodynamics such as those of Ben-Naim and co-workers(20) which treat solute molecules and the solvent associated with it for the longest time as a "solvaton" in a sea of solvent, do not account for differences in exchange rates at different moieties on the same solute molecule. These issues become significant when time and length scales associated with solvation and desolvation

become significant to the description of a process, as is the case for crystallization from solution.

The relationship between supersaturation and deviation from ideal solution behavior has often been used to define or describe structure in supersaturated solutions. The traditional and accepted analysis is based on a modified version of Kozak et. al's (60) approach of relating molecular neighbor pair potential functions to the excess Gibb's free energy and thus the activity coefficient for each molecular species in solution. Barone and co-workers (61-64) have demonstrated this technique. They analysed solution structure by examining the concentration dependence of the magnitude and nature of molecular pair potential functions calculated using a numerical approach..

Myerson and co-workers (Sorrel, (65) and Chang, (66-69)) have attempted to directly relate activity to solution structure through analytical correlations between activity and other solution properties. They painstakingly and meticulously measured diffusion coefficients of both non-electrolytes (urea, glycine, and glycine-valine) and electrolytes (sodium chloride and potassium chloride) in solute diffusion studies in concentrated aqueous solutions. Precipitous drops in diffusion coefficients were observed near the saturation point in each case. The results indicate formation of solute-solvent aggregates of an unknown composition. Whereas the measurement of the diffusion coefficient was careful and direct, in each case, the calculation of cluster size or aggregate size was not a very straight forward process and involved the implicit assumption that the solution may be treated as a continuum. Transport phenomena in solution are determined by non-equilibrium solvation dynamics which are governed by short range interactions. These take place on a variety of time and length scales that are shorter than the time and length scales associated with diffusion. This evidence will be reviewed in another section. Myerson and coworkers attempted to relate the diffusion

coefficients to the structure of the solution resulting from short range interactions without taking solvation dynamics into account.

Larson and Garside (24,25) performed an experiment with isothermal columns of concentrated, saturated, and supersaturated solutions of citric acid, urea, sodium nitrate, and potassium sulfate during which they observed concentration gradients along the length of the column for only the supersaturated solutions. Larson and Garside concluded that there must be solute structuring in supersaturated solutions. By making the classical assumption that all solute in solution must be associated with other solute molecules because of an absence of solvent to satisfy the solvation requirements, the solvent exclusive clusters were proposed to be comprised of several thousand molecules each. Myerson⁶³ in recent work has argued that if the constraint of solvent exclusion is relaxed, then the probable size of clusters would be two or three solvated molecules of solute. Cerreta and Berglund (51,71) used Raman spectroscopy of ammonium dihydrogen phosphate (ADP) to show that while no great differences could be observed in the spectra of very concentrated, saturated and supersaturated solutions, evidence did exist for dimer formation. Larson and Garside(24) cited Cerreta and Berglund (51) as well as the Raman studies of Hussman et al.(71) and MacMahon et al.(73) with alkali nitrates as evidence of pre-crystalline clusters in concentrated solutions.

Implicit to each approach is the assumption that any one molecule of a given chemical species is considered to be identical in function to any other molecule of that chemical species. Pair potential functions are time and space averaged and do not account for dynamic structure and/or interactions on submolecular scales in a manner that allows direct correlation with physical variables that can be directly measured; neither do excess energies and activity coefficients derived therefrom. The fact that some solvent is involved in solvation and other solvent behaves as a pure component is not accounted for, nor the dynamic nature of this distribution. The possibility of any

relation between deviation from ideal solution behavior and such a difference in the function of the solvent is *a-priori* excluded from such analyses. This limitation arises because of the implicit assumption that matter in solution is in a homogeneously continuous phase at all times.

2.3.3 Other Concepts of Solution Structure

The fact that all water molecules in solution at any given instant do not have identical solvation environments, even in pure solvent, has been accepted for a long time now, e.g. Bousfield and Lowry (74). From the earliest post-quantum discourses on solution structure and properties it is clear that a relationship between change in solution structure and deviations from ideal solution behavior was thought to exist although the specifics of cause-effect were undetermined. The focus on solution-structure has been primarily limited to the study of the immediate solvation environment of the solute molecules(75,76). In many cases the structure of this environment has been observed to change little, if at all, with solution concentration up to saturation, even though deviations from ideal solution behavior over the same range of solution concentrations are observed to be significant. As a result, strong correlations between structure and deviations from ideal solution behavior were not apparent. There has been some speculation as to changes in the structure of the solvent that does not participate in the solvation of solute with changes in concentration (77-81); however, until recently there were few reliable estimates regarding the nature of such changes(83).

Physical chemists at the turn of the century were well aware that solution structure (at that time attributed only to aqueous solutions) is a consequence of the functional distribution of water molecules into "bulk" and "solvated" microphases. This is to say that some of the water in solution behaves as if it is not associated (bulk or free), and some behaves as if it is (solvated or bound). Even in pure water not all the

water molecules (or even parts of water molecules) are associated to the same extent. Bousfield and Lowry thought that water molecules existed as "dimers and trimers"(74). Pauling championed the idea of "tetrahedral clusters" (75). Frank and Wen (84) modified the tetrahedral cluster concept to reflect the dynamic nature of distribution of water molecules between clusters of different sizes , or "dynamic or flickering clusters".

Most ideas regarding solution structure that are accepted today are in some way related to Hildebrand's work (85). He proposed that in order for a molecule of solute to enter solution it must first break the bonds with its nearest neighbors in the solid lattice, then displace a molecule of solvent from the solvent lattice, and finally develop bonds with its nearest neighbors in the solvent lattice.

Thus the processes of solvation and desolvation were proposed to be intimately connected with the concept of solution. Frank and Wen and Némethy and Scheraga (86) furthered the idea of structure in water by proposing the concept of a distribution of clusters and flickering clusters respectively, wherein the chemically identical water molecules are functionally distributed in solution according to how they participate in nearest neighbor interactions defined in a large part by their ability to participate in proton exchange.

A water molecule may be unable to participate in proton exchange in a solution if it is hydrogen bonded to either another water molecule or a solute molecule. Water that behaves in such a manner has been designated "associated", "bound", or "water of solvation (specifically applied to water hydrogen bonded in the proximity of a solute molecule)". Water molecules may also be able to participate in solvent exchange and exhibit behavior that is indicative of the absence of any solute molecules, such water has been designated "free", "unbound", or "unassociated". In this work we will refer to water which does not participate in solvent exchange on the time scale of the experiment as "solvation water", and water which behaves as if there were no solute molecules

present as "bulk water". Water which behaves in a manner which is not consistent with either solvation water or bulk water will be designated non-bulk-non-solvation water. From this discussion it is apparent that it is important to account for not only what points in space are occupied by solvent and solute molecules at given moments in time, but also what role each molecule of solvent takes on at that time. For this purpose we will use the terms spatial distribution, functional distribution, and functional microphase distribution. The term "spatial distribution" refers to how solute and water or other solvent molecules are distributed and arranged in space in a solution. The term "functional distribution" of solvent refers to the moles (or molecules) of water in solution which can be assigned to each category. The term "functional microphase distribution" refers to the number of water molecules in the neighborhood of a solute or probe molecule or moiety (when specifically designated) or some microscopic region in space less than 200 nm in extent (when no specific molecule is designated) which can be assigned to each category. It is also apparent from this discussion that the dynamics of the molecules in solution is intimately related to the solution structure. In an absolute sense, the discussion of one can only be incomplete without discussing the other. In the following discussion we therefore review information related to both structure and dynamics of aqueous sucrose solutions.

Franks (87-89), and Sugget (90-93) and coworkers in a series of studies on various sugar solutions demonstrated that water in both dilute and non-dilute solutions is also functionally distributed. Birch et. al. (94) demonstrated the functional distribution of water on the basis of proton exchange rates in pulsed NMR experiments, as did Richardson and Steinberg (83) in an NMR study of sucrose solutions of various concentrations (including nearly saturated, saturated, and supersaturated solutions) in the presence and absence of growing crystals. Each of these studies provides an estimate of the amount of water that immediately solvates the sugar molecule in solution, and thereby sheds light on the nature of short range and short time solute-

solvent interactions. None specifically addresses the issue of the structure or behavior of the non-solvation water, and if the microphase distribution changes with concentration.

Previous investigations have studied the nature of various molecular associations by utilizing a variety of means. In the study of supersaturated solution structure many studies have been conducted on the scale of molecular diffusion. Some of these include the column studies of Larson and Garside (24-26), the studies of Narayan and Youngquist (95), and the studies of Myerson and coworkers (65-69). Dielectric relaxation methods (Suggett and Clark (92)) have identified two distinct relaxation processes for water in sucrose solutions. These are designated associated water, hydrating the sucrose, and bulk water comprising the remaining water in solution, not associated with solute. Associated water has a longer relaxation time than the bulk water. The ^2H and ^{17}O NMR studies of Richardson and Steinberg (83), on the mobility of water in sucrose solutions, indicate three regions of decreasing rotational rates of water molecules with increase of sucrose concentration through saturation and continuing into the supersaturated regions. These effects were attributed to the development of an extensive but dynamic network of hydrogen bonds of water to sucrose, water bridging of the sucrose and direct sucrose to sucrose interactions (although no direct evidence of sucrose-sucrose interactions were observed). The bulk viscosities of these solutions also increase with increasing sucrose concentrations, in a manner consistent with the rest of the data, suggesting that the same short range interactions define both structure and transport.

The studies of Myerson and coworkers (65-69) are particularly interesting because they utilized Guoy Interferometry to measure diffusion coefficients. The interesting aspect is that Myerson used continuum arguments to reach his conclusions. This would indicate that for the systems under consideration the macroscopic transport

coefficients in supersaturated solution must be very similar to the microscopic transport coefficients in supersaturated solution.

2.3.4 Non-Continuum Descriptions of Solvation and Structure

A more recent trend in the description of solvation and solution structure is the effort to develop non-continuum models to describe order, dynamics and interactions. This work has been pioneered by the pico- and femto-second spectroscopy of Marcus and coworkers. Structure, transport properties and thermodynamics of phase equilibria are manifestations of interactions on submolecular length scales, e.g. hydrogen bonding, hydrophobic interactions, which require anywhere from a picosecond to a nanosecond to take place. The fact that solution structure and transport phenomena are related in a way that structure governs transport properties and transport phenomena are a directly measurable manifestation of structure, enables us to extract important information about the structure from the study of transport processes and vice versa. Transport properties in solution are governed by non-equilibrium solvation dynamics. There is evidence to suggest that transport phenomena are governed by short range interaction processes that take place on a variety of time and length scales, which are less than those associated with molecular diffusion (96,97). The work of Maroncelli et. al.(98), Kenney-Wallace, Jonah, and co-workers (99-102), Wolynes (103, 104), Cross and Simon (105,106), Migus et.al.(107), and Brady (108) demonstrates that the time scales involved in the solvation (and desolvation) process, as well as the molecular re-orientation process, are much faster than that of molecular diffusion. They suggest that the length scales involved in the interactions most significantly associated with desolvation and molecular reorientation, with respect to incorporation of solute molecules in the crystalline lattice, are small compared to those associated with molecular diffusion. Continuum models are still prevalent for solvation dynamics.

These models do justice to the long range interactions in solution, but fail to account for the details of structure and interaction of inner solvation shells which are often dominant factors (103).

There are now several non-continuum approaches to understanding solvation dynamics. They differ primarily in the choice of a basis set of significant length/time scales. One such widely discussed approach, the mean spherical approximation or MSA, indicates that solvation of an ion or molecule occurs on a range of time scales. A molecule can be thought to be made up of component dipoles. The limiting length scale of each such component is on the order of length of the hydrogen bond. Local solvent structure and dynamics near each of these components has been observed to differ significantly. Even the solvation of a simple alcohol must be described by at least two different time scales. One corresponds to the continuum longitudinal relaxation time, while the other is associated with the time required by solvent molecules to rearrange themselves near the dipole. For small dipoles or ions, in dilute solution, this time is of the order of a picosecond (103,104). Furthermore, the molecular dynamics simulations of Cross and Simon (105), suggests that if a dipole is strong enough (>17 D) then the two ends may start behaving like point dipoles in the sense that the localized solvent structure and dynamics may be different at each of the ends of the dipole. This is summed up by Maroncelli et. al.(98) who conclude that the solvation response in a polar solvent involves coupled reorientational dynamics that occur on time scales shorter than single particle diffusion. There have been studies in the solvation of an electron in water and alcohols, using picosecond and femtosecond time correlated spectroscopies, which indicate that solvent reorientational times are on the order of < 500 fs (107). Brady's study (108) of the molecular dynamics of solvated glucose in a 15 wt. % solution also indicates that the local structure and dynamics near each of the O or OH moieties of the glucose molecule differ, as do the solvent relaxation times.

The significance of this information, simply put, is this: although solvation and desolvation must necessarily play critical roles in the crystallization process, there are no parameters for either length or time scales involved in these phenomena, in the description of crystal growth or nucleation mechanisms, kinetics, transport, or subsequent analyses of crystallization processes. Furthermore most models of solvation in use are continuum models, it is not possible to use a non-continuum approach like MSA for a sucrose-water system because the relevant length scales or time scales have not yet been identified, besides which the large number of sites at which solvent exchange occurs on a sucrose molecules may make such an approach impractical. Therefore on the one hand non-continuum approaches are still in their developmental stages, and on the other the usefulness of any model of crystal growth based on an approach which does not account for solvation and or desolvation will necessarily be limited. The extent to which such limitations affect the ability to control crystallizations is not an easy issue to address, and is beyond the scope of this work.

2.4 Techniques commonly used to measure concentration in supersaturated solutions

For industrial sugar solutions temperature measurement at a known pressure is the most common technique of measuring supersaturation. Industrial sugar solutions are normally crystallized by means of evaporating the water by means of boiling the solution. On the basis of years of experience the temperature of a sugar solution can be accurately correlated to its concentration or supersaturation.

Refractive index, viscosity, and density are other common means of determining the concentration of a sugar solution. Additionally water of solvation data obtained via a variety of techniques like NMR and dielectric relaxation can be related to solution concentration.

2.4.1 Spectroscopic Sensing Techniques

All spectroscopic sensing techniques are based on extracting information about the structure of a molecule or a part of a molecule, its environment, or the interactions between them. The literature which describes these techniques is vast and the how and why of these techniques are largely not of significance to this work; however, the results of studies of solution structure using these techniques affect this work a great deal. A review of the results of various studies of aqueous sucrose solutions using these techniques follows.

2.4.1.1 Raman Spectroscopy

Recent experimental attempts to study interactions in supersaturated aqueous sugar solutions have involved the use of Raman, IR, and NMR spectroscopies and X-ray diffraction. X-ray diffraction, Raman and IR spectroscopy are sensitive to changes in vibrational frequencies and space lattice ordering that occur as the concentration of the solution increases. The effects of molecular association, and hydrogen bonding are observed in Raman and IR spectra. Mathlouthi et al.(109-111) performed vibrational spectroscopy of sugar solutions of various concentrations and observed that the characteristics of the spectra were concentration sensitive. Bands assigned to the asymmetric vibrations of the CH and OH groups are observed to shift in frequency. In an attempt to correlate the change in solution structure to change in concentration, the ratio of the integrated band intensity at 1460 cm^{-1} , assigned to the HCH bending mode, to that at 1640 cm^{-1} , assigned to the HOH bending mode was plotted as a function of concentration. The shift in these frequencies were plotted against sugar concentration. A ten wavenumber shift (approximately 1%) , from 1450 cm^{-1} to 1460 cm^{-1} , was observed in the band associated with the HCH bend as the concentration of sucrose in

solution increased from 10 to 66 wt%, and that of glucose increased from 5 to 54 wt%. This indicates that the HCH bend can be accomplished with less energy in dilute solution than in-vacuo or in crystalline form, the two standards that are commonly used for calculation of band positions and contributions (112, 113).

While this indicates that this particular vibrational mode is about as hindered in concentrated solution as it is in vacuo or in crystalline state, all one can safely conclude from this is that the CH₂ moiety must be hydrophobically hydrogen bonded to the same extent in solution as it is in a crystal or otherwise limited in its ability to bend. It is not clear from this observation per-se that the CH₂ group is associated to another sugar molecule: it might be associated with water. For similar reasons it cannot be concluded that the shift in the HOH bend frequency is evidence of solvent exclusive solute clustering; it can be concluded that some of the water molecules behave in an ice-like manner (are tetrahedrally coordinated) and the bending motion is hindered concentrated solutions. It cannot be said conclusively whether this hindering is due to association with the solvent or with the solute. In addition to this uncertainty of interpretation is the fact that Raman spectra are solute sensitive. As the concentration increases beyond saturation the changes in the spectra are less pronounced; Mathlouthi's observations do not extend into the supersaturated region.

2.4.1.2 Fourier Transform Infrared Spectroscopy

Evidence of solvent exclusive-solute clustering, if it occurs, could be observed in IR spectra (114). The unequivocal interpretation of IR and Raman spectra is severely hindered by the absence of accepted protocol for quantifying the effects of hydrogen bonding on the spectra, by the inability to account for the effects of hydrogen bonding in LCAO-MO or other calculations by means of which band assignments are accomplished (since these calculations are for molecules in-vacuo), by the general lack

of resolution observed in all regions of the spectrum associated with water and its vibrations, and by the lack of a clear understanding of the spectrum of liquid water. This is more so true for IR. Suggested methods for obtaining good quality spectra include the arbitrary subtraction of weighted solvent spectra; while this may be good enough for qualitative analysis it is unsatisfactory for interpreting structure and interactions. Although there is evidence that suggests solute-solute interactions in supersaturated solutions, there is also overwhelming evidence that all bands corresponding to vibrational modes sensitive to hydrogen bonding are intensified. Thus the possibility of solvent inclusive association cannot be ruled out.

2.4.1.3 X-ray Diffraction

Mathlouthi's X-ray diffraction studies (81) of sugar solutions indicate formation of intramolecular bonds with the increase in solute concentration. He was able to convincingly demonstrate that some sucrose molecules might be associating with some other sucrose molecules, a result consistent with the observations of band shifting and intensification in IR and Raman spectra. He was, however, unable to provide any convincing data or argument that suggests that such clusters are larger than two solute molecules or that they were exclusive of associated solvent.

2.4.1.4 NMR

Franks, Suggett and co-workers (87-93) used dielectric relaxation and NMR to determine solvation properties of sugars. Franks et al. (87, 88) confirmed the earlier results of Jones (75) and Phillips (76) for dilute solutions (an average of 6 water molecules of solvation per molecule of sucrose) and also confirmed that the sugar water interaction was about as strong as the water-water interaction. Harvey and Symons (82) used NMR to determine 11 water molecules of solvation per molecule of sucrose,

interpreted as 6 molecules of water strongly associated with the molecule of sucrose and the remaining molecules more dynamically associated. Birch et al.(94), in a pulsed NMR study of concentrated sucrose solutions, determined that there are four kinds of protons in solution: bulk water, solvated water, exchangeable sugar hydroxyl, and non-exchangeable ring (C-H) protons. Franks, Suggett and co-workers as well as Barone and co-workers (who used numerical simulations based on Kozak et al.'s (60) modification of McMillan Meyer (96) theory) initially hypothesized that solute-solute interactions in dilute solutions were unlikely. More recent work by Barone et al.(61) indicates that the nature of interactions in solution may be more complex than previously accepted without offering insight into the exact nature of the complexity. The ^{17}O NMR work of Richardson and Steinberg (83) indicates that sucrose solutions can be modelled using an isotropic two states of water exchange model, with no discontinuity in exchange rates related to saturation. The NMR work is sensitive to the time scales on which the exchange of proton takes place between different proton donor-acceptors. All of this work indicates that the solute molecules are at least partially solvated even in supersaturated solutions and that there is water, even in supersaturated solutions, that behaves like bulk water.

2.5 References

1. Jancic S.J. and E.J. de Jong eds., Industrial Crystallization '84, Elsevier, Amsterdam, (1984)
2. Levine I. N., Physical Chemistry, 2nd edition, McGraw Hill Inc., New York, NY, (1983)
3. Randolph A. D. and M. A. Larson, Theory of Particulate Processes, Academic Press, New York, NY (1971)
4. Randolph A. D. , *Can. J. Chem. Engg.*, **42**, 280, (1964).
5. Larson M.A. and A. D. Randolph , *Chem. Engg. Progress Symp. Ser.*, **65**(95), 1, (1969).
6. Mullin, J.W., Crystallization, Butterworths, London, pp. 35-52, (1971).
7. Kirk , and Othmer eds., Encyclopedia of Chemical Technology, 3rd ed., (1981).
8. Brice J. C., *J. Crystal Growth*, **1**, 218, (1967)
9. Bunn, C. W., *Disc. Faraday Soc.*, **5**, 32, (1949)
10. Berglund K. A., PhD Dissertation, Iowa State University, 1981.

11. Shiau L. D., PhD. Dissertation, Michigan State University, 1988.
12. Mason R. E. A. and R. F. Strickland-Constable, *Trans. Faraday Soc.*, **62**, 455, (1966)
13. Botsaris G. D., in J.W. Mullin ed. Industrial Crystallization, Plenum Press, New York, NY, 3-32, (1976)
14. Lal D. P., R. E. A. Mason, and R. F. Strickland Constable, *J. Crystal Growth*, **5**, 1, (1969)
15. Garside J. and R. J. Davey, *Chem. Engg. Com.*, **4**, 393-424, (1980)
16. a. Mullin, J.W. and C. Leci, *Philos. Mag.*, **19**, 1075 (1969).
b.. Mullin, J.W. and C. Leci, AIChE Symposium Series **68**, J. Estrin ed., **8**, (1972).
17. Clontz N. A. and W. L. Mc Cabe, *Chem. Engg. Prog. Symp. Ser.*, **67**(110), 6, 1971.
18. Strickland-Constable R.F., Kinetics and Mechanism of Crystallization, Academic Press, London, (1968)
19. Powers H.E. C., *Nature*, **178**, 139-140, (1956)
20. Ben-Naim, A. , Solvation Thermodynamics, Plenum Press, New York (1987).
21. Buckley H. E., Crystal Growth, Chapman and Hall, London, (1952)
22. Burton W.K., N. Cabrera, and F. C. Frank, *Phil. Trans.*, **A243**, 299, (1951)
23. Frank F. C., *Disc. Faraday Soc.*, **5**, 49, (1949)
24. Larson, M.A. and J. Garside, *Chem. Eng. Science*, **41**, 1285 (1986).
25. Larson, M.A. and J. Garside, *J. Crystal Growth*, **76**, 88 (1986).
26. Larson, M.A., *AIChE Symposium Series no.240*, **80**, 39-44 (1984).
27. Gilmer G.H. , R. Ghez, and N. Caberera, *J. Crystal Growth*, **8**, 79, (1971)
28. Chernov A. A., *Soviet Phys. Usp.*, **4**, 116, (1951)
29. Bennema P., in J.W. Mullin ed. Industrial Crystallization, Plenum Press, New York, NY, (1976)
30. Shiau L. D. and K. A. Berglund, *AIChE. J.*, **33**(6), 1028, (1987).
31. Shri Y. , R.W. Hartel, and B. Liang, *J. Dairy Science*, **72**(11), 2906-2915, (1989)
32. Cerreta, M.K. and K. A. Berglund, *J. Crystal Growth*, **102**, 869, (1990)
33. Addadi L., Z. Berkovitch-Yellin, N. Domb, E. Gati, M. Lahav, and L. Leiserowitz, *Nature*, **296**, 21, (1982).
34. Addadi L., Z. Berkovitch-Yellin, I. Weissbuch, M. Lahav, and L. Leiserowitz, *Mol. Cryst. Liq. Cryst.*, **96**, 1, (1983).
35. Addadi L., and S. Weiner, *Proc. Natl. Acad. Sci., USA*, **82**, 4110, (1985).
36. Addadi L., Z. Berkovitch-Yellin, I. Weissbuch, J. van Mil, L. J.W. Shimon, M. Lahav, and L. Leiserowitz, *Angew. Chem. Intl. Ed. Engl.*, **24**, 466, (1985).
37. Addadi L., and S. Weiner, *Mol. Cryst. Liq. Cryst.*, **134**, 305, (1986).
38. Berkovitch-Yellin, Z., L. Addadi, M. Idelson, L. Leiserowitz, and M. Lahav, *Nature*, **296**, 27, (1982).
39. Berkovitch-Yellin, Z., L. Addadi, M. Idelson, M. Lahav, and L. Leiserowitz, *Angew. Chem. Intl. Ed. Engl.*, **21**(8), 631, (1982).
40. Landau, E. M., M. Levanon, L. Leiserowitz, M. Lahav, and J. Sagiv, *Nature*, **318**, 353, (1985).
41. Landau, E.M., R. Popovitz-Biro, M. Levanon, L. Leiserowitz, M. Lahav, and J. Sagiv, *Mol. Cryst. Liq. Cryst.*, **134**, 323, (1986).
42. Weissbuch I., L. Addadi, Z. Berkovitch-Yellin, E. Gati, M. Lahav, and L. Leiserowitz, *Nature*, **310**, 161, (1984).
43. Weissbuch I., L. J. W. Shimon, E.M. Landau, R. Popvitz-Biro, Z. Berkovitch-Yellin, L. Addadi, M. Lahav, and L. Leiserowitz, *Pure and Appl. Chem.*, **58**(6), 947, (1986).
44. Dunning W.J. and N. Albon, in Growth and Perfection of Crystals, ed. R.H. Doremus, R.W. Roberts, and D. Turnbull, Wiley, London, 416, (1958).
45. Smythe B. M., *Aust. J. Chem.*, **20**, 1115, (1967).
46. Smythe B. M., *Sugar Technol. Rev.*, **1**, 191, (1971).
47. Tamman G., States of Aggregation, transl. R.F. Mehl, van-Nostrand, New York, (1925).

48. Elankovan, P. and K.A. Berglund, *AIChE J.*, **33**, 1844, (1987).
49. Elankovan, P., and K.A. Berglund, *Appl. Spectroscopy*, **40**, 712, (1986).
50. Cerreta, M.K. and K.A. Berglund, in Industrial Crystallization '84, S.J.Jancic and E.J. DeJong, (Eds.), Elsevier, Amsterdam, 21 (1984).
51. Cerreta, M.K. and K. A. Berglund, *Journal of Crystal Growth*, **84**, 577 (1987).
52. Smith, J. M. and H. C. Van Ness, Introduction to Chemical Engineering Thermodynamics, 3rd ed., McGraw Hill Inc., Singapore, (1975)
53. Labuza T. P. 1980. The effect of water activity on rection kinetics of food deterioration. *Food Technol.* **34**(4):36
54. Rockland L. B. and Nishi, S. K. 1980. Influence of water activity on food product quality and stability. *Food Technol.* **34**(4):42
55. Duckworth, R. B. 1975. *Water relations of Foods*. Academic Press, New York
56. Rockland, L. B. and Stewart, G. F. 1981. *Water Activity: Influences on Food Quality*. Academic Press, New York
57. Simato D. and Multon, J. L. 1985. Properties of Water in Foods. Martinus Nijhoff Publishers, Dordecht, The Netherlands
58. Le Maguer M. in Water Activity : Theory and Applications to Foods, L. B. Rockland and L. R. Beauchat eds., Marcel Dekker, Inc. , New York and Basel, pp. 1-25, (1987)
59. Johnston M.R. and R.C. Lin, in Water Activity : Theory and Applications to Foods, L. B. Rockland and L. R. Beauchat eds., Marcel Dekker, Inc. , New York and Basel, pp. 287-294, (1987)
60. Kozak, J.J., W.S. Knight and W. Kauzmann *J. Chem. Phys.*, **48**, 2, 675 (1968).
61. Barone, G., G. Castronuovo, P. Del Vecchio and V. Elia, *J. Solution Chem.*, **19**, 1, 41 (1990).
62. Barone, G., G. Castronuovo, P. Del Vecchio, V. Elia and M.T. Tosta, *J. Solution Chem.*, **17**, 10, 925 (1988)
63. Barone, G., G. Castronuovo, V. Elia and M.T. Tosta, *J. Solution Chem.*, **15**, 2, 199 (1986).
64. Barone, G., G. Castronuovo, V. Elia and V. Savino, *J. Solution Chem.*, **13**, 3, 209 (1984).
65. Myerson, A.S. and L.S. Sorrel, *AIChE Journal*, **28**, 778 (1982).
66. Myerson, A.S. and Y.C. Chang, in Industrial Crystallization '84, S.J. Jancic and E.J. DeJong (Eds.), Elsevier, Amsterdam, 27 (1984).
67. Chang, Y.C. and A.S. Myerson, *AIChE J.*, **31**, 980 (1985).
68. Chang, Y.C. and A.S. Myerson, *AIChE J.*, **32**, 1567 (1986).
69. Chang, Y.C. and A.S. Myerson, *AIChE J.*, **32**, 1747,(1986).
70. Myerson A.S.,
71. Cerreta, M.K., Ph.D thesis, Michigan State University (1988).
72. Hussman, G.A., M.A. Larson and K.A. Berglund, in Industrial Crystallization '84, S.J. Jancic and E.J. DeJong (Eds.), Elsevier, Amsterdam, 21 (1984).
73. MacMahon, P.M., K.A. Berglund and M.A. Larson in Industrial Crystallization '84, S.J. Jancic and E.J. DeJong (Eds.), Elsevier, Amsterdam, 229 (1984).
74. Bousfield, W.R. and T.M. Lowry, *Trans. Faraday Soc.*, **6**, 85 (1910).
75. Jones, H.C., *Amer. Chem. Journal*, **32**, 319 (1904).
76. Phillips, J.C., *Trans. Faraday Soc.*, **3**, 136 (1907).
76. Bernal, J.D. and R.H. Fowler, *J. Chem. Phys.*, **1**, 515 (1933).
78. Pauling, L. and O. Brockway, *Proc. Natl. Acad. Sci.*, **20**, 336 (1934).
79. Franks, F. in Hydrogen Bonded Solvent Systems, A.K. Covington and P.Jones (Eds), Taylor and Francis Ltd., London, 31-47 (1968).
80. Suggett, A., *J. Solution Chem.*, **5**, 1,33 (1976).
81. Mathlouthi M., *Carbohydrate Res.*, **91**, 113, (1981).
82. Harvey, J.M. and M.C.R. Symons, *J. Solution Chem.*, **7**(8), 571 (1978).
83. Richardson S.J. and M.P. Steinberg, in Water Activity: Theory and Applications to Food, L. B. Rockland and L.R. Beauchat eds., Marcel Dekker Inc., New York, 235, (1987).
84. Frank, H.S. and W.Y. Wen, *Disc. Faraday Soc.*, **24**, 1333 (1957).

85. Hildebrand, J.H., in *Solubility*, Wiley and Sons, N.Y., 2nd. ed., (1965).
86. Nemethy, G. and H.A. Scheraga, *J. Chem. Phys.*, **36**, 3401 (1962).
87. Franks, F., J.R. Ravenhill and D.S. Reid *J. Solution Chem.*, **1**, 1, 3 (1972).
88. Franks, F., M. Pedley and D.S. Reid, *J. Chem. Soc. Faraday Trans. I*, **72**, 359 (1976).
89. Franks, F., *Pure and Appl. Chem.*, **59**, 9, 1189 (1987).
90. Tait, M.J., A. Suggett, F. Franks, S. Ablett and P.A. Quickenden *J. Solution Chem.*, **1**, 2, 131 (1972).
91. Suggett, A. and A.H. Clark, *J. Solution Chem.*, **5**, 1, 1 (1976).
92. Suggett, A., *J. Solution Chem.*, **5**, 1, 33 (1976).
93. Suggett, A., S. Ablett and P.J. Lillford, *J. Solution Chem.*, **5**(1), 17 (1976).
94. Birch, G.G., J. Grigor and W. Derbyshire, *J. Solution Chem.*, **18**, 8, 795 (1989).
95. Narayanan, H. and G.R. Youngquist, *AIChE Symposium Series no. 253*, **83**, 1-7 (1987).
96. McMillan, W.G. and J.E. Mayer, *J. Chem. Phys.*, **13**(7), 276 (1945).
97. Migus A., Y. Gauduel, J.L. Martin, and A. Antonetti, *Phys. Rev. Lett.* , **58**(17), 1559, (1987).
98. a. Maroncelli M., J. MacInnis, and G.R. Fleming, *Science*, **243**, 1674, (1989).
b. Chapman C. F., R. S. Fee, and M. Maroncelli, *J. Phys. Chem.*, **94**, 4929, (1990).
99. Kenny Wallace G.A. and C.D. Jonah, *Chem. Phys. Lett.*, **39**(3), 596, (1976).
100. Kenny-Wallace G.A., *Can. J. Chem.*, **55**, 2009, (1977).
101. Kenny-Wallace G.A., G.E. Hall, L.A. Hunt, and K. Sarantidis, *J. Phys. Chem.*, **84**, 1145, (1980).
102. Kenney-Wallace G.A. and C.D. Jonah, *J. Phys. Chem.*, **86**, 2572, (1982).
103. Wolynes P.G., *Annu. Rev. Phys. Chem.*, **31**, 345, (1980).
104. Wolynes P.G., *J. Chem. Phys.*, **86**(9), 5133, (1987).
105. Cross, A. J. and J.D. Simon, *J. Chem. Phys.*, **86**, 7079, (1987).
106. Simon, J.D., *Acc. Chem. Res.*, **21**, 128, (1988).
107. Migus A., Y. Gauduel, J.L. Martin, and A. Antonetti, *Phys. Rev. Lett.* , **58**(17), 1559, (1987).
108. Brady J.W., *J. Am. Chem. Soc.*, **111**, 5155, (1989).
109. Mathlouthi M and D.V. Luu, *Carbohydrate Res.*, **78**, 225, (1980).
110. Mathlouthi M. and D.V. Luu, *Carbohydrate Res.*, **81**, 203, (1980).
111. Mathlouthi, M., C. Luu, M. Meffrov-Biget and D.V. Luu, *Carbohydrate Res.*, **81**, 213 (1980).
112. Cael J.J., J.L. Koenig and J. Blackwell, *Carbohydrate Res.*, **32**, 79, (1974).
113. Szarek W.A., S. Korppi-Tommola, H.F. Shurvell, V. H. Smith Jr., and O.R. Martin, *Can. J. Chem.*, **62**, 1512, (1984).
114. Back D.M., D.F. Michalska, and P. L. Polavarapu, *Appl. Spectroscopy*, **38**(2), 173, (1984).

Chapter Three

The use of pyranine as a trace fluorescent probe to study structure in aqueous sucrose solutions*

3.1 Background

The effect of supersaturation on crystal growth from solution was established by Ostwald in 1897, and the need to establish a relation between solubility and solution structure was recognized in 1910 by Bousfield and Lowry (10); but, the need to relate the properties of saturated and supersaturated solutions to structure and to thereby characterize the effect of solution structure upon crystal growth is fairly recent. In 1910 Bousfield and Lowry (10) accepted that water consisted mainly of dimers and trimers in the liquid state and that structure in aqueous solution was a primary consequence of ordering of water molecules. Jones (29) in 1904 showed that a molecule of sucrose is associated with 6 molecules of water on the average (values varied between 3 and 10), by measuring freezing point depression in aqueous sucrose solutions of up to 47 wt.%. Phillips (49) in 1907 obtained similar results (with a similar range of values) using hydrogen gas absorption in sucrose solutions. The mechanism of solvation was investigated by Eley (19), who proposed a 2 step solvation model which correctly predicted the relationship between temperature and heat capacity of solvation, but could not account for observed water of solvation of various compounds. Pauling (48) proposed a tetrahedral model for liquid water

* This material was published in part as R. Chakraborty & K. A. Berglund, "The Use of Pyranine as a Trace Fluorescent Probe to Study Structure in Aqueous Sucrose Solutions," *AIChE Symposium Series, no. 284*, p 113-124, (1991).

which could explain the solvation behavior of some ions, but could not account for the conductivity of water or rapid rates of proton transfer.

Meanwhile Bernal and Fowler (8) first used Raman spectra of water and Hg fluorescence of sugar solutions to speculate the relative strength of sugar-water interactions, concluding that they were of the same order of magnitude as the water-water interaction. Hildebrand (27) successfully explained solvation using a lattice model of solution in which he considered the interaction of a molecule with its six nearest neighbors. Thus, it was recognized that solution structure is the result of different molecular interactions ie. solute-solvent, solvent-solvent, and solute-solute. Solution structure was hence no longer understood to be an exclusive property of aqueous solutions.

The structure of liquid water nevertheless continued to be a subject of interest because a correct determination of the structure in liquid water defines the nature of solvent-solvent interactions in aqueous solution. Frank and Wen (21) proposed a flickering cluster model for water which allows dynamic interchange of single water molecules between clusters of 2 to 7 water molecules. Nemethy and Scheraga (45) authored another theory which assumes formation of clusters of a similar size with the absence of dynamic interchange at the molecular level. Both these views are widely accepted today. Once the nature of the solvent- solvent interaction was widely accepted the attention focused on determining the nature of solvent-solute and solute-solute interactions. The nature of these interactions is particularly complex in concentrated solutions; therefore, most of the work reported involves techniques developed for the study of undersaturated solutions.

Recent experimental attempts to verify concepts of solution structure have involved the use of Raman, IR, and NMR spectroscopies. The possibility that molecular conformation in solution could affect solution structure was recognized as an important issue in the early 70's. Franks, Suggett and co-workers

(2

so

P

al

to

m

re

st

pr

nc

w

mx

int

inc

pre

co

co

is

su

Al

inc

rela

supe

liqui

(22,23,24,25,53,54,55,56) used dielectric relaxation and NMR to determine solvation properties of sugars. Franks et al. confirmed the earlier results of Jones and Phillips for dilute solutions and also confirmed that the sugar water interaction was about as strong as the water-water interaction. Harvey and Symons (26) used NMR to determine 11 water molecules of solvation per molecule of sucrose, interpreted as 6 molecules of water strongly associated with the molecule of sucrose and the remaining molecules more dynamically associated. Birch et al. (9), in the only NMR study of concentrated sucrose solutions, determined that there are four kinds of protons in solution: bulk water, solvated water, exchangeable sugar hydroxyl, and non-exchangeable ring (C-H) protons, using pulsed NMR.

Franks, Suggett and co-workers (22-25,53-56) as well as Barone and co-workers (4-6) (who used numerical simulations based on Kozak et al.'s (33) modification of McMillan Meyer (39) theory) initially hypothesized that solute-solute interactions in dilute solutions were unlikely. More recent work by Barone et al. (3) indicates that the nature of interactions in solution may be more complex than previously accepted without offering insight into the exact nature of the complexity.

Mathlouthi et al. (38) attempted to use vibrational spectroscopy of concentrated solutions to correlate the change in solution structure to change in concentration. It was demonstrated that vibrational spectroscopy (ie. Raman and IR) is effective in solutions of low solute concentrations. Back et al. (1) used FTIR to successfully study the mutarotation behavior of glucose in dilute aqueous solutions. Although vibrational spectroscopy yields significant information about solute solvent interactions, in practice this information is very difficult to extract.

Larson (34) explicitly stated the need to understand and characterize the relationship between the properties of supersaturated solutions (degree of supersaturation) and concentrated solution structure. Work on cluster diffusion in liquids (Cussler, 18) was cited as evidence that properties of non-ideal solutions

could deviate greatly from those of ideal and dilute solutions. Subsequently Myerson and co-workers (14-16,42,43) performed diffusion studies in concentrated aqueous solutions of both non-electrolytes (urea, glycine, and glycine-valine) and electrolytes (sodium chloride and potassium chloride) that indicated formation of solute-solvent aggregates of an unknown composition as evidenced by precipitous drops in diffusion coefficients. Cerreta and Berglund (12,13) used Raman spectroscopy of ammonium dihydrogen phosphate (ADP) to show that while no great differences could be observed in the spectra of very concentrated, saturated and supersaturated solutions, evidence did exist for dimer formation. Larson and Garside (35) cited Cerreta and Berglund (13) as well as the Raman studies of Hussman et al. (28) and MacMahon et al. (37) with alkali nitrates as evidence of pre-crystalline clusters in concentrated solutions. Larson and Garside (35,36) performed an experiment with isothermal columns of concentrated, saturated, and supersaturated solutions of citric acid, urea, sodium nitrate, and potassium sulfate during which they observed concentration gradients along the length of the column for only the supersaturated solutions. Larson and Garside concluded that there must be solute structuring in supersaturated solutions. In other work, Narayanan and Youngquist (44) attempted to relate the onset of saturation with a marked change in measurable physical properties of bulk solution in solutions of sodium nitrate, potassium nitrate, magnesium sulfate, potassium ammonium sulfate, and ADP. No unusual changes in density, viscosity, or electrical conductivity with saturation and subsequent supersaturation were observed.

In each of the previous studies (with the exception of the NMR study of concentrated solutions) the approach has been to relate the behavior of the solute or the state of the solute to a marked change in an observable bulk solution property at or near saturation, then to correlate the changes in this property to degree of supersaturation. The results of these experiments have been less than definitive;

therefore, we elected to develop a complementary approach which probes the solvent rather than the solute.

3.2 Photochemical Techniques using Trace Fluorescent Probes

The unimolecular photochemical reaction of electronically excited molecules in homogeneous media can be used to study relaxation processes on a variety of time scales. Fluorescence is the consequence of fast radiative transition to the ground state in a molecule that has been excited by radiation to an allowed electronic state of higher energy. Fluorescence techniques have high quantum efficiencies (0.7-0.9) but are restricted in application to fast kinetic processes.

It is important to distinguish between the photochemical investigation of a fluorescent compound and the experiment utilizing a trace fluorescent probe. The experiment involving a trace fluorescent probe differs from the photochemical investigation of a fluorescent compound in several important respects. The former makes use of a compound for which the photochemical behavior is well known; the photochemistry of the compound is the subject of the latter. Probe experiments require very low molarities of the fluorescent compound; photochemical investigations require high molarities. Changes in the emission of the molecule can be correlated to corresponding changes in solvent properties in experiments using fluorescent probes. In a photochemical investigation changes in emission of the fluorescing species give information about its electronic state.

Often photochemical investigations are experimentally difficult because the high molarity of the fluorescent species gives rise to a host of associated phenomena which may also affect its excited state behavior. Fluorescent probes on the other hand are usually present in sufficiently low molarities to preclude any effect other than that due to the solvent environment of the probe (all other experimental conditions being

constant). In a homogeneous solvent or neat solution there is little possibility of non-uniform probe distribution. Additionally, judicious choice of a probe that has an affinity for a certain type of site on a molecule causes the nature of the microenvironment of the probe to be reflected in its emission properties. Often the sensitivity of a probe to solvent environment is enhanced in its excited state. Fluorescent compounds at very low molarities are thereby sensitive molecular probes of their solvent environment. Where the number of molecules that interact with the probe (hosts) is finite, a statistical analysis of the hosts is a useful approach to distinguish between various possible structural models. Information about the change in emission properties of the fluorescent probe can therefore be correlated with corresponding changes in solution properties to provide information about structure in solution provided the number of hosts is finite.

For this study, we required a probe that is known to have a highly sensitive, polarity dependent equilibrium between two excited states (both of which fluoresce) with the same chromophore differing only slightly in structure. We chose pyranine or 8-hydroxy-1,3,6-pyrenetrisulfonate, Fig. 3.1. Its photochemistry has been well characterized (Kondo et al., 32).

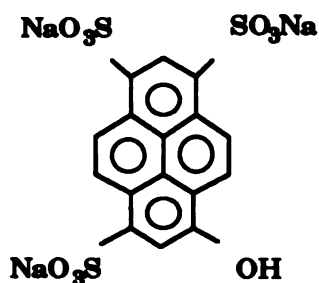


Figure 3.1. Chemical structure of pyranine or 8-hydroxy-1, 3, 6-pyrenetrisulfonate.

In solution pyranine exists with the sulfonate groups entirely dissociated. It has two excited fluorescent states: one where the hydroxyl proton is associated with the molecule which emits at about 440 nm and the other where the hydroxyl proton is dissociated from the molecule which emits at 511 nm, Fig. 3.2. Thus, the two excited states differ only in the hydroxyl proton. The pyrene ring acts as the chromophore in both cases. Pyranine in its excited state is sensitive to the presence or absence of exchangeable protons in the vicinity of the hydroxyl proton (i.e. polarity or pKa). Incident exciting radiation causes a $\pi-\pi^*$ singlet state transition in the probe molecule. This energy is then released mostly through a fast kinetic radiative path on the order of a 100 picoseconds with a quantum efficiency of nearly 80%.

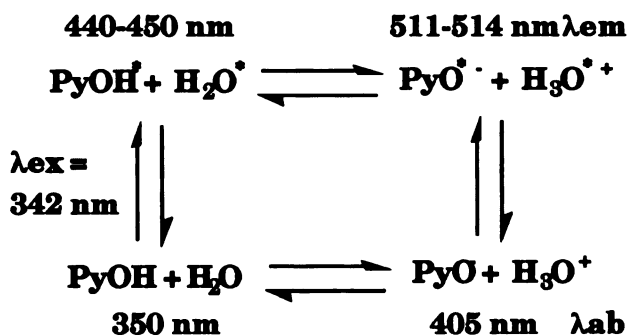


Figure 3.2. Emission equilibrium of pyranine. The equilibrium between the protonated form (absorbs at 350 nm and emits at 440 nm when excited at 342 nm) and the deprotonated form (absorbs at 405 nm and emits at 511 nm when excited at 342 nm) is determined by ability of the microenvironment of the hydroxyl group to participate in proton transfer.

The deprotonated state requires less energy of excitation and thus emits to the red of the protonated state. Whether the observed emission is from the excited deprotonated

or protonated form is determined by the molecular environment in its immediate vicinity. We can correlate changes in the fluorescence equilibrium between the two emitting forms of the probe to changes in the nature of the microenvironment of the hydroxyl moiety of the probe. Once we establish the nature of the microenvironment in terms of the species in solution we can then relate changes in the fluorescence equilibrium to changes in solution structure.

Pyranine has been used to probe water content of micellar dispersions (Clement and Gould, (17); Kano and Fendler, (30); Kondo et al., (32); Bardez et al., (2); and, Pines and Huppert, (47)), sols (Kaufman et al., (31)) and sol-gels (Pouxviel et.al., (50)) among other systems. It has been used to relate water content of these systems to the structure of various phases. It is photochemically active at concentrations of 1 ppm (1.9×10^{-6} M) or less. In addition, it is non-toxic, non-carcinogenic, and suitable for use in food grade applications (licensed for use as a food color additive, USDA regulations 1988).

The approach in this study is unique in two respects. First of all we decided to use a solvent sensitive technique to study concentrated and supersaturated solutions. We used pyranine as a trace fluorescent probe (very sensitive to solvent environment) and related changes in its state to changes in solvent environment. Secondly, we related changes in the state of the solvent to changes in solution structure. Our choice of bulk solution properties also differs from those chosen previously, by correlating changes in solvated and non-solvated (bulk) water with solute concentration, and in particular the degree of supersaturation (DS).

3.3 Materials and Methods:

Emission spectra were obtained with either a 200 W Xe/Hg or a 150 W Xe source in quartz cuvettes using an in-house constructed spectrometer described in detail elsewhere (Mussel and Nocera, (41)). The lamps were operated at 80% rated power. A Hamamatsu R1104 photomultiplier tube (maintained typically at 50% maximum voltage) was used in conjunction with a preamplifier (maintained at a sensitivity of 10^{-6}) and a Princeton Electronics lock-in amplifier (maintained at a sensitivity of 3V). The photomultiplier tube was maintained at -60 degrees C to improve the signal to noise ratio. A 375 nm KV or a 370 nm GG cutoff filter was used to filter out source excitation at 342 nm. A 3 mm slit width was used and shutters were kept fully open.

Reagent grade sucrose from Sigma Chemicals, 8-hydroxy 1,3,6, pyrenetrisulfonate (pyranine) from Eastman Kodak, and 18 Mohm reverse osmosis water were used. Stock solutions of 100 ppm (1.9×10^{-4} M) pyranine were prepared using 18 Mohm reverse osmosis water. Solutions of the 10 ppm (1.9×10^{-5} M) and 1 ppm (1.9×10^{-6} M) were prepared by dilution. The amount of sugar and water required for 10 grams (.01 kg) of each solution was calculated beforehand. Reagent grade sucrose samples were carefully measured out to +/- 1% of the required amount. Samples were prepared in 20 ml glass vials by adding the predetermined amount of stock solution to achieve the desired concentration. Samples varied in concentration between pure water and 80 wt.% sucrose. In undersaturated solutions samples were prepared in 10 wt.% intervals. Samples near saturation were taken at 2 wt.% intervals between 60 and 70 wt.%, and 76 wt.% and 80 wt.% solutions were also prepared. Supersaturated solutions were prepared by heating the vials in a water bath until the sugar dissolved. Spectra of the solutions were taken within 6 to 24 hours of

preparation to ensure equilibration of the sugar in solution and prevent biological contamination of the sugar solutions.

Pyranine doped sugar solutions - with pyranine concentrations of 1 ppm (1.9×10^{-6} M), 10 ppm (1.9×10^{-5} M), and 100 ppm (1.9×10^{-4} M)- showed little variation in peak intensity ratio (PIR). The PIR is defined as the ratio of the peak intensity at 440 nm to that at 511 nm. This is the same as the F ratio described in Pouxviel et.al. (50). It was decided to work at 100 ppm (1.9×10^{-4} M) levels of pyranine to maximize the signal to noise ratio. Small changes in instrument settings did not affect the values obtained for the PIR.

There was less than 3% variation in PIR of pyranine in undersaturated sucrose solutions over a 30 degree temperature span from 20 to 50 degrees C . This indicates that the equilibrium constant between the two excited states is not a strong function of temperature in this range of operation. Therefore temperature corrections were not applied.

Small variations in excitation wavelength (± 5 nm) did not change the PIR (less than 3%); however, large changes in the excitation wavelength (335-365 nm) indicated that the PIR were up to 5% less at longer wavelengths than at shorter ones. For a solution of given sucrose concentration doped with a fixed amount of pyranine the change in intensity of the peak at 511 nm with increase in wavelength is greater than that associated with the peak at 440 nm. This accounts for the difference in PIR due to large changes in excitation wavelength. In order to get consistent results an excitation wavelength of 342 nm was used for all experiments.

Emission spectra were obtained for each of the sample solutions prepared. The PMT response was about the same at 440 nm and 511 nm so the spectra were not corrected for PMT response.

3.4 Results and Analysis

The emission spectra for pyranine doped sucrose solutions of 0, 20,40,60, and 70 wt. % are shown in Fig. 3.3. It is evident that the intensity of both the blue (440 nm) and the green (511 nm) peaks change with the amount of sugar and water present in solution. The ratio of the peak intensity at 440 nm to that at 511 nm was defined previously as the peak intensity ratio (PIR).The PIR increases as the concentration of sugar increases and the concentration of water decreases. A clear isosbestic point is observed at 485 nm which also indicates the presence of two emitting species in equilibrium.

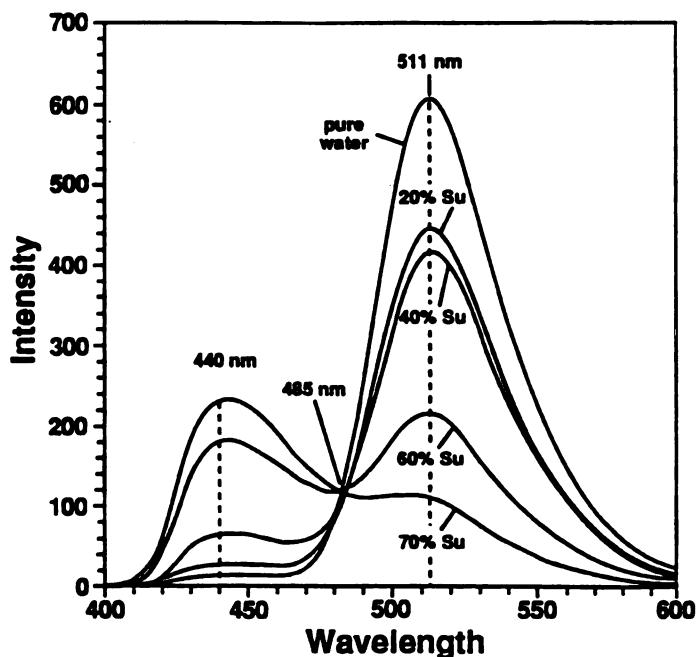


Figure 3.3. The emission spectra of pure water and sugar solutions of 20, 40, 60, and 70 wt. % sucrose doped with 100 ppm (1.9×10^{-4} M) pyranine at 20 degrees C. Emission maxima occur at 440 nm. and 511 nm. An isosbestic point is observed, represented by the pointer at 485 nm.

There are two possible emitting forms of pyranine. The form that contains the hydroxyl proton can exist only in an environment that does not facilitate the transfer of protons. The other form exists where it can transfer protons. The fact that emission from both forms is observed in solution leads us to conclude that microenvironments suitable to each species must co-exist in solution. This argument is along the same lines as that put forward by Zinsli (57) which led to a biphasic model for micelles.

In the current context microenvironments refer to the presence or absence of exchangeable protons in the immediate proximity of the pyranine hydroxyl proton. Emission observed at 440 nm indicates that there are protonated pyranine molecules in solution. These can exist because there are no protons available for exchange in the immediate vicinity of the pyranine hydroxyl proton. Similarly, emission observed at 511 nm indicates that there are deprotonated pyranine molecules in solution. So the PIR, according to this model, is a measure of the number of pyranine molecules in the protonated state versus the number in the deprotonated state. It is reasonable to assume that the accessibility of a molecule of pyranine to either environment is the same, because pyranine is present in very low molarity (of the order 10^{-7} or less) in solution. We now focus on what species or combination of species in solution could give rise to the observed behavior of the PIR.

Birch et.al. (9) observed three kinds of exchangeable protons in solutions of sucrose: bulk water, solvation water, and sucrose hydroxyl. Of these, the exchange rate of the sugar hydroxyls is somewhat slower than that of the solvation water. For reasons of mobility, it is unlikely that the sucrose molecules would be able to compete with water molecules in interacting with pyranine molecules to a significant extent. This leads us to propose that the pyranine is likely to interact only with water molecules.

A water molecule in contact with other water molecules that behave like pure water could provide an environment that is capable of proton exchange. If the

pyranine hydroxyl is in the proximity of such a water molecule it would emit at 511 nm. Thus, we propose that one of the two microenvironments is likely to be a bulk-water-like microphase. A pyranine hydroxyl group existing near solvation water already associated with a molecule of sucrose could not exchange protons and would emit at 440 nm. Thus the other likely microenvironment could be due to the presence of an envelope of solvation.

A graph of the PIR versus concentration of sucrose (wt.%) is shown in Fig. 3.4. Since pyranine has only one proton available for exchange, it is reasonable to conclude that only one molecule of water at a time can participate in the exchange process. It follows that the PIR (a ratio of pyranine molecules incapable of exchanging protons to that of pyranine molecules capable of exchanging protons) is also the ratio of water molecules that do not participate in proton exchange with the pyranine to those that do. In addition we can scale this per molecule of sucrose. This is purely for our convenience, because it then becomes possible to look at the solution in terms of water of solvation per molecule of sucrose (unavailable for proton exchange) and bulk water (available for proton exchange). These are terms that can be compared with existing data, at least for undersaturated solutions.

Assuming that the quantum yield of the two emitting species is the same (same chromophore), we can plot a graph of the number of molecules of water in each of these microenvironments per molecule of sucrose. We calculate 6 molecules of solvation water per molecule of sucrose in undersaturated solutions, dropping (insignificantly perhaps) to 5.8 molecules at the saturation point, 5.5 at 70 wt.%, 5.2 at 76 wt.%, and 4.0 at 80 wt%; see Tables 3.1 and 3.2. It would seem reasonable that solvation water per molecule would be a function of the molecular structure, more specifically the number of sites (and conformation of these sites) on the molecule that could hydrogen bond with nearby water. Perhaps more significantly the number of molecules of water in the bulk water like environment drops from 165 for

a 10% sucrose solution to about 3 for a highly supersaturated solution of 70% sucrose. It drops further to a value slightly less than 1.0 (0.83) for the 76% solution and stays about constant for the 80% solution.

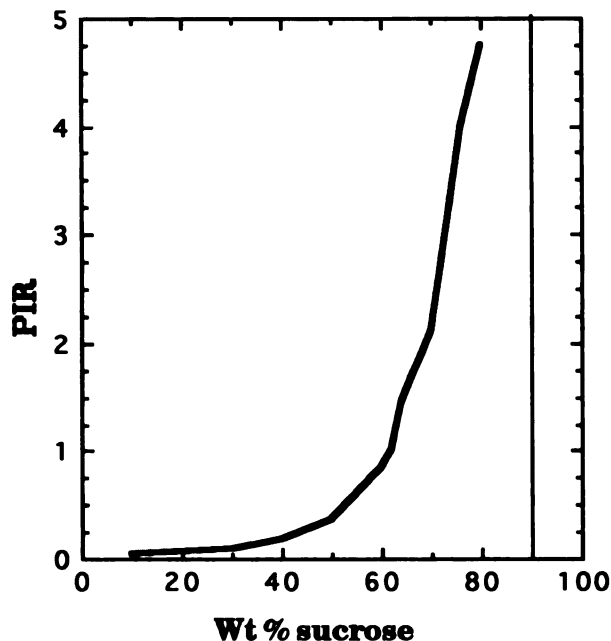


Figure 3.4. Graph of PIR (peak intensity ratio) vs. wt% sucrose in solution at 20 degrees C using 100 ppm (1.9×10^{-4} M) pyranine. The PIR is defined as the ratio of peak intensities at 440 nm and 511 nm. The arrow represents concentration at saturation.

Although the determination of water of solvation is in agreement with the results of Jones (29), Phillips (49), and Franks, Suggett and co-workers (22-25, 53-56), we were not entirely comfortable with the assumption of equal quantum yields for the two emitting species. In an attempt to isolate the two species and estimate relative quantum yield, spectra of equal amounts of carefully measured pyranine were obtained in methanol and water (under the same conditions as the rest of the experiments). The only peak observed in methanol was that at 430 nm. In water, a

weak shoulder was observed at 440 nm, but the emission was primarily due to the peak at 511 nm. The peak in methanol was approximately 1.8 times as intense as the peak in water for any given concentration of pyranine (between 1-80 ppm (1.9×10^{-8} and 1.6×10^{-5} M)). This would indicate 11 molecules of solvation water per molecule of sucrose, in agreement with the results of Harvey and Symons (26) and the earlier calculations of Stokes and Robinson (52). It would also indicate negative numbers for the bulk water like phase in the supersaturated region, which is unphysical. It is worth noting that the spectra in methanol were blue-shifted about 5-10 nm from those in water. This may be due to a difference in polarity of microenvironment or due to a green bleed through in the spectra in water. At this point we feel it is not appropriate to conclusively state that both emitting species have the same quantum efficiencies although there is some experimental evidence to support this and this is what our arguments would lead us to believe.

In either case (6 or 11 molecules of solvation water per molecule of sucrose) the surprising observation was that there should be any bulk phase water at all in saturated and supersaturated solutions. The number of water molecules in the bulk phase per molecule of sucrose decays exponentially with increase of sucrose concentration. Near saturation the number of water molecules per molecule of sugar in the bulk phase is roughly equal to the the number of molecules of water of solvation. For a highly supersaturated solution of 70% sucrose there are roughly three molecules of bulk phase water and six molecules of solvation water per molecule of sugar. It is probably the water in the bulk phase that is responsible for structurally "stable" supersaturated solutions. The ease with which sucrose can be dissolved in solution appears to be directly related to the amount of bulk phase water.

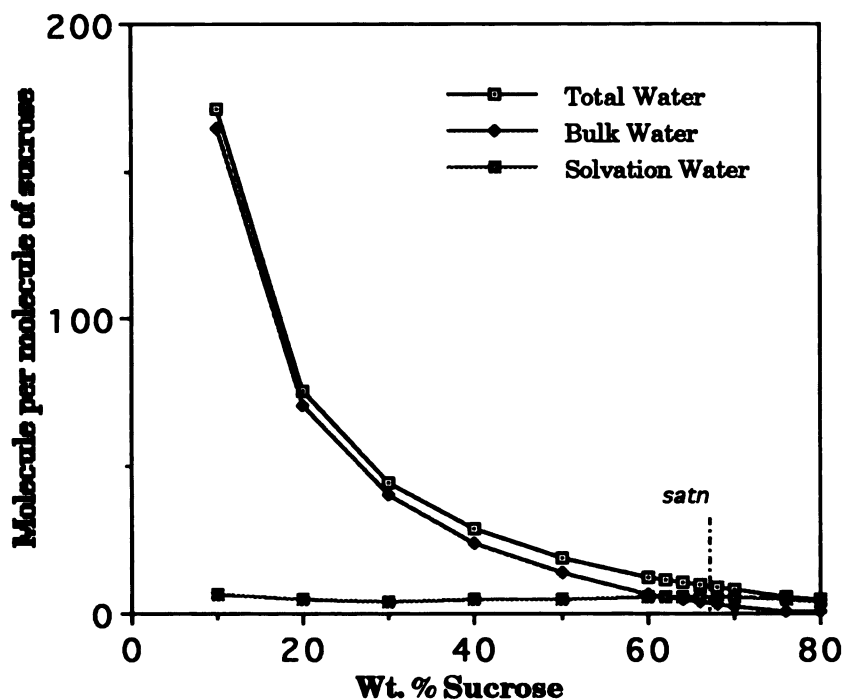


Figure 3.5. Total, bulk and solvation water (number of molecules of water per molecule of sucrose) vs. wt% sucrose in aqueous solution with 100 ppm (1.9×10^{-4} M) pyranine at 20 degrees C. The values on the graph are obtained from the analysis presented in Tables 1 and 2. The vertical line represents saturation.

An interesting feature of this analysis is that the water of solvation per molecule of sucrose becomes approximately equal to the bulk water per molecule of sucrose at saturation. In supersaturated solutions there is always less bulk water available per molecule of sucrose than solvation water. While this feature is apparent from Fig. 3.5, it becomes more so in Fig. 3.6. The crossing point of the two curves indicates equilibrium. At this point it becomes energetically unfavorable to add more solute to the solution without supplying external energy.

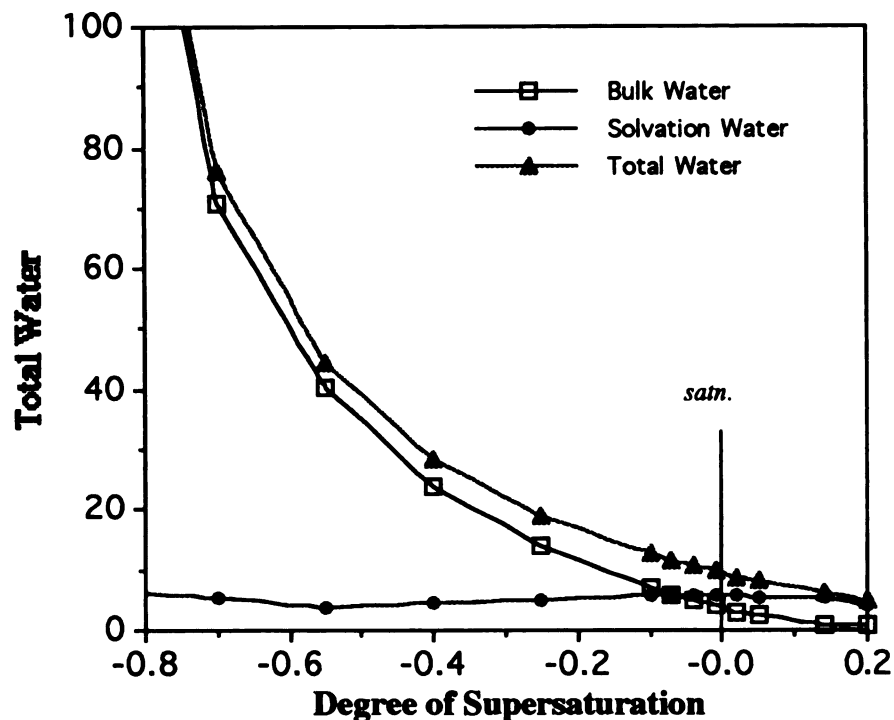


Figure 3.6. Graph of total water, bulk water and solvation water per molecule of sucrose in aqueous solutions doped with 100 ppm (1.9×10^{-4} M) pyranine at 20 degrees C versus the degree of supersaturation, DS. The DS is given by the difference between the solution concentration and the saturation concentration at 20 degrees C divided by the saturation concentration at 20 degrees C.

3.5 Conclusions

It appears that the PIR obtained from fluorescence spectra of aqueous sucrose solutions doped with trace amounts of pyranine show a marked change at saturation and are very sensitive to water content of supersaturated solutions. This is a sensitive technique for measuring degree of supersaturation.

Structurally, the solvent appears to distribute itself in two kinds of microenvironments. One is associated with the solvation envelope of the solute molecule, designated solvation water, and the other is non-solvated solvent,

designated bulk phase water. Both microenvironments exist in solutions of all concentrations examined. The amounts and ratio of water in each phase change with concentration of sucrose in solution. The water of solvation per molecule of sucrose seems to be a constant. The amount of water present in the bulk phase decreases exponentially with increase in sucrose concentration and correlates with the ease of solvation of sucrose. At the saturation point, the amount of water in the bulk phase per molecule of sucrose is roughly the same as the number of water molecules of solvation per molecule of sucrose.

3.6 Acknowledgements

The authors wish to thank Dr. D.G. Nocera, of the Department of Chemistry, Michigan State University for kindly permitting the use of the emission spectrometer in his laboratory. Financial assistance from the Department of Chemical Engineering and the Crop Bioprocessing Center/ Research Excellence Fund at Michigan State University is greatly appreciated.

3.7 Literature Cited

1. Back, D.M., D.F. Michalska and P.L. Polavarapu, *Applied Spectroscopy*, **38**, 2, 173 (1984).
2. Bardez, E., B.T. Gouguillon, E. Keh and B. Valeur, *J. Phys. Chem.*, **88**, 1909, (1984).
3. Barone, G., G. Castronuovo, P. Del Vecchio and V. Elia, *J. Solution Chem.*, **19**, 1, 41 (1990).
4. Barone, G., G. Castronuovo, P. Del Vecchio, V. Elia and M.T. Tosto, *J. Solution Chem.*, **17**, 10, 925 (1988).
5. Barone, G., G. Castronuovo, V. Elia and M.T. Tosta, *J. Solution Chem.*, **15**, 2, 199 (1986).
6. Barone, G., G. Castronuovo, V. Elia and V. Savino, *J. Solution Chem.*, **13**, 3, 209 (1984).
7. Ben-Naim, A. , Solvation Thermodynamics, Plenum Press, New York (1987).
8. Bernal, J.D. and R.H. Fowler, *J. Chem. Phys.*, **1**, 515 (1933).
9. Birch, G.G., J. Grigor and W. Derbyshire, *J. Solution Chem.*, **18**, 8, 795 (1989).
10. Bousfield, W.R. and T.M. Lowry, *Trans. Faraday Soc.*, **6**, 85 (1910).
11. Cerreta, M.K., Ph.D thesis, Michigan State University (1988).
12. Cerreta, M.K. and K.A. Berglund, *Journal of Crystal Growth* , **84**, 577 (1987).
13. Cerreta, M.K. and K.A. Berglund, in Industrial Crystallization '84, S.J.Jancic and E.J. DeJong, (Eds.), Elsevier, Amsterdam, 21 (1984).
14. Chang, Y.C. and A.S. Myerson, *AIChE J.*, **31**, 980 (1985).
15. Chang, Y.C. and A.S. Myerson, *AIChE J.*, **32**, 1567 (1986).

16. Chang, Y.C. and A.S. Myerson, *AIChE J.*, **32**, 1747,(1986).
17. Clement, N.R. and M. Gould, *Biochemistry*, **20**, 1534 (1981).
18. Cussler, E.L., *AIChE Journal*, **26**, 1, 43-51 (1980).
19. Eley, D.D., *Trans. Faraday Soc.*, **35**,1281 (1939).
20. Frank, H.S. and M.W. Evans, *J. Chem. Phys.*, **13**,11, 507 (1945).
21. Frank, H.S. and W.Y. Wen, *Disc. Faraday Soc.*, **24**, 1333 (1957).
22. Franks, F. in Hydrogen Bonded Solvent Systems, A.K. Covington and P.Jones (Eds), Taylor and Francis Ltd., London, 31-47 (1968).
23. Franks, F., J.R. Ravenhill and D.S. Reid *J. Solution Chem.*,**1**,1, 3 (1972).
24. Franks, F., M. Pedley and D.S. Reid, *J. Chem. Soc. Faraday Trans. I*, **72**, 359 (1976).
25. Franks, F., *Pure and Appl. Chem.*, **59**, 9,1189 (1987).
26. Harvey, J.M. and M.C.R. Symons, *J. Solution Chem.*, **7**(8), 571 (1978).
27. Hildebrand, J.H., in Solubility, Wiley and Sons, N.Y., 2nd. ed.
28. Hussman, G.A., M.A. Larson and K.A. Berglund, in Industrial Crystallization '84, S.J. Jancic and E.J. DeJong (Eds.), Elsevier, Amsterdam, 21 (1984).
29. Jones, H.C., *Amer. Chem. Journal*, **32**,319 (1904).
30. Kano, K. and J.H. Fendler, *Biochim. Biophys. Acta*, **509**, 289 (1978)
31. Kaufman, V.R., D. Avnir, E. Pines-Rojanski and D. Huppert, *J. Non-Crystalline Solids*, **99**, 397 (1988).
32. Kondo, H., I. Miwa and J. Sunamoto, *J. Phys. Chem.*, **86**, 4826 (1982).
33. Kozak, J.J., W.S. Knight and W. Kauzmann *J. Chem. Phys.*, **48**, 2, 675 (1968).
34. Larson, M.A., *AIChE Symposium Series no.240*, **80**, 39-44 (1984).
35. Larson, M.A. and J. Garside, *Chem. Eng. Science*, **41**, 1285 (1986).
36. Larson, M.A. and J. Garside, *J. Crystal Growth*, **76**, 88 (1986).
37. MacMahon, P.M., K.A. Berglund and M.A. Larson in Industrial Crystallization '84, S.J. Jancic and E.J. DeJong (Eds.), Elsevier, Amsterdam, 229 (1984).
38. Mathlouthi, M., C. Luu, M. Meffrov-Biget and D.V. Luu, *Carbohydrate Res.*, **81**, 213 (1980).
39. McMillan, W.G. and J.E. Mayer, *J. Chem. Phys.*, **13**(7), 276 (1945).
40. Mullin, J.W. and C. Leci, *Philos. Mag.*, **19**, 1075 (1969).
41. Mussel, R.D. and D.G. Nocera, *J. Am. Chem. Soc.*, **110**, 2764 (1988).
42. Myerson, A.S. and L.S. Sorrel, *AIChE Journal*, **28**,778 (1982).
43. Myerson, A.S. and Y.C. Chang, in Industrial Crystallization '84, S.J. Jancic and E.J. DeJong (Eds.), Elsevier, Amsterdam, 27 (1984).
44. Narayanan, H. and G.R. Youngquist, *AIChE Symposium Series no. 253*, **83**,1-7 (1987).
45. Nemethy, G. and H.A. Scheraga, *J. Chem. Phys.*, **36**, 3401 (1962).
46. Ostwald, W., *Z. Phys. Chem.*, **22**, 289-330 (1897).
47. Pines, E. and D. Huppert, *J. Phys. Chem.*, **87**, 4471 (1984).
48. Pauling, L. and O. Brockway, *Proc. Natl. Acad. Sci.*, **20**, 336 (1934).
49. Phillips, J.C., *Trans. Faraday Soc.*, **3**, 136 (1907).
50. Pouxviel, J.C., B. Dunn and J.I. Zink, *J. Phys. Chem.*, **93**, 2134 (1989).
51. Sorrel, L.S. and A.S. Myerson, *AIChE J.*, **28**, 772 (1982).
52. Stokes, R.H. and R.A. Robinson, *J. Phys. Chem.*, **76**, 2126 (1966).
53. Suggett, A. and A.H. Clark, *J. Solution Chem.*, **5**, 1, 1 (1976)
54. Suggett, A., S. Ablett and P.J. Lillford, *J. Solution Chem.*, **5**(1), 17 (1976).
55. Suggett, A., *J. Solution Chem.*, **5**, 1,33 (1976).
56. Tait, M.J., A.Suggett, F. Franks, S. Ablett and P.A. Quickenden *J. Solution Chem.*, **1**, 2, 131 (1972).
57. Zinsli, P.E., *J. Phys. Chem.*, **83**, 3223 (1979).

Table 3.1. Molar ratio of total water to sucrose at various concentrations.

Sucrose gm. (10^{-3} kg)	Water gm. (10^{-3} kg)	Sucrose moles N_{su}	Water moles N_{wat}	$N_w =$ N_{wat}/N_{su}
10	90	0.029	5.00	171.0
20	80	0.059	4.44	76.0
30	70	0.088	3.89	44.3
40	60	0.117	3.33	28.5
50	50	0.146	2.78	19.0
60	40	0.175	2.22	12.6
62	38	0.181	2.11	11.6
64	36	0.187	2.00	10.7
66	34	0.193	1.89	9.8
68	32	0.199	1.78	8.9
70	30	0.205	1.67	8.1
76	24	0.222	1.33	6.0
80	20	0.234	1.11	4.87

Table 3.2. Material Balances. Basis: 1 molecule sucrose. The entries in the second column are the same as those in the last column of Table 1. The entries in the third column are the PIR's (defined as the ratio of peak intensities at 440 nm and 511 nm) obtained experimentally. The PIR in each case is set, for the purposes of analysis, to the ratio of solvated water to bulk water. This is based on assignment of the peak at 440 nm to the microenvironment associated with solvated water and that at 511 nm to the bulk water. Total molecules of water are set equal to the sum of the water molecules in each microenvironment, thus yielding the values in the last two columns.

Wt. % Sucrose	Total molecules of water	Solvation water/ Bulk water	Bulk water	Solvation water
10	171.0	0.040	164.5	6.5
20	76.0	0.076	70.7	5.3
30	44.3	0.094	40.5	3.8
40	28.5	0.192	23.9	4.6
50	19.0	0.358	14.0	5.0
60	12.6	0.849	6.8	5.8
62	11.6	1.011	5.8	5.8
64	10.7	1.450	4.9	5.8
66	9.8	1.470	4.0	5.8
68	8.9	1.875	3.1	5.8
70	8.1	2.120	2.6	5.5
76	6.0	4.000	0.83	5.2
80	4.87	4.740	0.82	4.0

Chapter Four

Steady State Fluorescence Spectroscopy of Pyranine as a Trace Extrinsic Probe to Study Structure in Aqueous Sugar Solutions

4.1 Background

The structure of supersaturated solutions and its relationship with crystal nucleation and growth is an area of significant current activity. Myerson and co-workers^{19-21, 65, 66, 76} performed diffusion studies in concentrated aqueous solutions of both non-electrolytes (urea, glycine, and glycine-valine) and electrolytes (sodium chloride and potassium chloride) that indicated formation of aggregates of an unknown composition as evidenced by precipitous drops in diffusion coefficients. Tamman⁸³ and later Mullin and Leci⁶² demonstrated that certain substances, for instance citric acid in aqueous solutions, formed glass-like amorphous substances at high supersaturations which did not nucleate. Mullin and Leci concluded that the ability or inability of a solution to nucleate must somehow depend upon which molecules are contained in a supersaturated solution and how they are spatially distributed, which in turn depends upon the various molecular interactions. They reasoned that the molecular structure of citric acid favors intermolecular hydrogen bonding and association. Chains or clusters of solute molecules in supersaturated (and even concentrated but undersaturated) solutions were proposed as precursors to nuclei. Subsequently, Mullin and Leci⁶⁰ studied the desupersaturation of citric acid solutions, and applied the cluster hypothesis to explain how and why nucleation did or did not occur from supersaturated solutions.

In the study of contact nucleation of saccharides, Elankovan and Berglund^{27,28} and later Cerreta and Berglund¹⁵ showed that under certain conditions the contact of a parent crystal of a particular form and composition yielded some nuclei of a structure and composition different from that of the parent crystal, in addition to nuclei that were of the

same structure and composition of the parent crystal. They also observed that under certain conditions it is possible to grow crystals of one form on parent crystals of another form. Cerreta¹⁷ concluded that neither the attrition nor the cluster theory of origin of secondary nuclei provided satisfactory answers as to the origin and mechanism of this phenomena, and that there was probably a third mechanism responsible. As a result of this work it becomes clear that theories which are solvent exclusive in their descriptions of growth and nucleation phenomena, such as the attrition and cluster theory, are unsatisfactory because they cannot explain epitaxy and polymorphism. There is a growing amount of experimental evidence relating to growth and nucleation phenomena which cannot be explained on the basis of solute behavior alone. This leads us to believe that we must attempt to explain these phenomena in terms of both solute and solvent behavior. Solvent behavior in crystallization phenomena is not well understood. In order that the role of the solvent in growth and nucleation be understood, the structure and properties of supersaturated solutions must be determined.

Several attempts have been made to observe changes in macroscopic solution properties and to correlate these to changes in solution structure. Larson and Garside^{51,52} performed an experiment with isothermal columns of concentrated, saturated, and supersaturated solutions of citric acid, urea, sodium nitrate, and potassium sulfate during which they observed concentration gradients along the length of the column only for supersaturated solutions. They concluded that there must be solute structuring in supersaturated solutions. Narayanan and Youngquist⁶⁷ attempted to relate the onset of saturation with a marked change in measurable physical properties of bulk solution in solutions of sodium nitrate, potassium nitrate, magnesium sulfate, potassium ammonium sulfate, and ADP. No unusual changes in density, viscosity, or electrical conductivity with saturation and subsequent supersaturation were observed. The results of the experiments of Larson and Garside^{51,52} indicate changes which can be observed on a macroscopic scale

with the onset of saturation; however, it is not possible to accurately correlate these observations to changes in bulk solution structure at a molecular level.

Recent experimental attempts to study interactions in concentrated aqueous sugar solutions have involved the use of Raman, IR, and NMR spectroscopies and X-ray diffraction. These experiments will be summarized in turn as sugars are the object of the present study.

4.2 NMR

Franks, Suggett and co-workers^{32-36,78-80,82} used dielectric relaxation and NMR to determine solvation properties of sugars. Franks et al. confirmed the earlier results of Jones⁴¹ and Phillips⁷¹ for dilute solutions (an average of 6 water molecules of solvation per molecule of sucrose) and also confirmed that the sugar water interaction was about as strong as the water-water interaction. Harvey and Symons³⁸ used NMR to determine 11 water molecules of solvation per molecule of sucrose, interpreted as 6 molecules of water strongly associated with the molecule of sucrose and the remaining molecules more dynamically associated. Using a pulsed NMR study of concentrated sucrose solutions, Birch et al.¹⁰ determined that there are four kinds of protons in solution: bulk water, solvated water, exchangeable sugar hydroxyl, and non-exchangeable ring (C-H) protons. Franks, Suggett and co-workers^{32-36,78-80,82} as well as Barone and co-workers⁵⁻⁷ (who used numerical simulations based on Kozak et al.'s⁵⁰ modification of McMillan Meyer⁵⁸ theory) initially hypothesized that solute-solute interactions in dilute solutions were unlikely. More recent work by Barone et al.⁴ indicates that the nature of interactions in solution may be more complex than previously accepted without offering insight into the exact nature of the complexity.

Richardson and Steinberg⁷⁴ used ^{17}O and ^2H high field NMR to investigate sucrose-water or D_2O water systems over a wide range of concentrations and states. The

^{17}O NMR transverse relaxation rate (R_2) in D_2O increased markedly with sucrose concentration in supersaturated solutions of up to 70 wt.% sucrose. An isotropic two-state model of water with fast exchange was used to interpret results. Deviations in linearity in the results were hypothesized to be due to formation of intermolecular hydrogen bonds between water and sucrose, hydrogen bond bridging between water and sucrose molecules and sucrose-sucrose hydrogen bonding. No discontinuity in R_2 was observed with the onset of saturation.

4.3 Raman Spectroscopy

X-ray diffraction, Raman spectroscopy and IR spectroscopy are sensitive to changes in vibrational frequencies and space lattice ordering that occur as the concentration of the solution increases. The effects of molecular association, and hydrogen bonding are observed in Raman and IR spectra. Mathlouthi et al.⁵⁶ performed vibrational spectroscopy of sugar solutions of various concentrations and observed that the characteristics of the spectra were concentration sensitive. Bands assigned to the asymmetric vibrations of the CH and OH groups are observed to shift in frequency. In an attempt to correlate the change in solution structure to change in concentration, the ratio of the integrated band intensity at 1460 cm^{-1} , assigned to the HCH bending mode, to that at 1640 cm^{-1} , assigned to the HOH bending mode was plotted as a function of concentration. As the concentration of sucrose in solution increased from 10 to 66 wt%, and that of glucose increased from 5 to 54 wt%, a 10 cm^{-1} shift (approximately 1%), from 1450 cm^{-1} to 1460 cm^{-1} , was observed in the band associated with the HCH bend. This indicates that the HCH bend can be accomplished with less energy in dilute solution than in-vacuo or in crystalline form, the two standards that are commonly used for calculation of band positions and contributions (Cael et. al.¹³, Szarek et. al.⁸²). As a result one is tempted to conclude that the particular vibrational mode is about as hindered in concentrated solution as it is in vacuo or in

crystalline state; however, all one can safely conclude is that the CH₂ moiety must be hydrogen bonded to the same extent in solution as it is in a crystal. It is not clear from this observation per-se that the CH₂ group is associated to another sugar molecule; it might be associated with water. For similar reasons it cannot be concluded that the shift in the HOH bend frequency is evidence of solvent exclusive solute clustering; it can be concluded that some of the water molecules behave in an ice-like manner (are tetrahedrally coordinated) and the bending motion is hindered in concentrated solutions. It cannot be said conclusively whether this hindering is due to association with the solvent or with the solute. In addition to this uncertainty of interpretation is the fact that Raman spectra are solute sensitive. As the concentration increases beyond saturation the changes in the spectra are less pronounced; Mathlouthi's observations do not extend into the supersaturated region.

4.4 X-ray Diffraction

Mathlouthi's X-ray diffraction studies⁵⁷ of sugar solutions indicate formation of intramolecular bonds with increase in solute concentration. He was able to convincingly demonstrate that some sucrose molecules might be associating with some other sucrose molecules, a result consistent with the observations of band shifting and intensification in IR and Raman spectra. He was, however, unable to provide any convincing data or argument that suggests that such clusters are larger than two solute molecules or that they were exclusive of associated solvent.

4.5 Diffusion and Viscosity Measurements

Myerson and co-workers^{19-21,65,66} performed diffusion studies in concentrated aqueous solutions of both non-electrolytes (urea, glycine, and glycine-valine) and electrolytes (sodium chloride and potassium chloride) that indicated formation of an unknown composition as evidenced by precipitous drops in diffusion coefficients. Larson

and Garside^{51,52} performed an experiment with isothermal columns of concentrated, saturated, and supersaturated solutions of citric acid, urea, sodium nitrate, and potassium sulfate during which they observed concentration gradients along the length of the column for only the supersaturated solutions. Larson and Garside concluded that there must be solute structuring in supersaturated solutions. By making the classical assumption that all solute in solution must be associated with other solute molecules because of an absence of solvent to satisfy the solvation requirements, the solvent exclusive clusters were proposed to be comprised of several thousand molecules each.

4.6 Correlation of Macroscopic and Microscopic transport properties

Myerson⁶⁴ in recent work has argued that if the constraint of solvent exclusion is relaxed, then the probable size of clusters would be two or three solvated molecules of solute. The studies of Myerson and coworkers^{19-21,65,66,76} are particularly interesting because they utilized measurements on the time scale of diffusion. Transport properties in solution are governed by non-equilibrium solvation dynamics. There is evidence to suggest that such phenomena are governed by short range interaction processes that take place on a variety of time and length scales all of which are less than those associated with molecular diffusion (Wolynes^{86,87}). Continuum models are still prevalent for such dynamics. Such models do justice to the long range interactions in solution, but fail to account for the details of structure and interaction of inner solvation shells which are often dominant factors (Wolynes^{86,87}).

In the particular case of supersaturated solutions, where the molar ratio of solvation water to bulk water per mole solute is such that there is only enough water available on the average for one solvation shell or incomplete solvation shells, one would expect interactions to be dominated by the non-equilibrium behavior. There are now several non-continuum heuristic approaches to understanding such phenomena. One such widely

discussed approach, the mean spherical approximation or MSA, indicates that solvation of an ion or molecule occurs on a range of time scales. A molecule can be thought to be made up of component dipoles. The limiting scale of each such component is that of the order of the hydrogen bond. The local solvent structure and dynamics near each such component has been observed to differ significantly: even the solvation of a simple alcohol must be described by at least two different time scales. One corresponds to the continuum longitudinal relaxation time, the other is associated with the time required by solvent molecules to rearrange themselves near the dipole. For small dipoles or ions this time is of the order of a picosecond (Wolynes⁸⁷). Furthermore, the molecular dynamics simulations of Cross and Simon²⁴, suggests that if a dipole is strong enough (>17 D) then the two ends may start behaving like point dipoles in the sense that the localized solvent structure and dynamics may be different at the two ends of the dipole. This is summarized by Maroncelli et. al.⁵⁵ who conclude that the solvation response in a polar solvent involves coupled reorientational dynamics that occur on time scales shorter than single particle diffusion. There have been studies in the solvation of an electron in water and alcohols, using picosecond and femtosecond time correlated spectroscopies, which indicate that solvent reorientational times are on the order of < 500 fs.

Interestingly, Myerson used continuum arguments to reach his conclusions. This would indicate that for the systems under consideration the macroscopic transport coefficients in supersaturated solution must be very similar to the microscopic transport coefficients in supersaturated solution.

With the exception of NMR the focus of previous work has been primarily on solute sensitive techniques. Steady state fluorescence spectroscopy using extrinsic trace fluorescent probes is an experimental technique that is solvent sensitive like NMR, rich in information content, experimentally simple, yet not currently utilized for studying structure in solutions. This approach has been exploited and developed to a great degree of sophistication for studying microheterogeneous systems; Kalyansundaram⁴² has presented

a comprehensive treatise on principles involved and techniques available. The development and analysis of a steady state fluorescence technique based on monitoring the solvent sensitive emission behavior of an extrinsic fluorescent probe is discussed in the current work.

4.7 Photochemical Techniques using Extrinsic Trace Fluorescent Probes

Fluorescence spectroscopy of extrinsic probe molecules in solution offers a complementary approach to measuring many variables of interest. Fluorescence is the consequence of fast radiative transition to the ground state in a molecule that has been excited by radiation to an allowed electronic state of higher energy. Fluorescence techniques have high quantum efficiencies (0.7-0.9), but are restricted in application to fast kinetic processes. The unimolecular photochemical reaction of electronically excited molecules in homogeneous media can be used to study relaxation processes on a variety of time scales. Simple steady state measurements of intensity and wavelength of the observed fluorescence are rich in information about to the immediate molecular environment of the probe molecule (or moiety). The nature of the probe environment, concentrations, distances, accessibility, possible complexing, electric field, polarity, lateral diffusion, functional correlations, reactivities and pH are all reflected in the emission behavior of the probe⁸⁴.

It is important to distinguish between the photochemical investigation of a fluorescent compound and the experiment utilizing an extrinsic trace fluorescent probe. The experiment involving a trace fluorescent probe differs from the photochemical investigation of a fluorescent compound in several crucial aspects. The former makes use of a compound for which the photochemical behavior is well known; the photochemistry of the compound is the subject of the latter. Probe experiments require very low molarities of the fluorescent

compound; photochemical investigations may require high molarities. In a photochemical investigation changes in emission of the fluorescing species gives information about its electronic state. Changes in the emission of the extrinsic probe molecule (or moiety) can be correlated to corresponding changes in solvent properties. Often photochemical investigations are experimentally difficult because the high molarity of the fluorescent species gives rise to a host of associated phenomena which may also affect its excited state behavior. Extrinsic fluorescent probes, on the other hand, can be designed or judiciously chosen to be present at molarities low enough to preclude any effect other than that due to the solvent environment of the probe (all other experimental conditions being constant).

The way the microenvironment of the probe responds to the perturbation can yield valuable information about its structure. A probe that is chosen because it exhibits an affinity for a certain type of site on a molecule, or a certain kind of interaction, will reflect the nature of its microenvironment in its emission properties. Often the sensitivity of a probe to solvent environment is enhanced in its excited state. Fluorescent compounds at very low molarities are thereby sensitive molecular probes of their solvent environment.

For this study, we chose a water soluble probe that is known to have a highly sensitive, polarity dependent equilibrium between two excited states that fluoresce. We chose pyranine (or 8-hydroxy-1,3,6-pyrenetrisulfonate), Figure 4.1. Its photochemistry has been well characterized (Kondo et al.⁴⁹). In solution pyranine exists with the sulfonate groups entirely dissociated. It has two excited fluorescent states: one in which the hydroxyl proton is associated with the molecule and one in which it is dissociated, Figure 4.2. The two excited states differ only in the hydroxyl proton. Emission is observed from the molecule in the former state at 440 nm and from that in the latter at 511 nm, when excited at 342 nm corresponding to an absorption isosbestic point. Pyranine in its excited state is sensitive to the concentration of molecular moieties which can participate in exchange processes in the vicinity of the hydroxyl proton (i.e. polarity or pKa). Incident exciting radiation causes a π - π^* singlet state transition in the probe molecule. This energy is then

released mostly through a fast kinetic radiative path on the order of a 100 picoseconds with a quantum efficiency of nearly 80%. The deprotonated state requires less energy of excitation and thus emission from the molecule in this state is observed to the red of that emitting from the protonated state. Whether the observed emission is from the excited deprotonated or protonated form is determined by the molecular environment in its immediate vicinity. We can correlate changes in the fluorescence equilibrium between the two emitting forms of the probe to changes in the nature of the microenvironment of the hydroxyl moiety of the probe. Once we establish the nature of the microenvironment in terms of the species in solution we can then relate changes in the fluorescence equilibrium to changes in solution structure.

Pyranine has been used to probe water content of micellar dispersions^{3, 23, 43, 49, 72}, sols⁴⁴ and sol-gels⁷³ among other systems. It has been used to relate water content of these systems to the structure of various phases. It is photochemically active, even at concentrations of 1 ppm (1.9×10^{-6} M) or less. In addition, at these concentrations it is non-toxic, non-carcinogenic, and suitable for use in food grade applications (approved for use as a food color additive, USDA regulations 1988).

4.8 Materials and Methods

Emission spectra were obtained with either a 200 W Xe/Hg or a 150 W Xe source in quartz cuvettes using an in-house constructed spectrometer described in detail elsewhere (Mussel and Nocera⁶³). The lamps were operated at 80% rated power. A Hamamatsu R1104 photomultiplier tube (maintained typically at 50% maximum voltage) was used in conjunction with a preamplifier (maintained at a sensitivity of 10^{-6}) and a Princeton Electronics lock-in amplifier (maintained at a sensitivity of 3V). The photomultiplier tube was maintained at -60 degrees C to provide a large signal to noise ratio. A 375 nm KV or a

370 nm GG cutoff filter was used to filter out source excitation at 342 nm. A 3 mm slit width was used and shutters were kept fully open.

Reagent grade sucrose, glucose, and lactose monohydrate from Sigma Chemicals, fructose from A.E. Staley, 8-hydroxy 1,3,6, pyrenetrisulfonate (pyranine) from Eastman Kodak, and 18 Mohm reverse osmosis water were used. Stock solutions of 100 ppm (1.9×10^{-4} M) pyranine were prepared using 18 Mohm reverse osmosis water. Solutions of the 10 ppm (1.9×10^{-5} M) pyranine and 1 ppm (1.9×10^{-6} M) pyranine were prepared by dilution.

The amount of sugar and water required for 10 grams (.01 kg) of each solution was calculated. Reagent grade sucrose samples were carefully measured out to $\pm 1\%$ of the required amount. Samples were prepared in 20 ml glass vials by adding the predetermined amount of stock pyranine solution to achieve the desired concentration. Samples varied in concentration between pure water and 80 wt.% sucrose. In undersaturated solutions samples were prepared in 10 wt.% intervals. Samples near saturation were taken at 2 wt.% intervals, eg. for sucrose between 60 and 74 wt.%, and solutions at high concentrations, eg. 76 wt.% and 80 wt.% solutions of sucrose, were also prepared. Supersaturated solutions were prepared by heating the vials in a water bath until the sugar dissolved. Spectra of the solutions were taken within 6 to 24 hours of preparation to ensure equilibration of the sucrose in solution [with respect to temperature] and prevent biological contamination of the sugar solutions. Solutions of fructose, glucose, and lactose were prepared in a similar manner: by weighing out predetermined amounts of sugar and stock solution, by agitating, and heating to dissolve all the sugar, and followed by cooling to 20 °C in order to obtain supersaturated solutions. Fructose samples were prepared at 10 wt.% intervals up to 70 wt.% and then at 2 wt.% intervals up to 84 wt.%. Glucose solutions were prepared at 5 wt.% intervals upto 40 wt.% and then at 2 wt.% intervals from 43 wt.% to 55 wt.%. Lactose mono hydrate solutions were prepared at 5 wt.% intervals to 45 wt.%.

Pyranine doped sugar solutions - with pyranine concentrations of 1 ppm (1.9×10^{-6} M), 10 ppm (1.9×10^{-5} M), and 100 ppm (1.9×10^{-4} M)- exhibited little variation in peak intensity ratio (PIR). The PIR is defined as the ratio of the peak intensity at 440 nm to that at 511 nm. This is the same as the F ratio described in Pouxviel et.al. (50). It was decided to work at 100 ppm (1.9×10^{-4} M) levels of pyranine to maximize the signal to noise ratio. Small changes in instrument settings did not affect the values obtained for the PIR.

There was less than 3% variation in the PIR of pyranine in undersaturated sucrose solutions over a 30 degree temperature span from 20 to 50 degrees C . This indicates that the equilibrium constant between the two excited states is not a strong function of temperature in this range of operation. Therefore temperature corrections were not applied.

Small variations in excitation wavelength (± 5 nm) did not change the PIR (less than 3%); however, large changes in the excitation wavelength (335-365 nm) indicated that the PIR were up to 5% less at longer wavelengths than at shorter ones. This behavior can be explained on the basis of the difference in the amount of light absorbed by the two states of pyranine. For a solution of given sucrose concentration doped with a fixed amount of pyranine the change in intensity of the peak at 511 nm with increase in wavelength is greater than that associated with the peak at 440 nm. This accounts for the difference in PIR due to large changes in excitation wavelength. In order to get consistent results an excitation wavelength of 342 nm was used for all experiments.

Emission spectra were obtained for each of the sample solutions prepared. The PMT response was about the same at 440 nm and 511 nm so the spectra were not corrected for PMT response.

4.9 Results and Analysis

The emission spectra for pyranine doped sucrose solutions of 0, 20,40,60, and 70 wt. % are shown in Figure 4.3. The intensity of both the blue (440 nm) and the green (511 nm) peaks change with the amount of sugar and water present in solution. The ratio of the peak intensity at 440 nm to that at 511 nm was defined previously as the peak intensity ratio (PIR). The PIR increases as the concentration of sucrose increases and the concentration of water decreases. A clear isosbestic point is observed at 485 nm which also indicates the presence of two emitting species in equilibrium.

There are two possible excited states from which pyranine molecules may emit. The form that contains the hydroxyl proton can exist only in an environment that does not facilitate the transfer of protons. The other form exists where it can transfer protons. The fact that emission from both forms is observed in solution leads us to conclude that microenvironments suitable to each species must co-exist in solution. This argument is along the same lines as that put forward by Zinsli⁸⁸ which led to a biphasic model for micelles.

In the current context microenvironments refer to the presence or absence of exchangeable protons in the immediate proximity of the pyranine hydroxyl proton. Emission observed at 440 nm indicates that there are protonated pyranine molecules in solution. Protonated pyranine molecules exist where there are no protons available for exchange in the immediate vicinity of the pyranine hydroxyl proton. Similarly, emission observed at 511 nm indicates that there are deprotonated pyranine molecules in solution. So the PIR is a measure of the ratio of protonated to deprotonated pyranine in solution; and therefore (as explained in the following discussion) a measure of the ratio of water associated with the solute to that not associated with the solute.

According to the pulsed NMR work of Birch et al. there are 3 kinds of exchangeable protons in concentrated sucrose solutions: bulk water, solvation water, and sucrose hydroxyl. Of these, the exchange rate of the sugar hydroxyls is somewhat slower than that of the solvation water. For reasons of mobility and polarity, it is unlikely that the sucrose

molecules would be able to compete with water molecules in interacting with pyranine molecules to a significant extent.

A water molecule in contact with other water molecules that behave like pure water could provide an environment that is capable of proton exchange. If the pyranine hydroxyl is in the proximity of such a water molecule it would emit at 511 nm. Thus, we propose that one of the two microenvironments is likely to be a bulk-water-like microphase. A pyranine hydroxyl group existing near solvation water already associated with a molecule of sucrose could not exchange protons and would emit at 440 nm. Thus, the other likely microenvironment could be due to the presence of an envelope of solvation in general and more specifically due to the presence of water that chemically interacts with the molecule in the sense of the three-state model for solutions, as in NMR.

A graph of the PIR versus concentration of sucrose (wt. %) is shown in Figure 4.4. Since pyranine has only one proton available for exchange, it is reasonable to conclude that only one molecule of water at a time can participate in the exchange process. It follows that the PIR (a ratio of pyranine molecules incapable of exchanging protons to that of pyranine molecules capable of exchanging protons) is also the ratio of water molecules that do not participate in proton exchange with the pyranine to those that do. Furthermore, we can scale this per molecule of sucrose. This is purely for convenience. It then becomes possible to look at the solution in terms of water of solvation per molecule of sucrose (unavailable for proton exchange) and bulk water (available for proton exchange); terms that can be compared with existing data, at least for undersaturated solutions. Similar results were obtained from the analysis of glucose, fructose, and lactose, Figures 4.5, 4.6, and 4.7 respectively. It is apparent that the change in the PIR with saturation is not so marked in the case of glucose and lactose as it is for sucrose and fructose.

Assuming that the quantum yield of the two emitting species is the same (same chromophore), we can plot a graph of the number of molecules of water in each of these microenvironments per molecule of sucrose. We calculate 6 molecules of solvation water

per molecule of sucrose in undersaturated solutions, dropping to 5.8 molecules at the saturation point, 5.5 at 70 wt.%, 5.2 at 76 wt.%, and 4.0 at 80 wt%; see Tables 1 and 2. It would seem reasonable that solvation water per molecule would be a function of the molecular structure, more specifically the number of sites (and conformation of these sites) on the molecule that could hydrogen bond with nearby water. Of equal or greater significance is the behavior of the bulk water. The number of molecules of water in the bulk-water-like environment drops from 165 for a 10% sucrose solution to about 3 for a highly supersaturated solution of 70% sucrose. It drops further to a value slightly less than 1.0 (0.83) for the 76% solution and stays about constant for the 80% solution.

Although the determination of water of solvation is in agreement with the results of Jones⁴¹, Phillips⁷¹, and Franks, Suggett and co-workers^{32-35, 78-80, 82}, we were not entirely comfortable with the assumption of equal quantum yields for the two emitting species. In an attempt to isolate the two species and estimate relative quantum yield, spectra of equal amounts of carefully measured pyranine were obtained in methanol and water (under the same conditions as the rest of the experiments). The only peak observed in methanol was that at 430 nm. In water, a weak shoulder was observed at 440 nm, but the emission was primarily at 511 nm. The peak in methanol was approximately 1.8 times as intense as the peak in water for any given concentration of pyranine (between 1-80 ppm (1.9×10^{-8} and 1.6×10^{-5} M)). This would indicate 11 molecules of solvation water per molecule of sucrose, in agreement with the results of Harvey and Symons³⁸ and the earlier calculations of Stokes and Robinson⁷⁷. It would also indicate smaller numbers for both the bulk-water-like phase and the solvated water in the supersaturated region. The smaller amount of solvation water might indicate that the more dynamically associated water (according to Harvey and Symons) might be depleted in order to solvate solute in excess of the amount in a saturated solution. The basic concept that saturation occurs when it is no longer energetically favorable to solvate more solute molecules without supplying external energy, as evidenced by an equilibrium between the bulk and solvation water, remains

unchanged. It is worth noting that the spectra in methanol were blue-shifted about 5-10 nm from those in water. This may be due to a difference in polarity of microenvironment or due to a green bleed through in the spectra in water. At this point it is not appropriate to conclusively state that both emitting species have the same quantum efficiencies although this is what our arguments and observations would lead us to believe.

In either case (6 or 11 molecules of solvation water per molecule of sucrose) the surprising observation was that there should be any bulk phase water at all in saturated and supersaturated solutions. The number of water molecules in the bulk phase per molecule of sucrose decays exponentially with increase of sucrose concentration. Near saturation the number of water molecules per molecule of sugar in the bulk phase is roughly equal to the the number of molecules of water of solvation. For a highly supersaturated solution of 70% sucrose there are roughly three molecules of bulk phase water and six molecules of solvation water per molecule of sugar. It is probably the water in the bulk phase that is responsible for structurally "stable" supersaturated solutions. The ease with which sucrose can be dissolved in solution appears to be directly related to the amount of bulk phase water.

An interesting feature of this analysis is that the water of solvation per molecule of sucrose becomes approximately equal to the bulk water per molecule of sucrose at saturation. In supersaturated solutions there is always less bulk water available per molecule of sucrose than solvation water. While this feature is apparent from Figure 4.8, it becomes more so in Figure 4.9. The crossing point of the two curves indicates equilibrium. At this point it becomes energetically unfavorable to add more solute to the solution without supplying external energy.

When this analysis is applied to glucose (Figure 4.10), fructose (Figure 4.11), and lactose (Figure 4.12), essentially the same trends are observed, except that the bulk water and solvation water curves no longer cross at saturation in the case of glucose and lactose. If we draw upon NMR analogy, sucrose solutions can be represented well by a two-state

isotropic model for water as in the work of Richardson and Steinberg⁷⁴. Thus a two-state analysis as presented for sucrose is expected to work well, as it indeed does. Fructose which has several hydroxyl groups that exchange at a rate similar to bulk water is observed to have two molecules of water of solvation per molecule of fructose.

Pyranine can interact with water in one of two ways in the steady state emission experiment. Thus, it is possible to measure only two "kinds" of water: that which will exchange with it and that which will not. It is possible that glucose and lactose both associate with water in a third manner, so that pyranine interprets the water in the solvation shell as "free" for purposes of exchange, whereas in reality it exchanges at an intermediate rate, i.e., slower than bulk water but faster than solvation water.

In the case of glucose we may apply the following analysis. We observe from an initial analysis along the lines of that for sucrose, that there appear to be four waters of solvation per molecule of glucose. At saturation there now appear to be 8 molecules of bulk water per molecule of glucose. We ask ourselves if this water is capable of solvating more glucose then why is the solution saturated? Perhaps glucose molecules associate water at a rate that is faster than what our probe perceives to be associated water but slower than bulk water.

Brady's study of molecular dynamics of solvated glucose in a 15 wt% solution suggests that the residence times of water molecules near each of the sugar oxygen atoms is different. He observed that it takes a small (on the scale of several fs) but finite amount of time for solvent exchange to occur near each of the OH or O moieties in the glucose molecule. Thus on some very small but finite time scale each of these groups remains relatively "unattached" to any specific water molecule. Four of these times are relatively slow; two are of the same order of magnitude as the residence time of a water molecule near another water molecule: roughly twice as fast as the other four. All exchange processes and rotational correlation times can be classified into three groups. This is interesting in the light of our steady state emission studies with pyranine as an extrinsic trace fluorescent probe in

solution, because it supports the idea that at least three significant exchange time scales are involved.

Based on this information we assume that glucose associates 2 molecules of water per remaining sugar oxygen group (four of which are already accounted for as being solvated). This adds up to 4 more water molecules (each of the other groups associate with roughly double the water in the same period of time). When we take these extra molecules into account and apply it to our analysis we observe that the bulk water does indeed become equal to the solvation water at or near saturation (for $DS=0$). Thus, a three state model for water allows us to explain the behavior of aqueous glucose solutions well, Figure 4.13.

Lactose shows on the average of 3 waters of solvation per molecule, Figure 4.12. If the three state model is postulated for lactose and a correction of 2 water molecules is applied for each oxygen unaccounted for ie., $11-3=8$, the curves still do not cross at saturation, but a much better fit of data is obtained, Figure 4.14.

4.10 Conclusions

It is possible to calculate a quantity which we call the peak intensity ratio (PIR) from steady state emission spectra of trace quantities of pyranine in solutions of sucrose, fructose, glucose and lactose in polar solvents. It appears that the PIR obtained from fluorescence spectra of pyranine in aqueous sucrose solutions shows a marked change at saturation and is very sensitive to water content of supersaturated solutions. This is a sensitive technique for measuring degree of supersaturation. The PIR obtained from the fluorescence emission of pyranine in aqueous solutions of fructose also exhibits similar behavior. Such a marked change in PIR was not observed with the onset of saturation in the fluorescence emission of pyranine in aqueous solutions of glucose and lactose .

Structurally, the solvent appears to distribute itself in at least two, and in some cases three, kinds of microenvironments. One corresponds to the water strongly associated with the solute molecule, designated solvation water, and the other is solvent that associates primarily with other solvent molecules, designated bulk phase water. The third state corresponds to water in an envelope of solvation associated with the molecule in a more dynamic fashion and cannot be measured by the probe directly. This water is viewed by the probe to be bulk water. The amount of water present in the bulk phase decreases exponentially with increase in solute concentration and correlates with the ease of solvation of the solute. At the saturation point the amount of water in the bulk phase per molecule of sucrose is roughly the same as the number of water molecules of solvation per molecule of sucrose. This was also observed to be true for fructose. Lactose and glucose were observed to behave in roughly the same way if it was assumed that some water was available for exchange in a "third state", i.e., at a third or intermediate rate.

Most of the previous studies of structure in concentrated and supersaturated solutions have focused on solute-solute interactions and solute structuring or aggregation. We have developed a means of extracting information about the solvent distribution in sugar solutions using steady state fluorescence spectroscopy of an extrinsic trace fluorescent probe. We have demonstrated that this technique works well for analysis of aqueous solutions of polar organics and that the best data are obtained for systems that can be described by an isotropic two-state exchange model for water. Reasonably good results can be obtained for systems described by a three state model of exchange for water. Our results do not indicate the presence of solvent-exclusive precrystalline clusters; instead we observe the sugar molecules to be at least partially solvated in supersaturated solutions, even at moderate degrees of supersaturation. It is suggested that the results of the various studies in solution structure are not inconsistent with each other. We suggest they may be consistent with each other if the supersaturated solution contains some moieties, solvent

and/or solute, that participate in bulk-water-like fast exchange and at least some molecules of solute that are partially solvated at some moieties some of the time.

4.11 Acknowledgements

The authors wish to thank Dr. D.G. Nocera, of the Department of Chemistry, Michigan State University for kindly permitting the use of the emission spectrometer in his laboratory. Financial assistance from the Department of Chemical Engineering and the Crop and Food Bioprocessing Center/ Research Excellence Fund at Michigan State University is greatly appreciated. Support from the Cooperative State Research Service (CSRS) of the United States Department of Agriculture (Grant No. 90-24189-5014) is also acknowledged. R.C. wishes to thank Dr. R. I. Cukier, of the Department of Chemistry, Michigan State University for several very useful discussions and comments.

4.12 References

1. Back D.M., D.F. Michalska, and P. L. Polavarapu, *Appl. Spectroscopy*, **38**(2), 173, (1984).
2. Barbara P.F. and W. Jarzeba, *Acc. Chem. Res.*, **21**, 195, (1988).
3. Bardez, E., B.T. Gouguillon, E. Keh and B. Valeur, *J. Phys. Chem.*, **88**, 1909, (1984).
4. Barone, G., G. Castronuovo, P. Del Vecchio and V. Elia, *J. Solution Chem.*, **19**, 1, 41 (1990).
5. Barone, G., G. Castronuovo, P. Del Vecchio, V. Elia and M.T. Tosto, *J. Solution Chem.*, **17**, 10, 925 (1988)
6. Barone, G., G. Castronuovo, V. Elia and M.T. Tosta, *J. Solution Chem.*, **15**, 2, 199 (1986).
7. Barone, G., G. Castronuovo, V. Elia and V. Savino, *J. Solution Chem.*, **13**, 3, 209 (1984).
8. Ben-Naim, A. , Solvation Thermodynamics, Plenum Press, New York (1987).

9. Bernal, J.D. and R.H. Fowler, *J. Chem. Phys.*, **1**, 515 (1933).
10. Birch, G.G., J. Grigor and W. Derbyshire, *J. Solution Chem.*, **18**, 8, 795 (1989).
11. Bousfield, W.R. and T.M. Lowry, *Trans. Faraday Soc.*, **6**, 85 (1910).
12. Brady J.W., *J. Am. Chem. Soc.*, **11**, 5155, (1989).
13. Cael J.J., J.L. Koenig and J. Blackwell, *Carbohydrate Res.*, **32**, 79, (1974).
14. Cerreta, M.K. and K.A. Berglund, in Industrial Crystallization '84, S.J.Jancic and E.J. DeJong, (Eds.), Elsevier, Amsterdam, 21 (1984).
15. Cerreta, M.K. and K.A. Berglund, *Journal of Cryst. Growth*, **102**, 869, (1990).
16. Cerreta, M.K. and K.A. Berglund, *Journal of Crystal Growth*, **84**, 577 (1987).
17. Cerreta, M.K., Ph.D dissertation, Michigan State University (1988).
18. Chakraborty R. and K.A. Berglund, *AIChE Symposium Series no. 284*, 113, (1991).
19. Chang, Y.C. and A.S. Myerson, *AIChE J.*, **31**, 980 (1985).
20. Chang, Y.C. and A.S. Myerson, *AIChE J.*, **32**, 1567 (1986).
21. Chang, Y.C. and A.S. Myerson, *AIChE J.*, **32**, 1747,(1986).
22. Chapman C. F., R. S. Fee, and M. Maroncelli, *J. Phys. Chem.*, **94**, 4929, (1990).
23. Clement, N.R. and M. Gould, *Biochemistry*, **20**, 1534 (1981).
24. Cross, A. J. and J.D. Simon, *J. Chem. Phys.*, **86**, 7079, (1987).
25. Cussler, E.L., *AIChE Journal*, **26**, 1, 43-51 (1980).
26. Delhaye M. and P. Dhamelincourt, *J. of Raman Spectroscopy*, **3**, 33, (1975).
27. Elankovan, P. and K.A. Berglund, *AIChE J.*, **33**, 1844, (1987).
28. Elankovan, P., and K.A. Berglund, *Appl. Spectroscopy*, **40**, 712, (1986).
29. Eley, D.D., *Trans. Faraday Soc.*, **35**,1281 (1939).
30. Frank, H.S. and M.W. Evans, *J. Chem. Phys.*, **13**,11, 507 (1945).
31. Frank, H.S. and W.Y. Wen, *Disc. Faraday Soc.*, **24**, 1333 (1957).
32. Franks, F. in Hydrogen Bonded Solvent Systems, A.K. Covington and P.Jones (Eds), Taylor and Francis Ltd., London, 31-47 (1968).
33. Franks, F., J.R. Ravenhill and D.S. Reid *J. Solution Chem.*,**1**,1, 3 (1972).
34. Franks, F., M. Pedley and D.S. Reid, *J. Chem. Soc. Faraday Trans. I*, **72**, 359 (1976).
35. Franks, F., *Pure and Appl. Chem.*, **59**, 9,1189 (1987).
36. Giermanska J. and M.M. Szostak, *Journal of Raman Spectroscopy*, **22**, 107, (1991).
37. Hameka H.F., G.W. Robinson, and C.J. Marsden, *J. Phys. Chem.*, **91**, 3150,(1987).
38. Harvey, J.M. and M.C.R. Symons, *J. Solution Chem.*, **7**(8), 571 (1978).

39. Hildebrand, J.H., in Solubility, Wiley and Sons, N.Y., 2nd. ed., (1965).
40. Hussman, G.A., M.A. Larson and K.A. Berglund, in Industrial Crystallization '84, S.J. Jancic and E.J. DeJong (Eds.), Elsevier, Amsterdam, 21 (1984).
41. Jones, H.C., *Amer. Chem. Journal*, **32**, 319 (1904).
42. Kalyansundaram , Photochemistry in Microheterogeneous Systems,
43. Kano, K. and J.H. Fendler, *Biochim. Biophys. Acta*, **509**, 289 (1978).
44. Kaufman, V.R., D. Avnir, E. Pines-Rojanski and D. Huppert, *J. Non-Crystalline Solids*, **99**, 397 (1988).
45. Kenney-Wallace G.A. and C.D. Jonah, *J. Phys. Chem.*, **86**, 2572, (1982).
46. Kenny Wallace G.A. and C.D. Jonah, *Chem. Phys. Lett.*, **39**(3), 596, (1976).
47. Kenny-Wallace G.A., *Can. J. Chem.*, **55**, 2009, (1977).
48. Kenny-Wallace G.A., G.E. Hall, L.A. Hunt, and K. Sarantidis, *J. Phys. Chem.*, **84**, 1145, (1980).
49. Kondo, H., I. Miwa and J. Sunamoto, *J. Phys. Chem.*, **86**, 4826 (1982).
50. Kozak, J.J., W.S. Knight and W. Kauzmann *J. Chem. Phys.*, **48**, 2, 675 (1968).
51. Larson, M.A. and J. Garside, *Chem. Eng. Science*, **41**, 1285 (1986).
52. Larson, M.A. and J. Garside, *J. Crystal Growth*, **76**, 88 (1986).
53. Larson, M.A., *AIChE Symposium Series no.240*, **80**, 39-44 (1984).
54. MacMahon, P.M., K.A. Berglund and M.A. Larson in Industrial Crystallization '84, S.J. Jancic and E.J. DeJong (Eds.), Elsevier, Amsterdam, 229 (1984).
55. Maroncelli M., J. MacInnis, and G.R. Fleming, *Science*, **243**, 1674, (1989).
- 56.a. Mathlouthi M and D.V. Luu, *Carbohydrate Res.*, **78**, 225, (1980).
b. Mathlouthi M. and D.V. Luu, *Carbohydrate Res.*, **81**, 203, (1980).
c. Mathlouthi, M., C. Luu, M. Meffrov-Biget and D.V. Luu, *Carbohydrate Res.*, **81**, 213 (1980).
57. Mathlouthi M., *Carbohydrate Res.*, **91**, 113, (1981).
58. McMillan, W.G. and J.E. Mayer, *J. Chem. Phys.*, **13**(7), 276 (1945).
59. Migus A., Y. Gauduel, J.L. Martin, and A. Antonetti, *Phys. Rev. Lett.* , **58**(17), 1559, (1987).
60. Mullin, J.W. and C. Leci, *AIChE Symposium Series no 68*, J. Estrin ed., **8**, (1972).
61. Mullin, J.W. and C. Leci, a. *Philos. Mag.*, **19**, 1075 (1969).
b. *J. Crystal Growth*, **5**, 75, (1969).
62. Mullin J.W. and C. Leci, *Chem Ind.*, 1517, (1968).
63. Mussel, R.D. and D.G. Nocera, *J. Am. Chem. Soc.*, **110**, 2764 (1988).
64. Myerson A.S., private communications to K. A. B.

65. Myerson, A.S. and L.S. Sorrel, *AICHE Journal*, **28**,778 (1982).
66. Myerson, A.S. and Y.C. Chang, in Industrial Crystallization '84, S.J. Jancic and E.J. DeJong (Eds.), Elsevier, Amsterdam, 27 (1984).
67. Narayanan, H. and G.R. Youngquist, *AICHE Symposium Series no. 253*, pp. 1-7 (1987).
68. Nemethy, G. and H.A. Scheraga, *J. Chem. Phys.*, **36**, 3401 (1962).
69. Ostwald, W., *Z. Phys. Chem.*, **22**, 289-330 (1897).
70. Pauling, L. and O. Brockway, *Proc. Natl. Acad. Sci.*, **20**, 336 (1934).
71. Phillips, J.C., *Trans. Faraday Soc.*, **3**, 136 (1907).
72. Pines, E. and D. Huppert, *J. Phys. Chem.*, **87**, 4471 (1984).
73. Pouxviel, J.C., B. Dunn and J.I. Zink, *J. Phys. Chem.*, **93**, 2134 (1989).
74. Richardson S.J. and M.P. Steinberg, in Water Activity: Theory and Applications to Food, L. B. Rockland and L.R. Beauchat eds., Marcel Dekker Inc., New York, 235, (1987).
75. Simon, J.D., *Acc. Chem. Res.*, **21**, 128, (1988).
76. Sorrel, L.S. and A.S. Myerson, *AIChE J.*, **28**, 772 (1982).
77. Stokes, R.H. and R.A. Robinson, *J. Phys. Chem.*, **76**, 2126 (1966).
78. Suggett, A. and A.H. Clark, *J. Solution Chem.*, **5**, 1, 1 (1976).
79. Suggett, A., *J. Solution Chem.*, **5**, 1,33 (1976).
80. Suggett, A., S. Ablett and P.J. Lillford, *J. Solution Chem.*, **5**(1), 17 (1976).
81. Szarek W.A., S. Korppi-Tommola, H.F. Shurvell, V. H. Smith Jr., and O.R. Martin, *Can. J. Chem.*, **62**, 1512, (1984).
82. Tait, M.J., A.Suggett, F. Franks, S. Ablett and P.A. Quickenden *J. Solution Chem.*, **1**, 2, 131 (1972).
83. Tamman G., States of Aggregation, transl. R.F. Mehl, van-Nostrand, New York, (1925).
84. Teale, F.W.J. and D. Constable, "Intramolecular Thiol-specific Probes" in Fluorescent Probes G.S. Beddard and M.A. West (Eds.), Academic Press, New York, 1-19, (1981)
85. Walafren G.E., in Water a Comprehensive Treatise, Vol. 1, F. Franks ed., Plenum Press, New York, 151, (1972).
86. Wolynes P.G., *Annu. Rev. Phys. Chem.*, **31**, 345, (1980).
87. Wolynes P.G., *J. Chem. Phys.*, **86**(9), 5133, (1987).
88. Zinsli, P.E., *J. Phys. Chem.*, **83**, 3223 (1979).

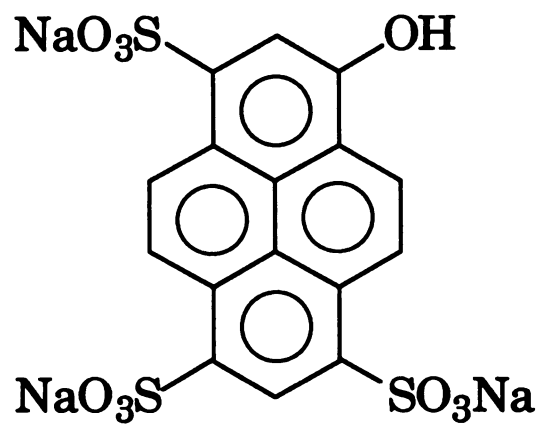


Figure 4.1. Chemical structure of pyranine or 8-hydroxy-1, 3, 6-pyrenetrisulfonate

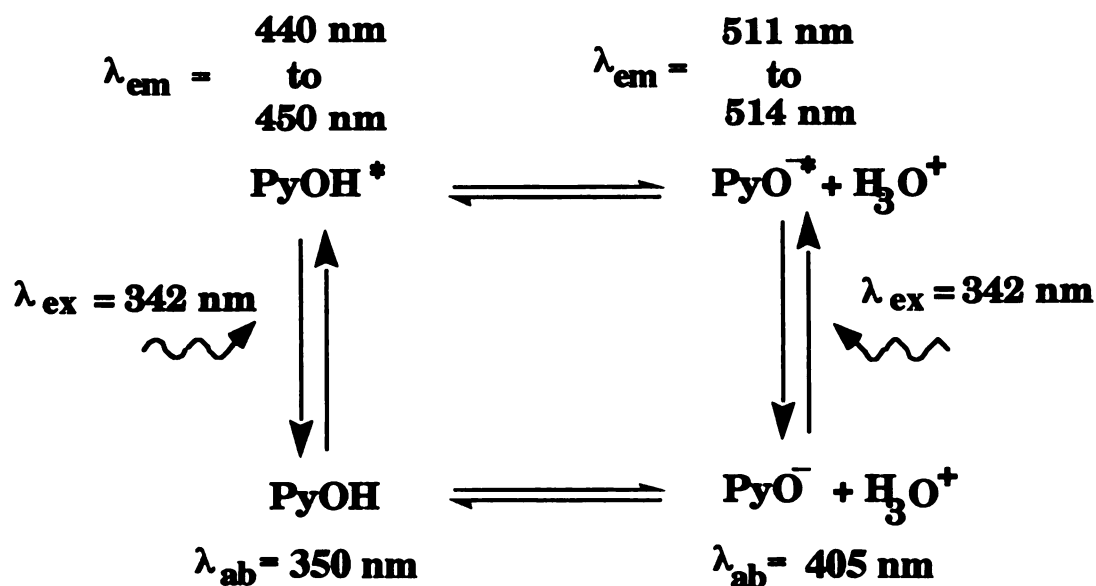


Figure 4.2. Emission equilibrium of pyranine. The equilibrium between the protonated form (absorbs at 350 nm and emits at 440 nm when excited at 342 nm) and the deprotonated form (absorbs at 405 nm and emits at 511 nm when excited at 342 nm) is determined by ability of the microenvironment of the hydroxyl group to participate in proton transfer.

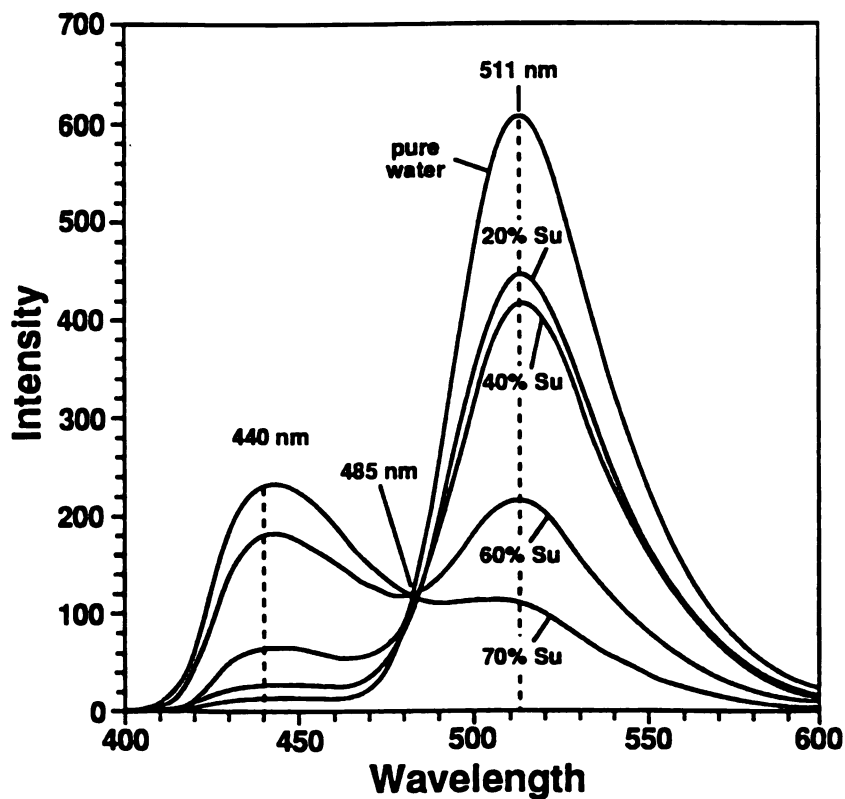


Figure 4.3. The emission spectra of pure water and sugar solutions of 20, 40, 60, and 70 wt.% sucrose doped with 100 ppm (1.9×10^{-4} M) pyranine at 20 degrees C. Emission maxima occur at 440 nm. and 511 nm. An isosbestic point is observed, represented by the pointer at 485 nm.

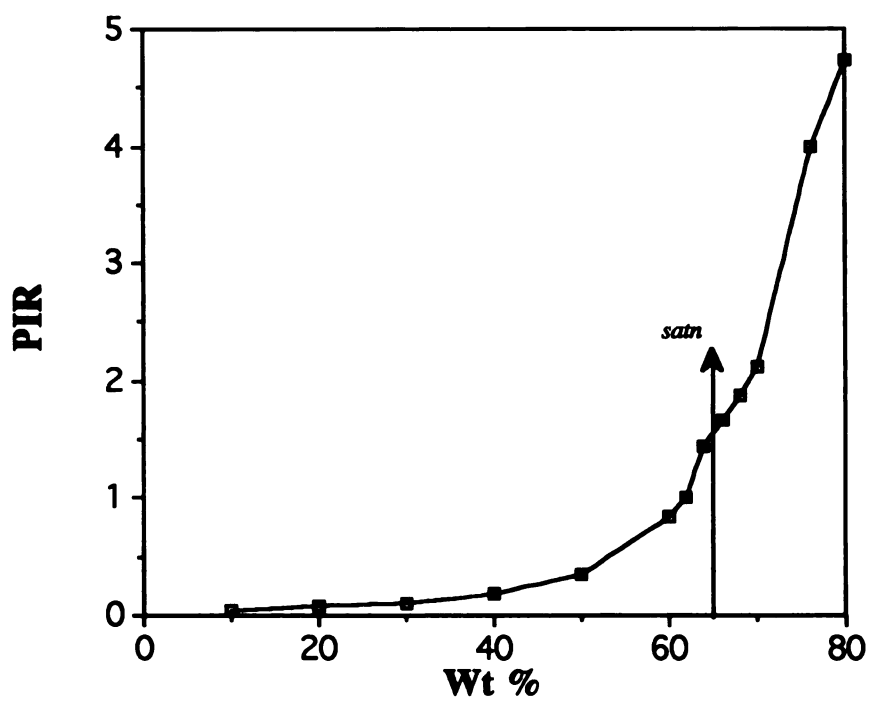


Figure 4.4. Graph of PIR (peak intensity ratio) vs. wt% sucrose in solution at 20 degrees C using 100 ppm (1.9×10^{-4} M) pyranine. The PIR is defined as the ratio of peak intensities at 440 nm and 511 nm. The arrow represents concentration at saturation.

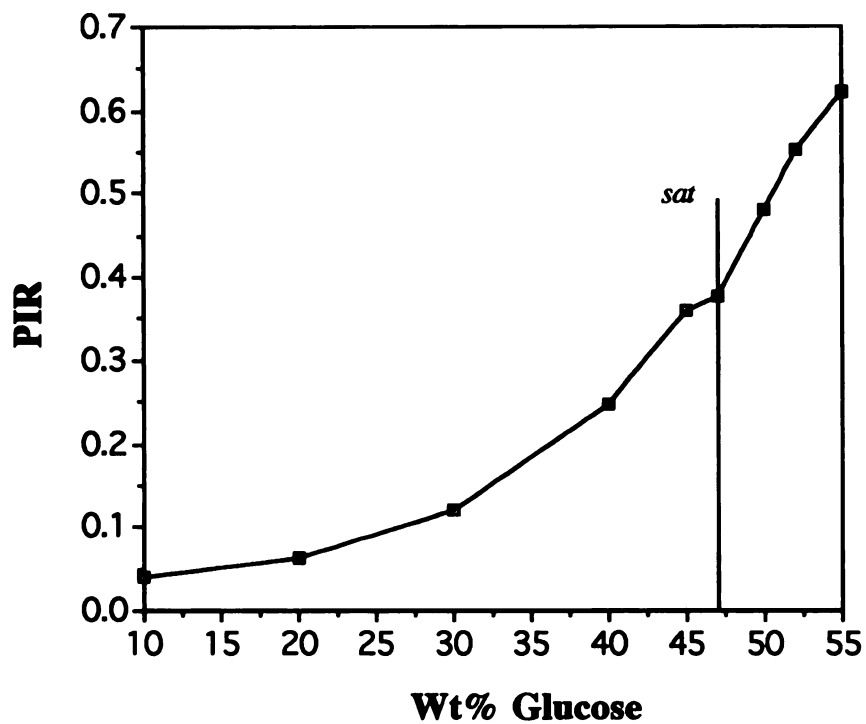


Figure 4.5. Graph of PIR (peak intensity ratio) vs. wt% glucose in solution at 20 degrees C using 100 ppm (1.9×10^{-4} M) pyranine. The PIR is defined as the ratio of peak intensities at 440 nm and 511 nm. The dashed line represents concentration at saturation.

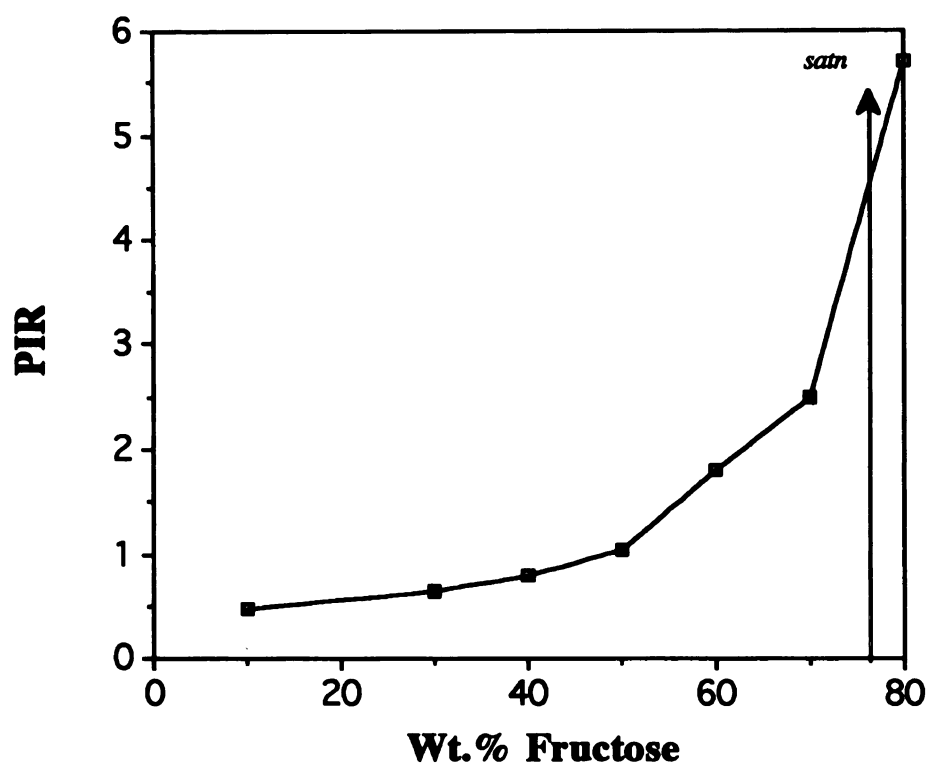


Figure 4.6. Graph of PIR (peak intensity ratio) vs. wt% fructose in solution at 20 degrees C using 100 ppm (1.9×10^{-4} M) pyranine. The PIR is defined as the ratio of peak intensities at 440 nm and 511 nm. The arrow represents concentration at saturation.

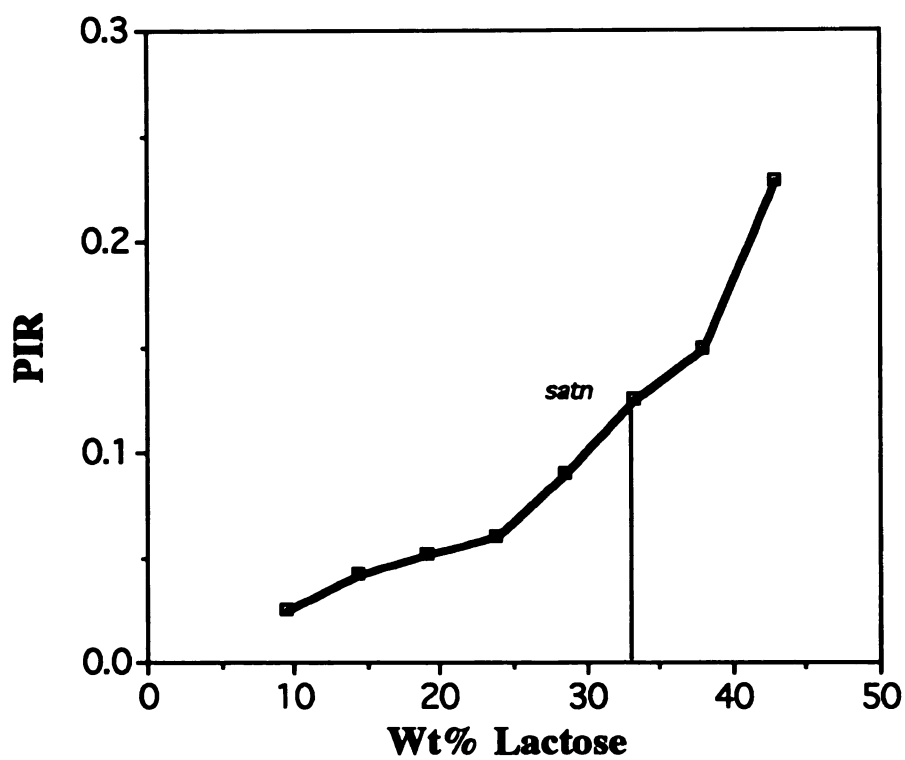


Figure 4.7. Graph of PIR (peak intensity ratio) vs. wt% lactose in solution at 20 degrees C using 100 ppm (1.9×10^{-4} M) pyranine. The PIR is defined as the ratio of peak intensities at 440 nm and 511 nm. The dashed line represents concentration at saturation.

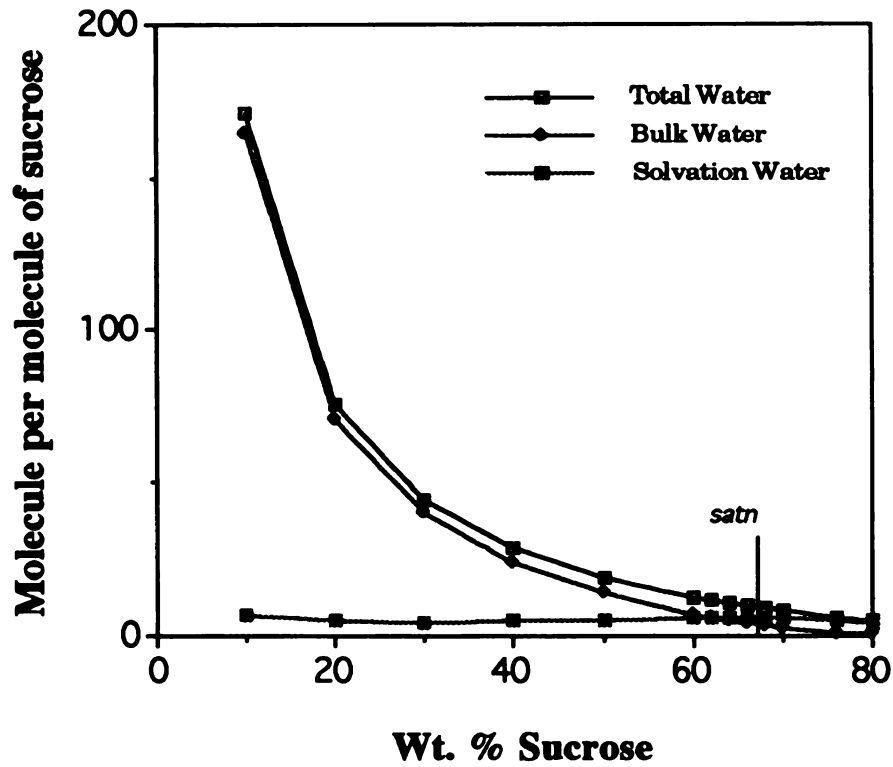


Figure 4.8. Total, bulk and solvation water (number of molecules of water per molecule of sucrose) vs. wt% sucrose in aqueous solution with 100 ppm (1.9×10^{-4} M) pyranine at 20 degrees C. The values on the graph are obtained from an analysis using a two state model for water. The vertical line represents saturation.

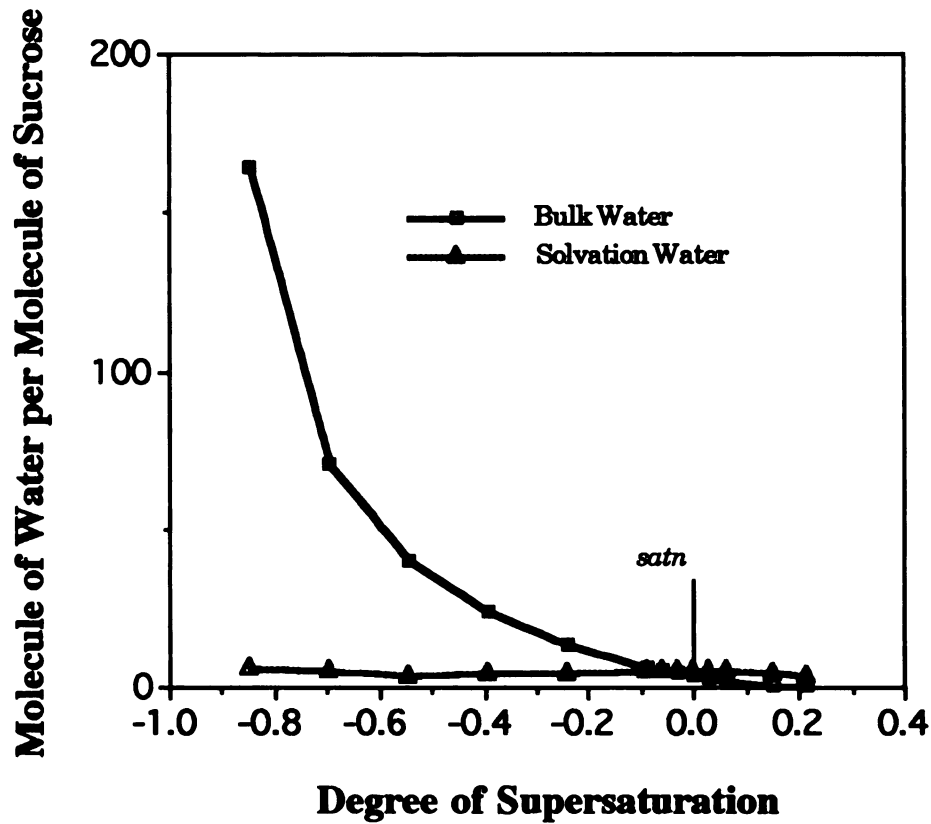


Figure 4.9. Graph of bulk water and solvation water per molecule of sucrose in aqueous solutions doped with 100 ppm (1.9×10^{-4} M) pyranine at 20 degrees C versus the degree of supersaturation, DS. The DS is given by the difference between the solution concentration and the saturation concentration at 20 degrees C divided by the saturation concentration at 20 degrees C.

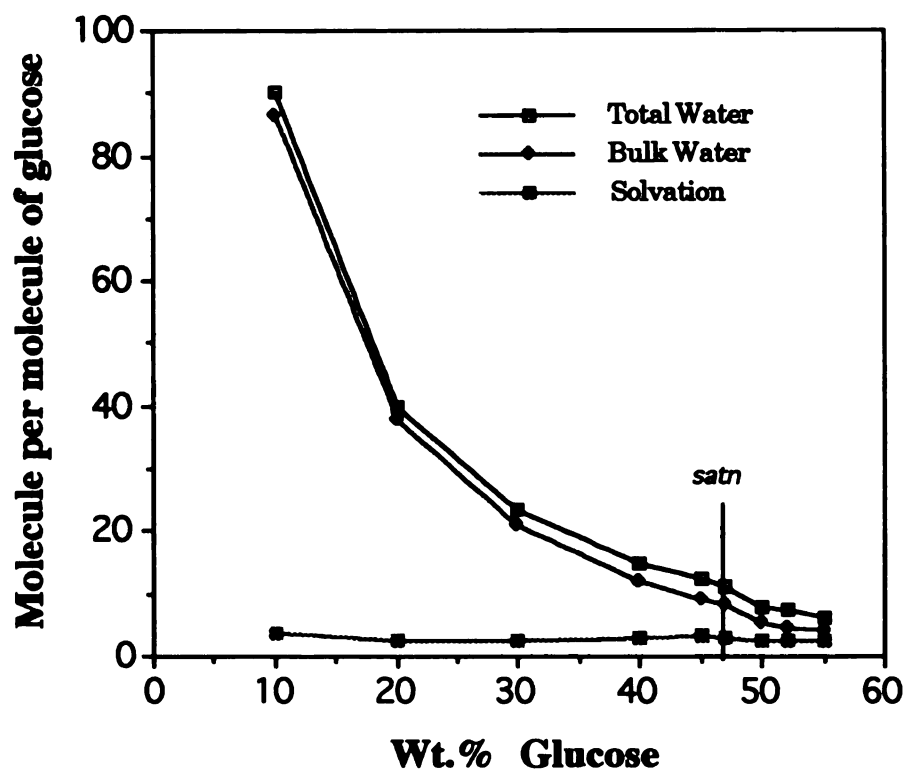


Figure 4.10. Total, bulk and solvation water (number of molecules of water per molecule of glucose) vs. wt% glucose in aqueous solution with 100 ppm (1.9×10^{-4} M) pyranine at 20 degrees C. The values on the graph are obtained from an analysis using a two state model for water. The vertical line represents saturation.

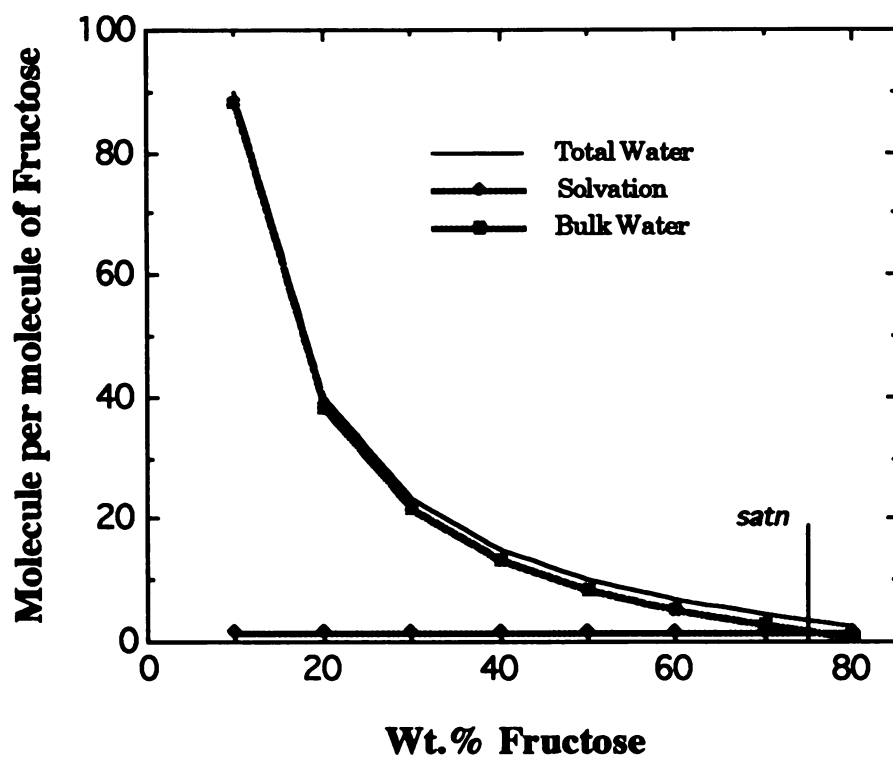


Figure 4.11. Total, bulk and solvation water (number of molecules of water per molecule of fructose) vs. wt% fructose in aqueous solution with 100 ppm (1.9×10^{-4} M) pyranine at 20 degrees C. The values on the graph are obtained from an analysis using a two state model for water. The vertical line represents saturation.

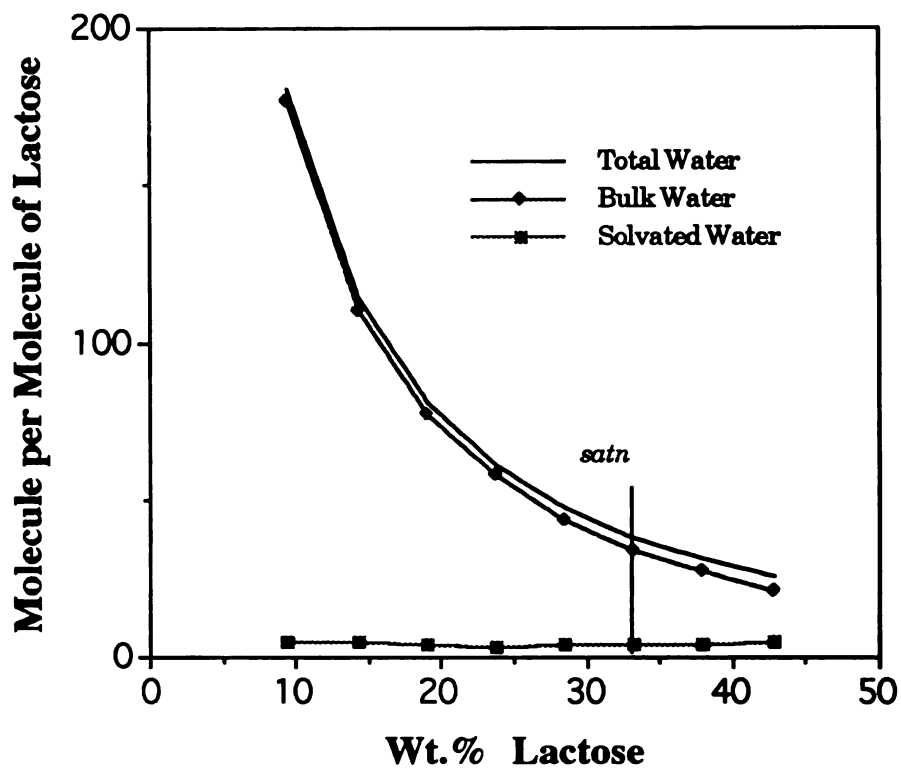


Figure 4.12. Total, bulk and solvation water (number of molecules of water per molecule of lactose) vs. wt% lactose in aqueous solution with 100 ppm (1.9×10^{-4} M) pyranine at 20 degrees C. The values on the graph are obtained from an analysis using a two state model for water. The vertical line represents saturation.

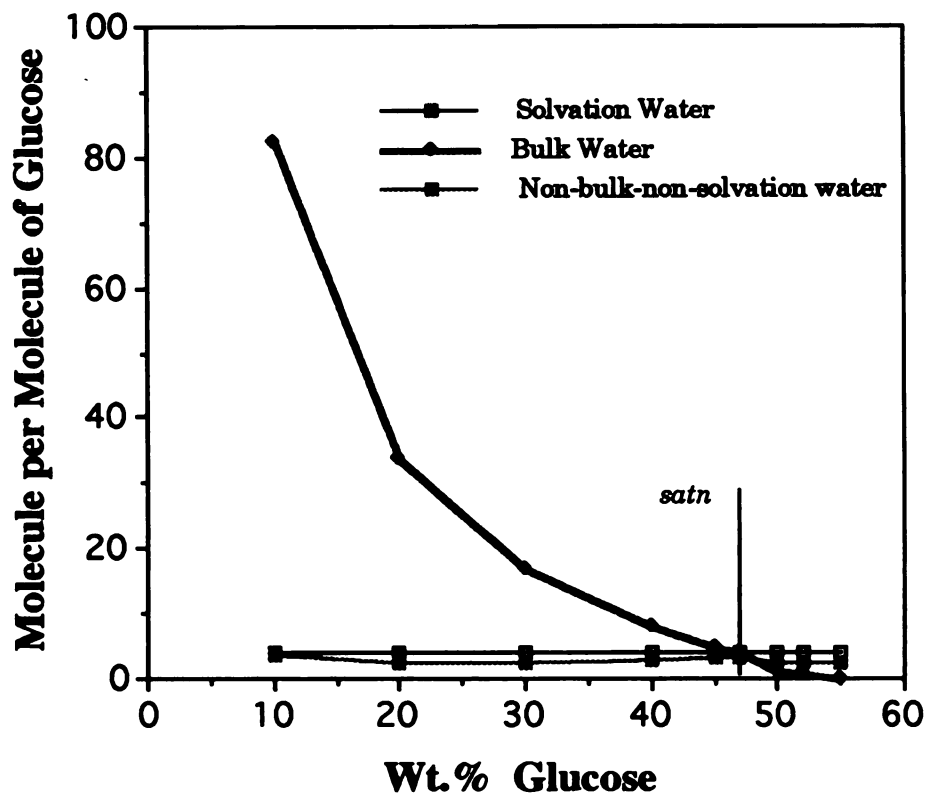


Figure 4.13. Bulk water, solvation water, and non-bulk-non-solvation water (number of molecules of water per molecule of glucose) vs. wt% glucose in aqueous solution with 100 ppm (1.9×10^{-4} M) pyranine at 20 degrees C. The values on the graph are obtained from an analysis using a three state model for water. The vertical line represents saturation.

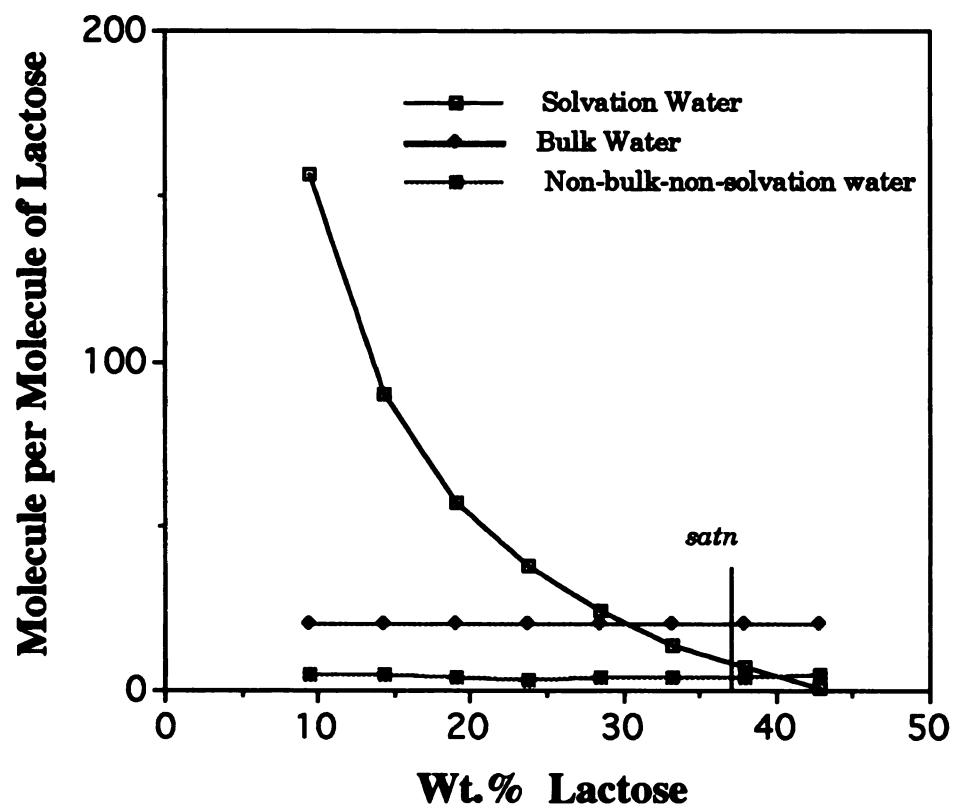


Figure 4.14. Bulk water, solvation water, and non-bulk-non-solvation water (number of molecules of water per molecule of lactose) vs. wt% lactose in aqueous solution with 100 ppm (1.9×10^{-4} M) pyranine at 20 degrees C. The values on the graph are obtained from an analysis using a three state model for water. The vertical line represents saturation.

Chapter Five

The PIR as a measure of deviation from Ideal Solution Behavior

5.1 Background

The focus on solution-structure has been primarily limited to the study of the immediate solvation environment of the solute molecules. In many cases the structure of this environment has been observed to change little, if at all, with solution concentration up to saturation, even though deviations from ideal solution behavior over the same range of solution concentrations are observed to be significant. As a result, strong correlations between structure and deviations from ideal solution behavior were not apparent. A relationship between change in solution structure and deviations from ideal solution behavior has been surmised although the specifics of cause-effect are yet undetermined. There has been some speculation as to changes in the structure of the solvent that does not participate in the solvation of solute with changes in concentration; however, until recently there were no reliable estimates regarding the nature of such changes.

In a study of structure in aqueous sucrose solutions we used the solvation environment related changes in the excited state equilibrium of trace quantities of pyranine (a fluorescent probe molecule extrinsic to the system) to determine the peak intensity ratio, or PIR (the ratio of water involved in solvating sugar molecules to water to water that is not). We found to our surprise that while the immediate solvation environment of the solute molecule remained fairly constant even in supersaturated solutions; the amount of water per solute molecule not involved in its solvation (designated bulk water in the case of sucrose) changed almost exponentially as a function of solution concentration. In an extension of this work, with Pan's measurements using time resolved fluorescence spectroscopy of pyrene butyric acid

and pyranine, we observed that the structure of the bulk water changed with solution concentration as well. The most marked changes were observed in supersaturated solution. Consequently, we were encouraged to search for a possible relationship between deviation from ideal solution behavior for a solution of a given concentration and either the ratio of solvation to bulk water per molecule of solute, or the amount of bulk water per molecule of solute.

The obvious choice as a measure of deviation from ideal solution behavior is the activity coefficient or the activity. In the particular case of sugar water systems this is of considerable practical significance because the correlation between shelf life, texture, biological stability of foods, and water activity, a_w , is well documented. Several comprehensive reviews of the influence of water on chemical reactions in food are available¹⁻⁵. The measurement of a_w , in concentrated and metastable aqueous solutions of sugars is also an area of active interest⁶.

Rugged, stable, rapid and precise techniques for evaluation of a_w are required; as are techniques that can rapidly, accurately, and simultaneously measure solute concentration and water activity. Official Methods of Analysis of the AOAC (1984) 32.004-32.009 details analytical methods for determination of a_w . Hair hygrometers, electronic hygrometers, and isopiestic methods are commonly used. Electronic hygrometers work on the principle that that changes in conductance, resistivity, impedance, resistance, or capacitance of a thin film or an aqueous solution of a hygroscopic substance can be correlated to corresponding changes in a_w ⁷. In this work we will demonstrate for aqueous sucrose and glucose solutions, that a single measurement of the emission spectrum of a trace fluorescent probe in a solution sample can be used in practice to obtain both concentration and a_w . We will suggest that this is possible because the same structure-interaction effects are responsible for changes in both the water activity as well as the ratio of solvation to bulk water.

5.2 Materials and Methods

Reagent grade sucrose and reagent grade glucose were obtained from Sigma Chemicals, and pyranine from Eastman Kodak. Water used was 18 Mohm reverse osmosis water. Stock solutions of 100 ppm (1.9×10^{-4} M) pyranine were prepared by measuring out 0.1 gms of pyranine to an accuracy of ± 0.0002 gms and diluting with 0.001 m^3 water. Sugar solutions of known wt % were made in 20 ml scintillation vials by measuring out the required amount of sugar to ± 0.0002 gms, and adding the required amount of stock solution. Sucrose solutions were obtained in 10 wt% intervals upto 60 wt% and in 2 wt % intervals upto 74%. Glucose solutions were obtained in 5 wt% intervals upto 40% and at 2 or 3 wt % intervals upto 55 wt %. All concentrated solutions were made by heating the mixture of sugar and pyranine doped water until the sugar completely dissolved. Solutions were then slowly cooled back to 293 K. Solutions were used within 6 to 24 hours to ensure equilibration, as well as avoid biological contamination.

Emission spectra were obtained with either a 200 W Xe/Hg or a 150 W Xe source in quartz cuvettes using an in-house constructed spectrometer described in detail elsewhere (Mussel and Nocera⁹). The lamps were operated at 80% rated power. A Hamamatsu R1104 photomultiplier tube (maintained typically at 50% maximum voltage) was used in conjunction with a preamplifier (maintained at a sensitivity of 10^{-6}) and a Princeton Electronics lock-in amplifier (maintained at a sensitivity of 3V). The photomultiplier tube was maintained at 213 K to improve the signal to noise ratio. A 375 nm KV or a 370 nm GG cutoff filter was used to filter out source excitation at 342 nm. A 3 mm slit width was used and shutters were kept fully open. Upon obtaining the emission spectra of sucrose solutions doped with pyranine at 100 ppm (1.9×10^{-4} M) varying in concentration from 0.5 wt% sucrose to 80 wt% sucrose, clearly a

contribution from molecules in each emitting form of pyranine was observed for each solution examined. Results are shown in Figure 5.1. Similar results were observed for glucose solutions examined.

5.3 Results

The structure of pyranine is presented in Figure 5.2. The equilibrium behavior of pyranine is described in Figure 5.3. In other work we have shown that the peak intensity ratio (PIR), the ratio of peak intensity at 440 nm to that at 511 nm for a solution excited at 342 nm, can be correlated to solute concentrations in concentrated and supersaturated solutions of sugars⁸.

The water activity for aqueous sucrose was determined from the data of Stokes and Robinson¹⁰. The $x_w \ln \gamma_w$ were plotted against experimentally obtained $\ln \text{PIR}$ in Figure 5.4. In each case the data fit well to a straight line. The activity coefficients for aqueous glucose were obtained using UNIFAC⁶. A reasonable linear fit is obtained for a plot similar to that presented in Figure 5.4. It is interesting to note that the fit improves considerably when a three state model for water is invoked and the $x_w \ln \gamma_w$ is plotted vs the natural log of the ratio of chemically associated water to bulk water as opposed to PIR, Figure 5.5. The chemically associated water is obtained as a derived quantity from experiment, by introducing a correction which is discussed in detail elsewhere⁸.

5.4 Analysis

We will attempt to relate the dissociation equilibrium of the probe to the solvation of solute and dissociation equilibrium of water via the coupled species

equilibria. The various relations for a system of solute, Su, and water at a known concentration, volume and temperature are presented briefly.

For a given unit volume V, and temperature T:

let there be

n_w^0 = total molecules of water in pure solvent

n_b = molecules in "bound" state

n_f = molecules in "free" state

n_{bulk} = molecules in bulk water phase

n_{solvated} = molecules in solvated phase

n_w = molecules of water in solution

n_s = molecules of solute in solution

now $n_w^0 = n_b + n_f$ although n_b and n_f need not be constant from moment to moment or from one point in solution to another.

$n_{\text{solvated}} = 6 n_s + n_b$

$n_{\text{bulk}} = n_f$

(although for most experiments we take $n_{\text{solvated}} = 6 n_s$

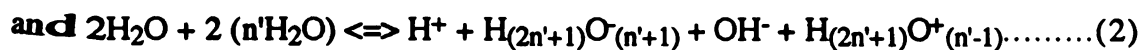
$n_{\text{bulk}} = n_f + n_b$)

$n_w = n_{\text{solvated}} + n_{\text{bulk}}$

$PIR = n_{\text{solvated}} / n_{\text{bulk}}$

Let us assume all the solute is solvated at any given moment.

Therefore the equilibria which affect the analysis are:



The solute molecules are entirely solvated

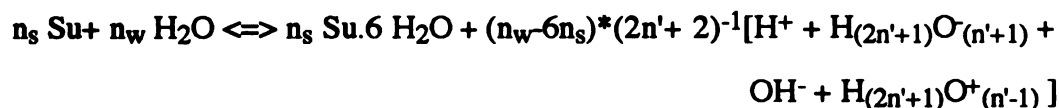


Let us recapitulate for the sake of clarity:

water involved in solvation of solute = $6 n_s$

water not involved in solvation of solute = $n_w - 6 n_s$

So in a sense:



and $\text{PIR} = \text{PyOH} / \text{PyO}^-$

Our argument has been that since there are on the order of 10^6 molecules of water for every probe molecule, it is the behavior of this water that affects the local and global instantaneous and time averaged equilibrium behavior of the probe. For this reason,

$$[\text{PyO}^-] \propto [\text{H}^+] + [\text{H}_{(2n'+1)}\text{O}^{+(n'-1)}] + [\text{OH}^-] + [\text{H}_{(2n'+1)}\text{O}^{(n'+1)}]$$

$$\text{and } [\text{PyOH}] \propto [\text{Su} \cdot 6 \text{ H}_2\text{O}] + [\text{H}_2\text{O}] + [n' \text{ H}_2\text{O}]$$

We find that when $n_s=0$, in pure solvent, PIR is approximately zero, thus, for all practical purposes we can assume that from the point of view of the probe molecule the equilibrium of the water lies far to the right. Consequently:

$$[\text{PyO}^-] \propto n_w - 6n_s \text{ and } [\text{PyOH}] \propto 6n_s,$$

so that $\text{PIR} \approx \phi 6n_s / (n_w - 6n_s)$ where ϕ = a proportionality constant.

$$\therefore \ln \text{PIR} = \ln 6\phi + \ln n_s - \ln n_{\text{available}} \text{ where } n_{\text{available}} = n_w - 6n_s$$

$$\therefore d \ln \text{PIR} / d n_w = (n_w + n_s) / n_s (n_w - 6n_s).$$

$$\text{Now } x_w = n_w / (n_w + n_s)$$

$$\begin{aligned} \text{so } d x_w &= (n_w + n_s) d n_w - n_w d(n_s + n_w) / (n_w + n_s)^2 \\ &= 1 / (n_w + n_s) d n_w \text{ also } d x_w = -d x_s = -1 / (n_w + n_s) d n_s \end{aligned}$$

$$\therefore \text{ but, for the sucrose-water system } \ln \gamma_w = C_1 x_w x_s^2 \text{ and } \ln \gamma_s = D_1 x_s x_w^2$$

$$\begin{aligned} \text{so } d \ln \gamma_w / d x_w &= C_1 x_s^2 - 2C_1 x_w x_s \text{ and } d \ln \gamma_s / d x_s = D_1 x_w^2 - 2D_1 x_w \\ &\approx -C_1 x_s (2x_w - x_s) \end{aligned}$$

$$\text{so } d \ln \gamma_w / d \ln \text{PIR} = -C_1 x_s (2x_w - x_s) [x_s (x_w - 6x_s)]$$

104

$$= -C_1[2x_w^2x_s^2-13x_wx_s^3-6x_s^4]$$

$$\approx -C_1[2x_s^2-17x_s^3+11x_s^4]$$

\approx fairly constant because both x_s and C_1 are small

numbers and x_s^2 does not change very much over the range of concentrations considered.

$$\text{and } d x_w \ln \gamma_w / d \ln \text{PIR} = x_w d \ln \gamma_w / d \ln \text{PIR} + \ln \gamma_w dx_w / d \ln \text{PIR}$$

= also fairly constant for the same reason.

5.5 Discussion

The PIR, and mol fraction, are both intensive state variables of the system. They are directly obtained from measurements of the concentration of different species in solution. The activity coefficient, γ_w , is not a directly measured variable; instead it is obtained by estimating how much the contribution of the mol fraction of each species in solution would have to change in order to correctly estimate a concentration dependent system variable which can be directly measured, using a thermodynamic relationship valid for an ideal solution. The deviation of the value of the activity coefficient from unity is a measure of the deviation of the properties of the solution from those of an ideal solution. To the extent that the actual value of the activity coefficient is related to the values of system variables which are obtained from direct measurements, the activity coefficient is also a measured quantity. The failure to reproduce any experimentally observed correlation between such measured quantities via modelling or argument must therefore be due to inherent flaws in the analysis or modelling and not in the experimental observation (provided the experimental data are fairly accurate).

It is clear that we observe a linear correlation between PIR and $x_w \ln \gamma_w$ (on logarithmic coordinates). The analysis suggests this result, however, does not lead to it

in a direct and conclusive manner. A large part of this has to do with accuracy of the model for the activity coefficient which is used to relate it to mol fractions. Structural effects on solution properties are expressed via this model. The current practice in order to form such a model is to start with an equation of state (of sorts) for the solution where each of the coefficients represents the contribution of nearest neighbour interactions, next nearest neighbor interactions, and so forth; where, "nearest neighbor" invariably refers to a molecule and "interactions" refer to interactions between molecules (on the scale of a molecule). Current practice is to consider each molecule of a particular species exactly identical to every other molecule of that species. Functional distribution of solvent cannot thus be accounted for, although strong correlations between the deviations from ideal solution behavior and the change in microphase distribution are experimentally observed. It is intuitively clear that both the change in the PIR and the deviation from ideal solution behavior are both due to similar physico-chemical reasons.

One of the ways to include the effects of structure would be to provide an alternate model for the activity coefficient that takes into account the localized non-continuum nature of the interactions between the solvent and the solute. The basis for such an approach lies in extending the principles of solvation thermodynamics as developed by Ben Naim and colleagues, with the help of experiments and molecular dynamics. This should allow the development of models which account for the structural reasons for deviations from ideal solution behavior without having to account for the exchange rates at each and every single atom of each molecular species separately.

5.6 Conclusions

It has been shown that a single emission spectrum of a sample of aqueous sucrose or glucose solution previously doped with pyranine can be analysed to yield a_w and concentration simultaneously because the solvation equilibria for all species in solution are coupled via a mass balance on the solvent i.e. water. This analysis is derived specifically for sucrose in water with pyranine as a probe, however, it may be equally valid for other systems. The good correlation between derivation and experiment point the way to the development of an optical sensor for water activity.

5.7 Notation

$[A]$ = concentration of A, moles/ volume of solution (molality) $[ML^{-3}]$

K_p = equilibrium constant for dissociation of pyranine, [dimensionless]

K_s = equilibrium constant for solvation of solute, [dimensionless]

K_w = equilibrium constant for dissociation of water, [dimensionless]

a_w = activity of water, [dimensionless]

x_i = mole fraction of i, [dimensionless]

γ_i = activity coefficient of i, [dimensionless]

R = gas constant

T = absolute temperature, K, [T]

M = mass, kg, or moles, [M]

L = length, meters, [L]

$n(A)$ = moles of A per unit volume of solution

ΔG_s = Gibbs' Free Energy of Solvation, such that $\Delta G_s/RT$ = [dimensionless]

5.8 References

1. Labuza T. P. 1980. The effect of water activity on reaction kinetics of food deterioration. *Food Technol.* **34**(4):36
2. Rockland L. B. and Nishi, S. K. 1980. Influence of water activity on food product quality and stability. *Food Technol.* **34**(4):42
3. Duckworth, R. B. 1975. *Water relations of Foods*. Academic Press, New York
4. Rockland, L. B. and Stewart, G. F. 1981. *Water Activity: Influences on Food Quality*. Academic Press, New York
5. Simato D. and Multon, J. L. 1985. *Properties of Water in Foods*. Martinus Nijhoff Publishers, Dordrecht, The Netherlands
6. Le Maguer M. 1987. Mechanics and Influence of Water Binding on Water Activity, in *Water Activity : Theory and Applications to Foods*, L. B. Rockland and L. R. Beauchat eds., Marcel Dekker, Inc. , New York and Basel, pp. 1-25
7. Johnston M.R. and R.C. Lin, 1987. FDA Views on the Importance of a_w in Good Manufacturing Practice. in *Water Activity : Theory and Applications to Foods*, L. B. Rockland and L. R. Beauchat eds., Marcel Dekker, Inc. , New York and Basel, pp. 287-294
8. Chakraborty R. and K. A. Berglund 1992. *J. of Crystal Growth*. submitted
9. Mussel, R.D. and D.G. Nocera, *J. Am. Chem. Soc.*, **110**, 2764 (1988).
10. Robinson R.A. and Stokes, R. H. 1965. *Electrolyte Solutions*, 2nd Edition (revised), Butterworths, London.

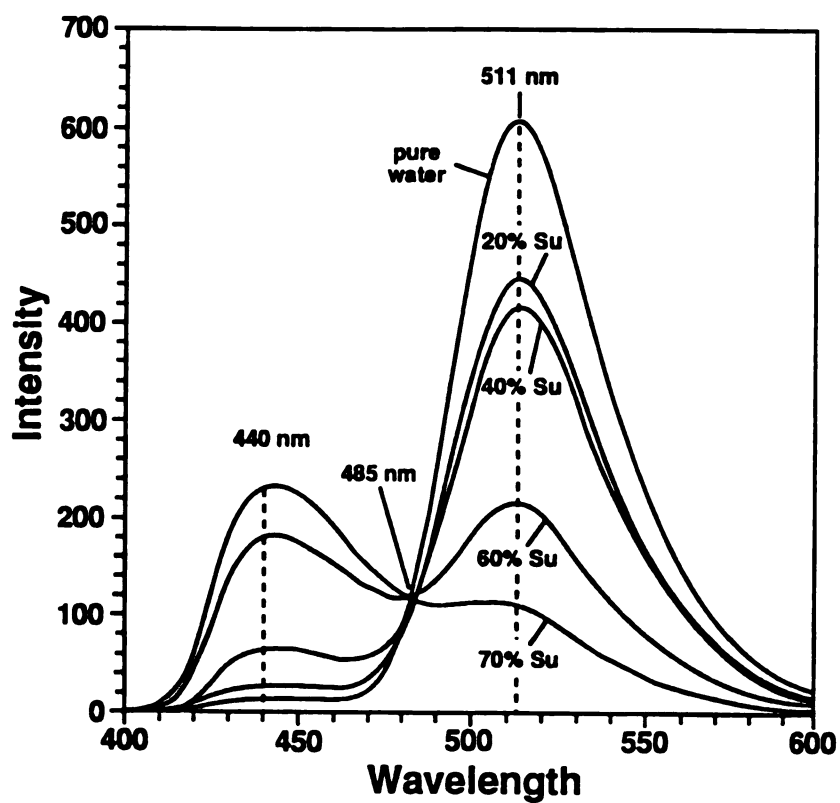


Figure 5.1. The emission spectra of pure water and sugar solutions of 20, 40, 60, and 70 wt.% sucrose doped with 100 ppm (1.9×10^{-4} M) pyranine at 293 K. Emission maxima occur at 440 nm. and 511 nm. An isobestic point is observed, represented by the pointer at 485 nm.

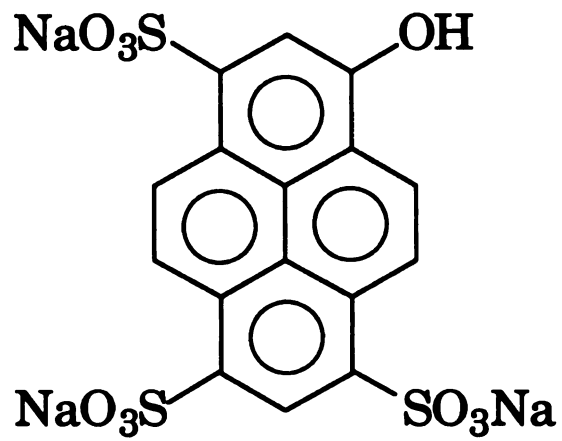


Figure 5.1. Chemical structure of pyranine or 8-hydroxy-1, 3, 6-pyrenetrisulfonate

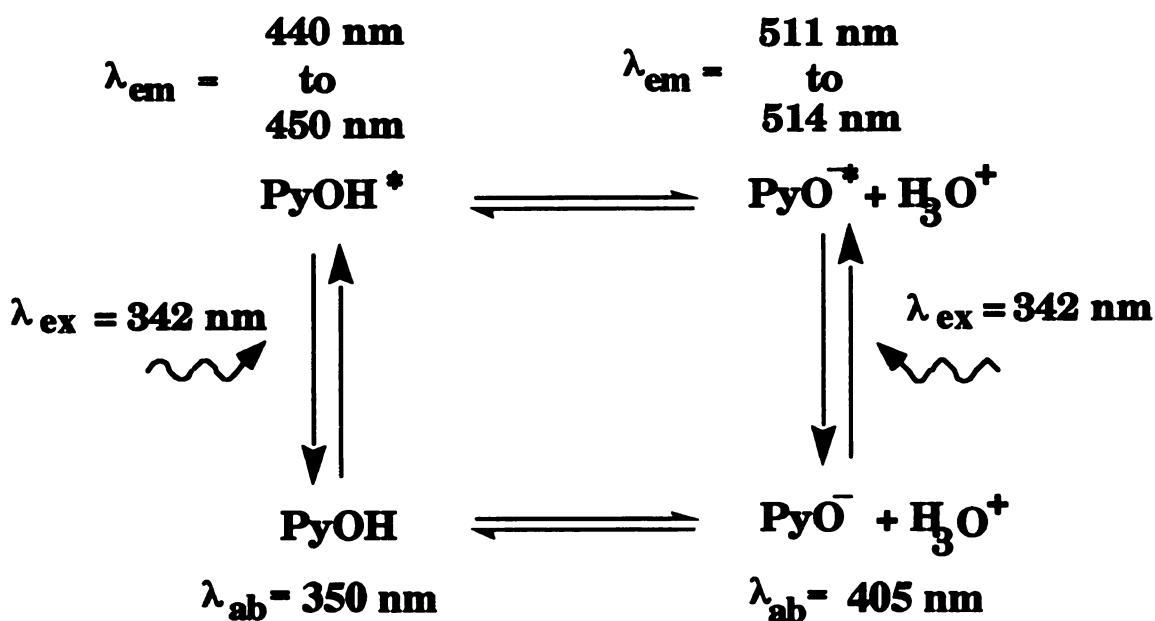


Figure 5.3. Emission equilibrium of pyranine. The equilibrium between the protonated form (absorbs at 350 nm and emits at 440 nm when excited at 342 nm) and the deprotonated form (absorbs at 405 nm and emits at 511 nm when excited at 342 nm) is determined by ability of the microenvironment of the hydroxyl group to participate in proton transfer.

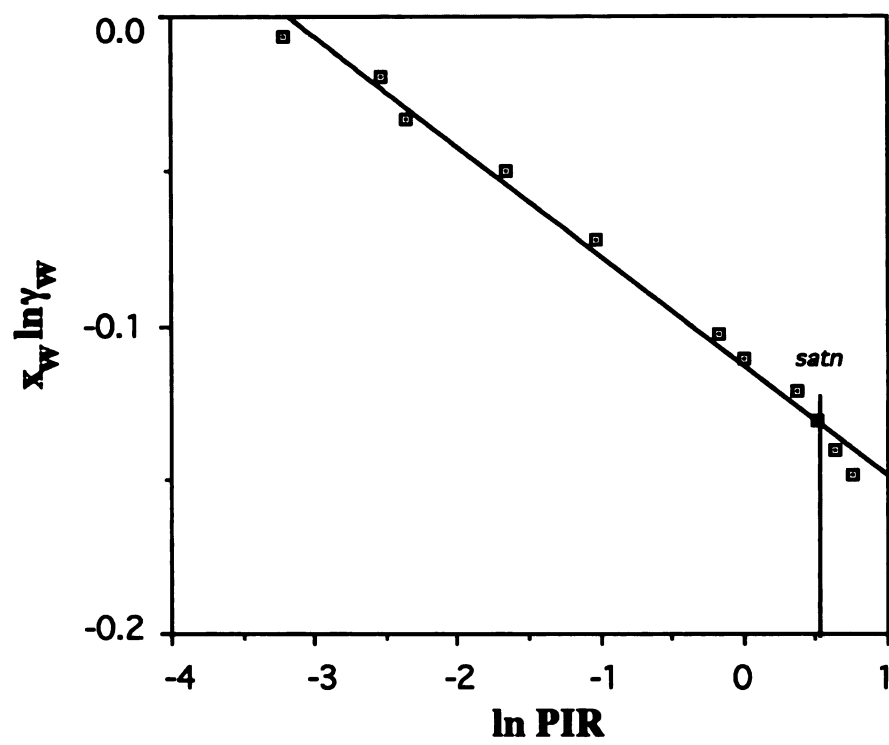


Figure 5.4. Graph of $x_w \ln \gamma_w$ versus $\ln \text{PIR}$ for aqueous sucrose solutions at 293 K.

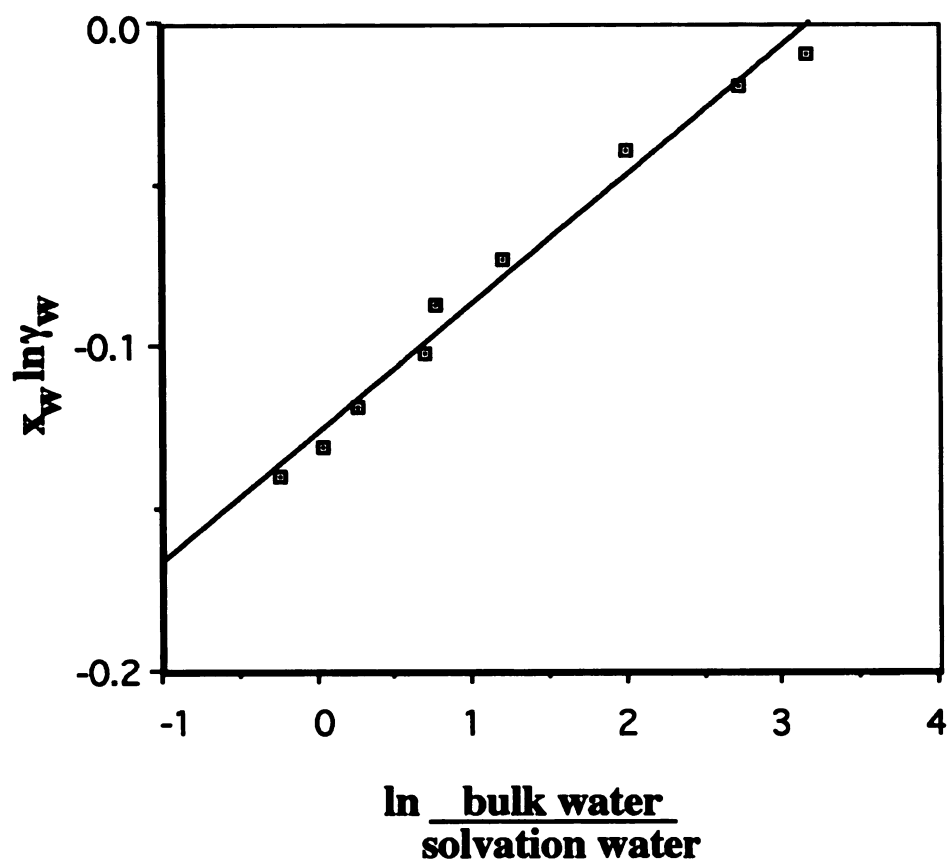


Figure 5.5 Graph of $x_w \ln \gamma_w$ versus \ln Bulk water/Solvation Water (excluding non-bulk-non-solvation water) for aqueous glucose solutions at 293 K.

Chapter Six

The Study of Structure in Saturated and Supersaturated Sucrose Solutions using Steady State and Time Resolved Fluorescence Spectroscopy*

6.1 Background

Structure, transport properties and thermodynamics of phase equilibria are manifestations of interactions on submolecular length scales, e.g. hydrogen bonding, hydrophobic interactions, which require anywhere from a picosecond to a nanosecond to take place. The fact that solution structure and transport phenomena are related in a way that structure governs transport properties and transport phenomena are a directly measurable manifestation of structure, enables us to extract important information about the structure from the study of transport processes and vice versa.

Transport properties in solution are governed by non-equilibrium solvation dynamics. They are governed by short range interaction processes that take place on a variety of time and length scales, which are less than those associated with molecular diffusion. Continuum models are still prevalent for such dynamics. These models do justice to the long range interactions in solution, but fail to account for the details of structure and interaction of inner solvation shells which are often dominant factors (1,2). In the particular case of supersaturated solutions, a previous study of the steady state fluorescence spectroscopy of pyranine in sucrose solutions of various concentrations indicates the molar ratio of solvation water to bulk water per

* Some of this material was published as a part of : B. Pan, R. Chakraborty, & K. A. Berglund, "Steady State and Time Resolved Fluorescence Spectroscopy of Sucrose Solutions," *Journal of Crystal Growth*, **130**, pp. 587-599, (1993). Time Resolved Fluorescence Spectroscopy Data were collected and analysed by B. Pan. Steady State data were collected and analysed by this author. That part of the results and discussion which this author contributed significantly to is included here. Some of Pan's data are mentioned here in support of analysis presented. The reader is referred to the paper for a complete discussion of materials, methods, and analysis.

mole solute is such that there is only enough water available on the average for one solvation shell or an incomplete solvation shell per molecule of solute (3). For this reason, one would expect transport governing interactions in supersaturated solution to be dominated by short range non-equilibrium solvent-solute interactions. The absolute times required for these interactions to take place in supersaturated solutions may be tens, hundreds, or even thousands of times longer than in dilute solution; yet, in terms of distances involved, they are still short range.

There are now several non-continuum heuristic approaches to understanding solvation dynamics. Even the solvation of a simple alcohol must be described by at least two different time scales. For small dipoles or ions, in dilute solution, the time required for solvent response is of the order of a picosecond (1,2). Furthermore, the molecular dynamics simulations of Cross and Simon (4), suggests that if a dipole is strong enough (>17 D) then the two ends may start behaving like point dipoles in the sense that the localized solvent structure and dynamics may be different at each of the ends of the dipole. This is summed up by Maroncelli et. al.(5) who conclude that the solvation response in a polar solvent involves coupled reorientational dynamics that occur on time scales shorter than single particle diffusion. There have been studies in the solvation of an electron in water and alcohols, using picosecond and femtosecond time correlated spectroscopies, which indicate that solvent reorientational times are on the order of < 500 fs (6). Brady's study (7) of the molecular dynamics of solvated glucose in a 15 wt. % solution also indicates that the local structure and dynamics near each of the O or OH moieties of the glucose molecule differ, as do the solvent relaxation times. In each of these studies in dilute solution there is a large amount of non-solvation solvent. Transport coefficients in sucrose solutions of a wide range of concentrations have been reported in literature by Stokes and Robinson (concentrated solutions(8)), and more recently by Sorrel and Myerson (supersaturated(9)). In each case the transport coefficients in

concentrated, saturated, and supersaturated solutions are observed to be much lower. One would expect that response and reorientation times would be much greater as the amount of bulk water decreases in the system, or the solvation to solvation distance decreases, however there are no experimental data in literature which directly measure such parameters.

Previous investigations have studied the nature of these molecular associations by utilizing a variety of means. In the study of supersaturated solution structure many studies have been conducted on the scale of molecular diffusion. Some of these include the column studies of Larson and Garside (10-12), the studies of Narayan and Youngquist (13), and the studies of Myerson and co-workers (9,14-19). Dielectric relaxation methods (20) have identified two distinct relaxation processes for water in sucrose solutions. These were designated as associated water, hydrating the sucrose, and bulk water comprising the remaining water in solution, not associated with solute. Associated water has a longer relaxation time than the bulk water. The ^2H and ^{17}O NMR studies of Richardson and Steinberg(21), on the mobility of water in sucrose solutions, indicate three regions of decreasing rotational rates of water molecules with increase of sucrose concentration through saturation and continuing into the supersaturated regions. These effects were attributed to the development of an extensive but dynamic network of hydrogen bonds of water to sucrose, water bridging of the sucrose and direct sucrose to sucrose interactions (although no direct evidence of sucrose-sucrose interactions were observed). The bulk viscosities of these solutions also increase with increasing sucrose concentrations, in a manner consistent with the rest of the data, suggesting that the same short range interactions define both structure and transport.

Techniques like x-ray diffraction (22) probe order on the right length scales but may still be very noisy because many separate phenomena happen on similar length/time scales and no single process can be distinctly identified. Vibrational

spectroscopy (non-time correlated), like IR or Raman spectroscopy (23, 24-26) probes faster time scales and smaller length scales than those involved, subsequently important information is often impossible to extract or resolve because of poor "signal to noise" ratios.

Both steady state and time resolved fluorescence spectroscopy of trace fluorescent probes, like PBA and pyranine, yield data that directly measure transport coefficients as well as data that can be indirectly related by means of correlations to activity coefficients. Steady state fluorescence spectroscopy of pyranine is sensitive to the time scale where the exchange of the hydroxyl proton of the pyranine occurs. As the solution grows more concentrated the time required for such an exchange increases but the time required for exchange of the hydroxyl proton increases in the same way, and the distance that is effectively probed remains the same.

Time resolved fluorescence techniques are able to resolve information on the organization and dynamics of the intermolecular interactions in the microenvironment of a probe molecule (27). The advantage of time resolved fluorescence spectroscopy is its ability to probe the solvation environment of the entire probe molecule via measurement of lifetime and anisotropy. It is sensitive to the longer times scales of molecular diffusion in the context of the microenvironment of a probe molecule. In the nanosecond time resolved fluorescence experiment, we use a nanosecond pulse of light to excite a sample of solution doped with a fluorescent probe and detect the output emission. This signal, a waveform in the form of an exponential decay, is fed to an oscilloscope (the triggering of which is described later). The output is then analyzed to yield the emission lifetime and the anisotropic rotational decay. Rotational correlation times can be subsequently calculated. The emission lifetime of the fluorescent probe is highly sensitive to its solvation microenvironment and can provide information on the polarity of the constituents of the solvent environment and the diffusive behavior of collisional

quenche
about the
of the p
investig

6.2 Ex

6.2

PBA (C
which
highly
 $1 \times 10^{-}$
long l
of lon

proto
mice
al, (3
(33)
sodiu
it is a
studie
wavel
maxin

quenchers. Measurement of the anisotropic rotational decay can provide information about the microscopic transport properties and packing of the solvation environment of the probe molecule. This work concerns the use of fluorescence techniques to investigate microscopic transport in supersaturated solutions.

6.2 Experimental Methods

6.2.1 Fluorescent probes:

For this study we chose two fluorescent probes. In addition to pyranine, PBA (1-pyrene butyric acid, Figure 6.1) is a well characterized fluorescent probe which has been extensively used as an oxygen sensor(27). The PBA molecule is highly hydrophobic and readily forms excimers in water at concentrations above 1×10^{-3} M. It has a blue emission with peaks at 380 nm and 398 nm and an unusually long lifetime (~ 100 nsec). The long lifetime makes this probe useful in measurements of long rotational correlation times.

Pyranine (Figure 6.1), with its dissociable proton, is highly sensitive to proton transfer processes and has been applied to the study of water content of micellar dispersions (Clement and Gould, (28); Kano and Fendler, (29); Kondo et al., (30); Bardez et al., (31); and, Pines and Huppert, (32)), sols (Kaufman et al., (33)) and sol-gels (Pouxviel et.al., (34)) among other systems. Because the sodium ions of pyranine are believed to be completely dissociated in ionic solutions, it is a highly soluble probe in water. The photochemistry of pyranine has been studied and is described elsewhere (Kondo, 35). The protonated form emits with a wavelength maxima at 440 nm, while the dissociated form emits with a wavelength maxima at 511 nm. Competition between these two forms determines the relative

intensities of the fluorescence maxima and influences the apparent fluorescence lifetimes of each species. PBA and pyranine were obtained from Eastman Kodak and were used without further purification.

6.2.2 Preparation of Solutions

Samples for the time resolved experiments were prepared in the following manner: Ultrapure sucrose was obtained from Boehringer Mannheim. Sucrose solutions were prepared at $\sim 80^{\circ}\text{C}$ by dilution of a 80 wt.% solution with either 10 mM sodium borate buffer at pH 8.5, for sufficient solubility of PBA, or 18 Mohm reverse osmosis water, for pyranine, to make 10 g samples with concentrations ranging from 0 wt.% to 80 wt.%. The concentration of PBA used was 2×10^{-6} mole/Kg of solution, while the concentration of pyranine was 1×10^{-5} mole/Kg of solution. The fluorescent probes were added to both the 80 wt.% solution and water prior to dilution. Samples were then allowed to cool to 22°C at least 3 hours and were not deoxygenated prior to measurements. Suprasil Quartz cuvettes were used to contain the samples during the measurements.

For the steady state fluorescence, and UV absorption experiments, reagent grade sucrose from Sigma Chemicals, and 18 Mohm reverse osmosis water were used. Stock solutions of 100 ppm (1.9×10^{-4} M) pyranine were prepared using 18 Mohm reverse osmosis water. Solutions of the 10 ppm (1.9×10^{-5} M) and 1 ppm (1.9×10^{-6} M) were prepared by dilution. The amount of sugar and water required for 10 grams (.01 kg) of each solution was calculated beforehand. Reagent grade sucrose samples were weighed to $\pm 1\%$ of the required amount. Samples were prepared in 20 ml glass vials by adding the predetermined amount of stock solution to achieve the desired concentration. Samples varied in concentration between pure water and 80 wt.% sucrose. In undersaturated solutions, samples were prepared in

10 wt.% intervals. Samples near saturation were taken at 2 wt.% intervals, eg. for sucrose between 60 and 74 wt.%, and solutions at high concentrations, eg. 76 wt.% and 80 wt.% solutions of sucrose, were also prepared. Supersaturated solutions were prepared by heating the vials in a water bath until the sugar dissolved. Spectra of the solutions were taken within 6 to 24 hours of preparation to ensure equilibration of the sugar in solution and prevent biological contamination of the sugar solutions.

6.3 Results and Discussion

6.3.1 Steady State Fluorescence Spectra and UV Absorption

Steady state fluorescence spectra of pyranine in sucrose solutions of various concentrations have been presented elsewhere. UV absorption spectra of pyranine in sucrose solutions are presented in Figure 6.2. These spectra were obtained in quartz cuvettes of 10 mm path length at 298 K using a Perkin Elmer Lambda Array UV-Vis spectrophotometer. These follow the same general trends as the steady state fluorescence emission spectra (presented elsewhere) and exhibit an absorption isosbestic point at 342 nm. Peaks at 350 nm and 400 nm correspond to absorption of the protonated and deprotonated forms of pyranine. Note that the UV absorption spectrum of pyranine in water follows the same general trends in profile as the spectra of the pyranine doped solutions of sugar but exhibits an isobestic point at 325 nm instead of 342 nm. Two less concentration sensitive bands are observed at 280 nm and 220 nm respectively. The spectra in saturated sucrose solution and the 76 wt.% solution show a peak at 400 nm and 525 nm respectively. The intensity of the UV absorption peaks at 350 nm and 342 nm are a function of concentration

though not nearly as well behaved and sensitive to concentration as the fluorescence spectra. It is worth noting that the UV absorption and steady state fluorescence spectra are related in such a manner as to suggest that fluorescence is observed from single probe molecules and that no excimer formation is observed.

6.3.2 Time resolved Fluorescent Lifetimes

The total fluorescence lifetime measures the average time for a population of probe molecules to return to the ground state from the photoexcited state. Total fluorescence lifetimes of PBA, vary as a function of concentration, Figure 6.3. At sucrose concentrations below 50%, the fluorescence decay at an emission wavelength of 380 nm was adequately fit by a single exponential term, while two exponential terms were required at higher concentrations. The value of the longer lifetime is 100 ns in the buffer and increases to about 125 ns at 55 wt.%. Above this concentration, the longer lifetime remains constant up to 80 wt.%. Values for the short lifetime ranged from 0 to 40 ns. The ratio of the pre-exponential terms for the fast component to the long component is shown in Figure 6.4. Remaining at a constant value of 0.1 from 50 wt.% to about 70 wt.% the ratio increases dramatically near the saturation concentration. At 400 nm, as seen in Figures 6.5 and 6.6, the short component is present at all concentrations measured and shows a higher intensity relative to the long component than at 380 nm. The same trend is seen at both 380 nm and 400 nm as the sucrose concentration is increased.

The fluorescence lifetimes of pyranine in sucrose solutions displays greater variation than the lifetimes of PBA as the concentration increases as depicted in Figure 6.7. Three regions are again present for both wavelengths as the concentration increases to 80 wt.%. For the emission at 440 nm, two exponential components are required to fit the total fluorescence decay for concentrations up to

40 wt.%. A low intensity long component (not shown), of about 10 ns, is present along with the dominant short component. The pre-exponential factor for the low intensity decay is less than approximately 2 % of the dominant decay. Because of the relatively large intensity of the 511 nm band at these concentrations, the long lifetime component is likely due to overlap from this emission. The fluorescence decay at 511 nm, attributed to the deprotonated form, can be fit by a single exponential term throughout the entire range of concentrations. In the dilute solutions, the apparent lifetimes of both species are relatively constant, with the protonated form exhibiting a value of 0.5 ns and the deprotonated form exhibiting a value of 5.5 ns. At 40 wt.% the lifetime at 440 nm begins to increase, while the lifetime at 511 nm shows a slight decrease to 5.4 ns and remains relatively constant up to a concentration of 66 wt.%. In saturated solutions, the lifetime at 511 nm decreases sharply to a value of 4.4 ns at 80 wt.%. The lifetime at 440 nm continues to increase less sharply and plateaus to 3.6 ns near 80%.

The increase in the lifetime of PBA is most likely due to the combined effects of the decreased collisional quenching by oxygen and the decreased polarity of the solvent. Because of the long lifetime of PBA, its diffusional radius in the excited state is also large. Interactions with collisional quenchers are possible during this period which lead to a decrease in the fluorescence lifetime of PBA. At dilute concentrations of sucrose, the lifetime may be shortened by collisions with dissolved oxygen. As the solutions becomes more concentrated, the diffusion of both pyrene and oxygen is hindered, causing an increase in the lifetime of PBA. Additionally, PBA is known to have a longer lifetime in more hydrophobic solvents, due to an increased rate of radiationless transitions from the excited state to the ground state for more polar solvents. The increase in the lifetime of PBA is most likely due to the decreased diffusional radius of oxygen in the excited state of PBA and the increased hydrophobicity of the solvent.

The component that fluoresces with a lifetime of 0-40 ns in PBA doped supersaturated solutions observed at 380 nm and 400 nm and pyranine doped solutions observed at 440 nm could be due to some impurity in sucrose. This impurity is probably natural or could occur as the result of the way the solutions were prepared. It probably competes with the sucrose for water of solvation and becomes more concentrated as the availability of bulk water decreases with increase in concentration, contributing significantly to the fluorescence only in very concentrated solutions. The fact that the contribution due to this component in dilute solutions is low compared to the probe emission indicates that either the impurity has a low quantum yield and/or the concentration of impurity in dilute solutions is very low. Because of the high percentage of the total fluorescence that is attributed to this impurity at high sucrose concentrations, it is likely that in these solutions it is present in concentrations higher than that of the probe (which probably has a higher quantum efficiency) which suggests that it may be a natural impurity or the result of some reaction that takes place at 80°C involving the breakdown of sugar.

The changes in the fluorescent lifetimes of pyranine are probably caused by changes in the rates of protonation and deprotonation. Pyranine is highly sensitive to the proton accepting abilities of the solution. The various forms of the pyranine probe as a proton donor in a two-state excited-state reaction are depicted in Figure 6.8. In bulk water, the protonated and the deprotonated ground state forms of pyranine exist at equilibrium with a pKa of 7.5. Upon excitation, the pKa for the molecules in the excited state decreases to 0.5, causing a shift to the deprotonated form. The rates for this process in water have been reported to be 2.1×10^9 and about 10^{15} s^{-1} for the forward and reverse rates, respectively (Kondo, 35). Thus, the excited pyranine probe exists almost completely in the deprotonated form in bulk water. The observed fluorescence lifetime of each form of pyranine is dependent on the intrinsic rate of excited state decay, k_i , the rate of radiationless decay, k_r , and the

rates of exchange between the protonated and deprotonated forms. The lifetime of fluorescence emission, excluding the effects of proton exchange, is related to the intrinsic and radiationless decay rates by,

$$\tau = \frac{1}{k_f} = \frac{1}{k_i + k_r}$$

where $k_f = k_i + k_r$. A value of $1.6 \times 10^8 \text{ s}^{-1}$ for k_f has been found and corresponds to a lifetime of about 6 ns. This value agrees with the observed lifetime of the deprotonated form and indicates that the reverse reaction is negligible at bulk water conditions.

It has been argued that the relative increases of the steady state fluorescence intensity of the protonated form as compared to the deprotonated form, due to solvent effects, can be attributed to decreases in k_1 (Kondo, 35). Otherwise, the unlikely possibility that the intrinsic fluorescence lifetime must decrease, in order to account for this effect, must occur. Thus, the observed increase in the apparent lifetime at 440 nm can be attributed to a decreased rate of deprotonation. Similarly, the decrease in the apparent lifetime at 511 nm indicates an increase in the rate of protonation. Together, these rates determine the equilibrium observed in the steady state spectra of pyranine. The rate effects are related to the availability of solvation water and its distribution in sucrose solutions. Physically, the proton transfer processes can be related to the associations of the water molecules in solution. A water molecule not associated with solute is able to accept protons from donor molecules owing to its ability to transfer the protons to other free water molecules in proximity. However, if all of the tetrahedral hydrogen bonding sites of water are occupied, proton exchange cannot occur. The time scales of the molecular motions and associations are the determining factors governing the specific behavior of these

exchange effects. When water is involved in the solvation of sucrose, interacting indirectly or directly, its mobility may be hindered by the sucrose molecule and cause the subsequent decrease in the rate of proton transfer. This leads to the view that the protonated form of pyranine interacts with the water involved with the solvation of sucrose, while the deprotonated form interacts with the bulk water.

From PIR ratios of the steady state fluorescence spectra, the ratio of the solvation and bulk water molecules decreases as the sucrose concentration increases and at saturation, there is one mole of solvation water for every mole of bulk water. Furthermore, the behavior of the fluorescent lifetime of pyranine can provide dynamic information on the structure of sucrose solutions. In the dilute region the relatively constant lifetimes of both the protonated and deprotonated species indicate that the environment of pyranine does not change appreciably. As the concentration is increased in the 40 wt. % to 66 wt. % range, the behavior of the lifetimes suggests that the water associated with sucrose becomes increasingly less mobile, while the bulk water experiences a decrease in its mobility at 40 wt. % but remains relatively mobile up to 66 wt. %. At saturation, the bulk water begins to experience additional effects of the sucrose by becoming less mobile.

6.3.3 Time Resolved Fluorescence Anisotropy

The rotational correlation time of the probe in solution is a measure of the time required for reorientation of its excited state dipole moment and is related to its rotational diffusion. Another indication of the nature of short range interactions between the probe and its solvation environment is found in the nature of the relationship between the rotational correlation time and viscosity. Rotational correlation times of PBA in sucrose solutions are shown in Figure 6.9. It is apparent that there are three regions as the concentration varies from 0 wt. % to 80 wt. %. In

the first region, with sucrose concentrations between 0 wt.% to about 40 wt.% the measured rotational correlation times are nearly instantaneous relative to values at higher concentrations. The accurate determination of these values are beyond the limits of the instrumentation used. A more apparent increase occurs above about 40-45 wt.% up to about the saturation concentration (67 wt.%), in the second region. In the third region, above about 66 wt.%, two components in the anisotropic decay become present. The fast component increases linearly as the concentration increases from a value near zero up to about 10 ns. In contrast, a dramatic increase of almost three orders of magnitude is seen in the long component. Figure 6.10 shows the dependence of the rotational correlation time on viscosity up to 74 wt.% sucrose. The short rotational correlation time increases only slightly as the viscosity increases. A linear relation between the rotational correlation time and viscosity is seen for the long component. The slope of the linear fit is 6.2×10^{-2} ns/cP with an intercept at 0.94 ns.

Another depiction of the three regions of concentration dependent behavior is illustrated in Figure 6.11 with the rotational correlation time of pyranine. The rotational correlation times of the protonated and deprotonated form of pyranine are, within experimental error, the same in the entire concentration range. In the low concentration range, below 40 wt.%, the rotational correlation time is nearly zero. Above this concentration, the rotational correlation time increases as the concentration increases. However, the increase above the saturation concentration is less than that with PBA. This is seen more clearly in Figure 6.12, where the rotational correlation time is plotted against viscosity. Below a concentration of about 66 wt.%, the rotational correlation time increases linearly in relation to the viscosity with a slope of 1.5×10^{-1} ns/cP for both the protonated form and the deprotonated form. The intercepts occur at 1.7 ns and 0.6 ns, for the protonated

form and deprotonated form, respectively. These values clearly level off, however, as the solution becomes supersaturated up to 74 wt. % sucrose.

The bulk viscosity shows three characteristic regions of structural organization. The relationship between rotational correlation time and viscosity is linear for PBA. In the case of pyranine, this relationship is nonlinear above 66 wt. % sucrose. This behavior may be interpreted in terms of the difference in molecular structure and geometry, and the difference in the way each probe interacts with its solvent environment. Both nonsphericity of the probe molecule and solvent interactions contribute to the rotational behavior of the probe.

PBA can form hydrogen bonds only at the carboxyl group of its side chain and has minimal interactions with solvent. However, pyranine has up to three negatively charged sulfonate groups directly on the pyrene which can exert a greater effect on its solvation shell. A molecule of PBA in aqueous solution can be approximated by an oblate spheroid within its solvation shell. Because of the additional polar groups on pyranine, however, this molecule may exist in a more spherical cavity and thus rotate at a greater rate. From the slopes of the rotational correlation time versus the viscosity the diameter of the spherical rotational cavity for PBA is found to be 8 Å. This corresponds well to the actual 7 Å value for the largest diameter of a pyrene group. At concentrations below 60 wt. % sucrose, the diameter for the spherical rotation of pyranine is found to be slightly larger at 11 Å. This may reflect the slightly larger size or greater charge interactions of the pyranine molecule in solution. However, neither molecule is strongly solvated by water, because of the similarity of the hydrodynamic diameters to actual molecular dimensions. Above saturation, the rotational correlation rate for pyranine does not vary linearly with viscosity and partial slip boundary conditions are observed. This may be interpreted, in view of the shape and free space arguments, as an increased ordering of the solvent shell around the pyranine molecule. The ordered shell provides a cavity

within the solution in which pyranine may rotate with a decreased degree of solvent displacement. In this ordered shell, the electropositive hydrogen atoms of the solvent would interact with the negatively charged groups allowing additional rotational movement with minimal disruption of the hydrogen bonding organization in the surrounding fluid. As the pyranine probe rotates, charges on it may be relayed among the hydrogen atoms, in a manner similar to the transfer of protons in bulk solution. This notion is supported by NMR studies, showing that the transverse relaxation rates for ^2H are an order of magnitude faster than the relaxation rate than that of ^{17}O . Likewise, the linear relationship observed with PBA may be explained by the nature of its rotational cavity. A possibility may be that the solvation environment of the PBA molecule is less polar and more homogeneously distributed about the pyrene molecule, and does not provide for the formation of a spherical cavity. Because the rotational cavity of PBA may be considered more oblate than that of the pyranine molecule, out of plane rotations would necessitate a greater degree of solvent reorientation in the immediate solvation microenvironment of the probe.

This analysis is particularly interesting because it calls upon a macroscopic hypothesis to explain a microscopic situation. An important issue is why this kind of reasoning should apply at all. One reason could be that, at these concentrations, the fluid environment of the probe is homogeneous. So the crux of the issue is the structure of the solvent environment of each of these probes. At concentrations of sucrose below saturation, the rotation of small probe molecules are essentially similar. However, a marked divergence is seen at saturation indicating a fundamental structural change in the structural organization of the solution. Regardless of the specific explanations for increased rotational mobility, it is clear that solute mobility in sucrose solutions decreases as the concentration is increased.

6.4 Structural Characteristics of Sucrose Solutions from Transport Properties

The solution structure of dilute solutions up to a concentration of about 35-45 wt.% has been described in terms of an isotropic two state model (e.g. (21)) in which the rotational mobility of water is a weighted average of the rotational mobilities of solvation water and bulk water. Anomalous behavior has been observed in solution between 30 and 40 wt.% in FTIR and Raman spectra and X-ray diffusion as well. The increase in the fluorescence lifetime of PBA at around 40 wt.%, is likely explained by the same underlying cause. The PIR calculated from steady state fluorescence spectra of pyranine, the fluorescence lifetimes of the protonated and deprotonated forms of pyranine and the rotational correlation times of PBA and pyranine exhibit relatively small changes in this region. Thus, although the solution becomes more concentrated and more water is bound to the sucrose, the behavior of the rotational correlation times indicates that the structure of the bulk phase water does not change appreciably from that of pure water.

As the concentration increases from 40 % to about 66 % sucrose, the behavior of the fluorescence properties of the probes indicates a nonlinear structural transformation where the solution becomes less fluid. This structural transformation has been characterized in NMR and X-ray diffraction studies as the formation of a network type structure of hydrogen bonding throughout the solution. These hydrogen bonds have been postulated to be comprised of the water-water interactions, hydrogen bond bridging between sucrose molecules and sucrose-sucrose interaction. However, it is not possible to correlate these microscopic interactions to specific locations relative to the sucrose molecule. Because of the almost identical rotational correlation times measured for the protonated and

deprotonated forms of pyranine, the mobilities of the solvation water and bulk water appear to behave similarly at the nanosecond time scales of these measurements. From this, it can be inferred that these solutions are isotropic at this time scale so that sucrose-sucrose interactions if they occur at all are minimal, and the associated water is not locally "bound" to sucrose. When in addition the steady state fluorescence data are taken into account, it is clear that sucrose-sucrose interactions in these solutions are unlikely to occur because on the average the sucrose molecules appear to be completely solvated and there is still enough bulk water in solution to achieve the complete solvation of all sucrose molecules. The average solvation microenvironments of both protonated and deprotonated forms of the pyranine molecule is indicated to be roughly the same although the local solvation environment around the probe hydroxyl moiety differs.

This region corresponds to the point where the number of molecules of bulk water per molecule of sucrose decreases from about 40 to about 6. This is also the region in which the sharpest changes in IR and Raman spectra are observed. A molecule of solute in 35 - 45 wt. % solution of sucrose is effectively still in a dilute solution because there are enough water molecules around it so that this water is still not influenced by the effect of nearby sucrose molecules. As the number of solute molecules increases, first, the effect of the water molecules dynamically associated to solute and then, that of water more strongly associated, exerts itself on water molecules not participating in the solvation of sucrose. Over a relatively small concentration range, the number of molecules of bulk water drops exponentially. This should be reflected by a sharp decrease in the rotational correlation time of the probe however no such sharp decreases are observed. Most of the molecules of water solvating the probe in solutions at these concentrations are already partially associated, either strongly or dynamically, to the solute molecules. Transport in this concentration range changes over from that governed essentially by the interaction of

probe with bulk water, to that resulting from the interaction of the probe with at least partially solute associated water. It is likely that in this region the changes observed are due to changes in structure associated with the solvation water.

Near the saturation point, another structural transformation is evident from the sharp decrease in the lifetime of the deprotonated pyranine, the rapid increase in the rotational correlation time of PBA and the relative leveling of rotational correlation time of pyranine. Additionally, the PIR indicates that the molar ratio of bulk to solvation water per molecule of sucrose is approximately unity. At this point, it is likely that the structure of the bulk water phase is considerably different from that of pure water. There are not enough water molecules per molecule of solute to support the variety of flickering clusters that are found in pure liquid water under identical conditions. The attractive forces between water molecules may take precedence over the attractive forces between the deprotonated pyranine and water for reasons of structural stability. It could be that there is enough bulk water to dissociate a few pyranine molecules but not for as long a time as in dilute solutions, because it is more important for the water to form clusters with other bulk water molecules. As the bulk water continues to decrease in quantity and change in structure and average coordination, the effects of molecular structure and solvation environment on rotational correlation time and viscosity become more pronounced.

The most surprising and interesting observation, however, concerns the implication of the sharp drop in the lifetime of the deprotonated pyranine on the dynamics of the bulk water. The UV-vis absorption and the steady state fluorescence spectra indicate that the absorption or emission is due to photon transfer between the same excited states: i.e.; the decrease in lifetime can be attributed to a decrease in the rate of radiative transfer as opposed to a decrease in the rate of non-radiative transfer. The behavior of the fluorescent lifetime, remaining more or less constant up to the saturation point, indicates that the "lifetime" (the interaction time) of the bulk

water up to the saturation point remains more or less the same despite the change in structural organization. At saturation, the sudden drop in the lifetime of deprotonated pyranine must also reflect an equivalent change in the "lifetime" of the bulk water. The bulk water is not only reduced in quantity and changed in structure, it is also available to pyranine for less time which means it must spend time trying to find other water molecules to coordinate with and/or moving faster to satisfy all its needs i.e., solvating deprotonated pyranine, finding other water molecules to coordinate with, coordinating with other water molecules, maintaining structural integrity of the solution etc.

One might object to the idea that bulk water moves faster in supersaturated solutions than in undersaturated ones because it seems contrary to intuition. However, when the energetics of the formation of a supersaturated solution are considered, this notion begins to make sense. It is impossible to make a phase transition from undersaturated to supersaturated solution without the addition of large amounts of external energy. This energy serves to increase the disorder of the solution and also increase the probability that enough bulk water molecules will be present in the vicinity of all the unsolvated solute molecules (one at a time) to solvate them (one at a time). The most common way of accomplishing this is to heat the solution until all the solute dissolves. Then as the solution cools, the solvated solute molecules transfer their kT energy to the surroundings, and become less mobile, (accounting for most of the cooling effect since these contain most of the mass) and the bulk water loses some kT energy as well. Under identical conditions of pressure and temperature, a supersaturated solution contains more energy per unit mass and volume than a saturated solution. In addition, the energy in a supersaturated solution is probably partitioned differently. If we compare a supersaturated solution with a saturated solution, the solvated solute in the supersaturated solution is much less mobile. It contains most of the potential energy of the solution but very little of the

translational energy. The difference in energy between the two solutions cannot be accounted for in terms of potential effects alone because there is an additional large energy barrier that must be overcome in order to reach supersaturation. What then is responsible for keeping the supersaturated solution at a higher energy? One factor might be that the bulk water moves faster relative to solvated water in supersaturated solution than in a saturated solution; even though on an absolute basis, both bulk and solvation water are less mobile.

The transport of solute and solvent in supersaturated solutions are not necessarily coupled in the same manner as in dilute solution. The solute is solvated and the time correlated fluorescence anisotropy measurements in supersaturated solutions indicate that the solvation microenvironment of the probe molecule behaves as if it is a homogeneous mixture of solvations (solvated solute molecules). We were thus, at the time this work was done, led to believe that in supersaturated solution the diffusional motion of the solute is closely coupled to that of the solvation shell surrounding it. That is to say the solute molecule is not likely to diffuse independently of a solvation shell on the time scale required for diffusion. The solvent, in addition to the option of being able to diffuse through the solution as bulk solvent, or with the solute as a part of the solvation shell, also has the option of being transported through exchange processes. These exchanges may be slower in supersaturated solution than in dilute solution, but are still faster on a relative basis than diffusion processes. Therefore it may be possible for water not to build up locally due to release of solvent or to associate locally over short periods of time if transported through solvent exchange. The solvent exchanged at one point in solution is not the same molecule that participates in an exchange process elsewhere, but it doesn't have to be so long as local requirements for order are met.

6.5 Self-Diffusion and Structure

In retrospect the increase in viscosity, and decrease in diffusion coefficients take on a different significance. Pan's data indicate that both the solvation water and the non-solvation water exhibit decreased mobility and increased correlation times in supersaturated solutions. In dilute solution where the solvation water is not strongly associated with the solute is somewhat more appropriate to describe diffusion in terms of solute and solvent, than in non-dilute solutions. When the solvation water mobility is such that it becomes strongly associated with the solute it is necessary to consider a solvaton as the appropriate unit to describe diffusion. As the solute concentration increases in solution the average distance between solvatons decreases, and the amount of total non-solvation water exponentially decreases. Once the concentration is such that the solvatons are likely to solvate the non-solvation water, the solvatons are the primary source of transport resistance.

It is useful to consider the resistance to mass transfer during self-diffusion of a species in solution in terms of the time required for that species to encounter a solvation environment identical to its initial solvation environment. The surface area of the sphere with a radius equal to the distance a solvaton must travel from its initial position to encounter an identical solvation environment divided by the time required for it to travel that distance represents the coefficient of self-diffusion for the solvaton. The viscosity can then be thought of as the ratio of the force of resistance experienced by the solvaton in traveling this distance to the diffusion coefficient. As the radius of the sphere approaches zero, so does the coefficient of self diffusion for the solvaton, while the viscosity of the solution approaches some large number. In dilute solution where the distance between solvatons (which are themselves more loosely associated) is large and the mobility is high, diffusion coefficients are fairly

high, and viscosity is fairly low. As the solution becomes more concentrated the radius of the sphere decreases as does the mobility of both the solvations and the bulk water, and the time required to diffuse increases, consequently the diffusion coefficient decreases and the viscosity increases. While this is true in general of non electrolytes, in the case of electrolytes the mobility of the hydrated ions will generally remain high as the time required to travel between identical solvation environments decreases. Therefore the self-diffusion coefficients in electrolyte solutions may appear to increase up to the saturation point, after which the radius of the sphere decreases so much as to cause the diffusion coefficient to drop precipitously. In supersaturated solutions of non-electrolytes where the solvation environment of the solvations are fairly identical from point to point, the distance the solvation must travel to experience an identical solvation environment approaches zero, and so does the coefficient of self-diffusion. The measurements of Sorrel and Myerson (9,14), and Myerson and Chang (15-18) indicate that this is indeed the case for many systems. Pan's observations also lend support to this interpretation.

6.6 Conclusions

We have demonstrated that fluorescence techniques provide a means by which transport and microenvironmental properties can be measured and consequently, the molecular structure of solutions can be inferred. As a result of the time resolved measurements with PBA and pyranine in sucrose solutions, further evidence is available suggesting that the structure and composition of bulk water changes with an increase in sucrose concentration from a nearly pure water like structure to a very different structure in supersaturated solutions. Information on the localized structure can be extracted from this data and incorporated with information obtained from other means. As the solution becomes more concentrated, the structure of the water transforms from a relatively unperturbed form to one in which a hydrogen bonding network between dispersed sucrose molecules are bridged by the solvation water with minimal effect on the bulk water. In supersaturated solutions, however, the remaining bulk water also becomes associated to the sucrose forming a third type of solvent interactions. The water in supersaturated solutions is likely to exist in tetrahedrally coordinated form for much shorter times than those observed bulk water at saturation.

Analysis of the difference in the nature of the correlation between rotational correlation time and viscosity for the two different probe molecules confirms the importance of understanding the short range interactions that govern transport. In concentrated sucrose solutions, it may prove useful to describe the solution as a homogeneous network of solvated solute molecules connected by more mobile and dynamic bulk solvent molecules. In the case of water as a solvent, it may be more important for structural integrity for the bulk water to form stable coordinated structures than to make itself available for solvation of probe molecules.

We saw evidence of both bulk and solvation water in solutions of all concentrations examined. No indication of microheterogeneities in solution microstructure was observed. The solutions appear to be isotropic and thus, no apparent microscopic clustering of the sucrose molecule is present in noncrystallizing solutions. On the basis of our investigation of sucrose solutions using steady state and time resolved fluorescence spectroscopy of fluorescent probes we can conclude that it is unlikely that there are solvent exclusive clusters of solute molecules in the metastable supersaturated sucrose solutions.

6.7 References

1. Wolynes P.G., *Annu. Rev. Phys. Chem.*, **31**, 345, (1980).
2. Wolynes P.G., *J. Chem. Phys.*, **86**(9), 5133, (1987).
3. Chakraborty R. and K. A. Berglund, *AIChE Symposium Series no. 284*, 114, (1991).
4. Cross, A. J. and J.D. Simon, *J. Chem. Phys.*, **86**, 7079, (1987).
5. Maroncelli M., J. MacInnis, and G.R. Fleming, *Science*, **243**, 1674, (1989).
6. Migus A., Y. Gauduel, J.L. Martin, and A. Antonetti, *Phys. Rev. Lett.* , **58**(17), 1559, (1987).
7. Brady J.W., *J. Am. Chem. Soc.*, **11**, 5155, (1989).
8. Stokes, R.H. and R.A. Robinson, *J. Phys. Chem.*, **76**, 2126 (1966).
9. Sorrel, L.S. and A.S. Myerson, *AIChE J.*, **28**, 772 (1982).
10. Larson, M.A. and J. Garside, *Chem. Eng. Science*, **41**, 1285 (1986).
11. Larson, M.A. and J. Garside, *J. Crystal Growth*, **76**, 88 (1986).
12. Larson, M.A., *AIChE Symposium Series no.240*, **80**, 39-44 (1984).
13. Narayanan, H. and G.R. Youngquist, *AIChE Symposium Series no. 253*, **83**,1-7 (1987).
14. Myerson, A.S. and L.S. Sorrel, *AIChE Journal*, **28**,778 (1982).

15. Myerson, A.S. and Y.C. Chang, in Industrial Crystallization '84, S.J. Jancic and E.J. DeJong (Eds.), Elsevier, Amsterdam, 27 (1984).
19. Ginde R. and A. S. Myerson, *AIChE Symposium Series no. 284*, 124, (1991).
16. Chang, Y.C. and A.S. Myerson, *AIChE J.*, **31**, 980 (1985).
17. Chang, Y.C. and A.S. Myerson, *AIChE J.*, **32**, 1567 (1986).
18. Chang, Y.C. and A.S. Myerson, *AIChE J.*, **32**, 1747,(1986).
20. Suggett, A. and A.H. Clark, *J. Solution Chem.*, **5**, 1, 1 (1976).
21. Richardson S.J. and M.P. Steinberg, in Water Activity: Theory and Applications to Food, L. B. Rockland and L.R. Beauchat eds., Marcel Dekker Inc., New York, 235, (1987).
22. Mathlouthi M., *Carbohydrate Res.*, **91**, 113, (1981).
23. Back D.M., D.F. Michalska, and P. L. Polavarapu, *Appl. Spectroscopy*, **38**(2), 173, (1984).
24. Mathlouthi M and D.V. Luu, *Carbohydrate Res.*, **78**, 225, (1980).
25. Mathlouthi M. and D.V. Luu, *Carbohydrate Res.*, **81**, 203, (1980).
26. Mathlouthi, M., C. Luu, M. Meffrov-Biget and D.V. Luu, *Carbohydrate Res.*, **81**, 213 (1980).
27. Kalyanasundaram K., Photochemistry in Microheterogeneous Systems, Academic Press Inc., (1987).
28. Clement, N.R. and M. Gould, *Biochemistry*, **20**, 1534 (1981).
29. Kano, K. and J.H. Fendler, *Biochim. Biophys. Acta*, **509**, 289 (1978).
30. Kondo, H., I. Miwa and J. Sunamoto, *J. Phys. Chem.*, **86**, 4826 (1982).
31. Bardez, E., B.T. Gouguillon, E. Keh and B. Valeur, *J. Phys. Chem.*, **88**, 1909, (1984).
32. Pines, E. and D. Huppert, *J. Phys. Chem.*, **87**, 4471 (1984).
33. Kaufman, V.R., D. Avnir, E. Pines-Rojanski and D. Huppert, *J. Non-Crystalline Solids*, **99**, 397 (1988).
34. Pouxviel, J.C., B. Dunn and J.I. Zink, *J. Phys. Chem.*, **93**, 2134 (1989).
35. Kondo, H., I. Miwa and J. Sunamoto, *J. Phys. Chem.*, **86**, 4826 (1982).

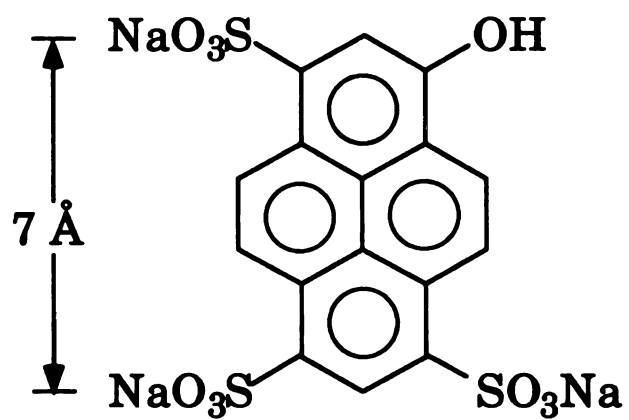
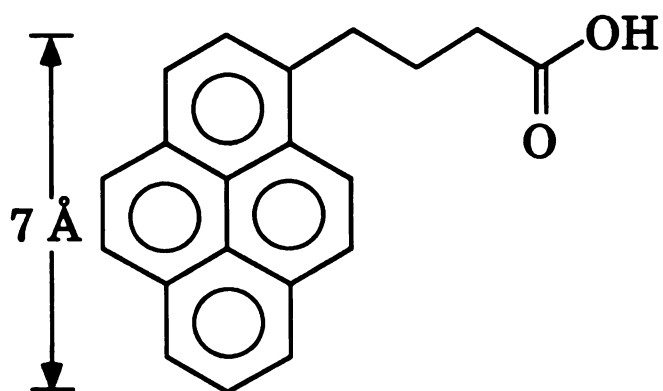


Figure 6.1. Structures of PBA (top) and pyranine (bottom).

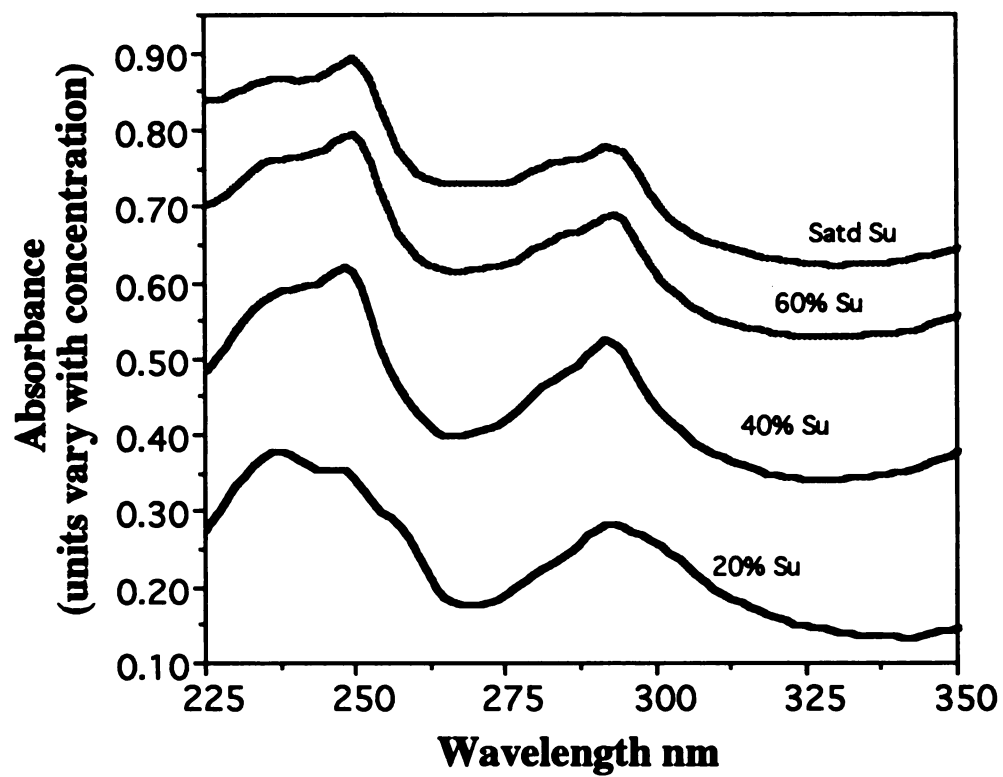


Figure 6.2 UV-vis spectra of 10 ppm pyranine in aqueous sucrose solutions of various concentrations at 293 K.

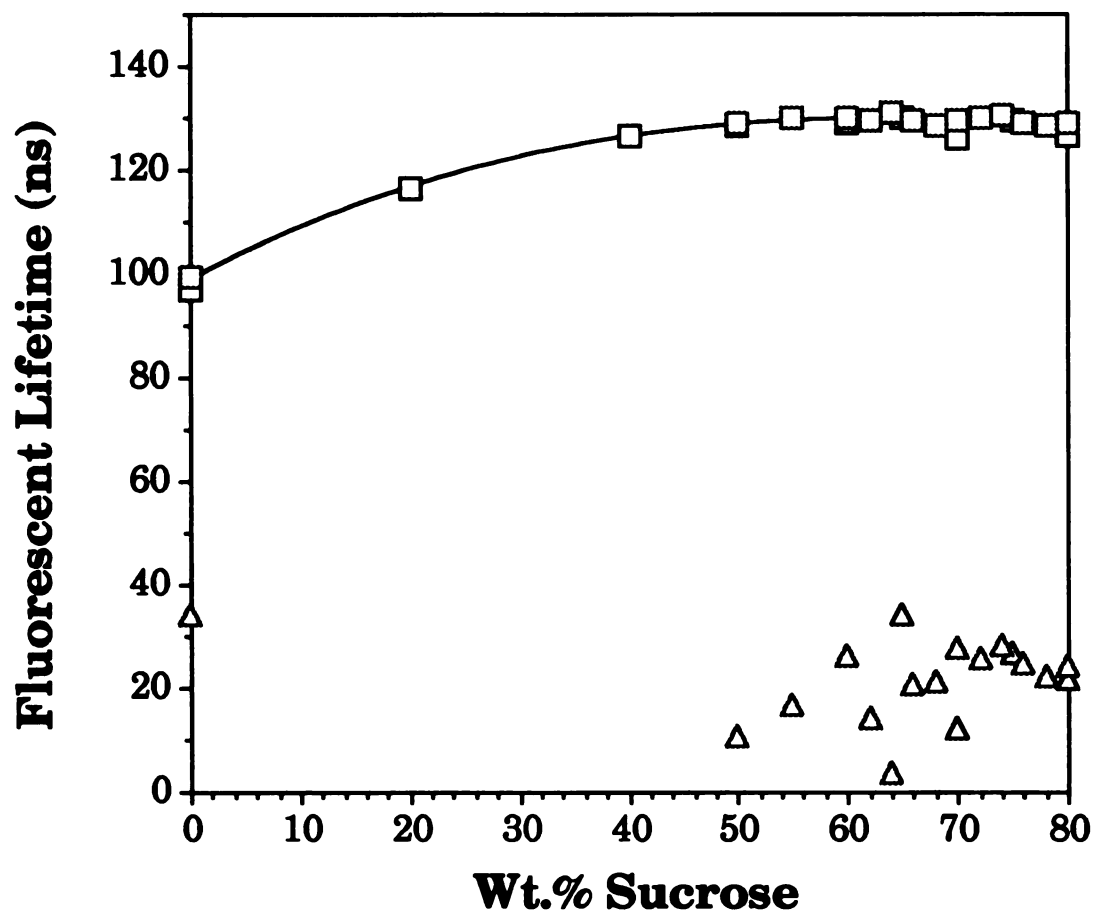


Figure 6.3. Fluorescent lifetimes of PBA in sucrose solutions observed at 380 nm and 293K as a function of sucrose concentration. Squares (□) represent the long lifetime component and triangles (Δ) represent the short lifetime component.

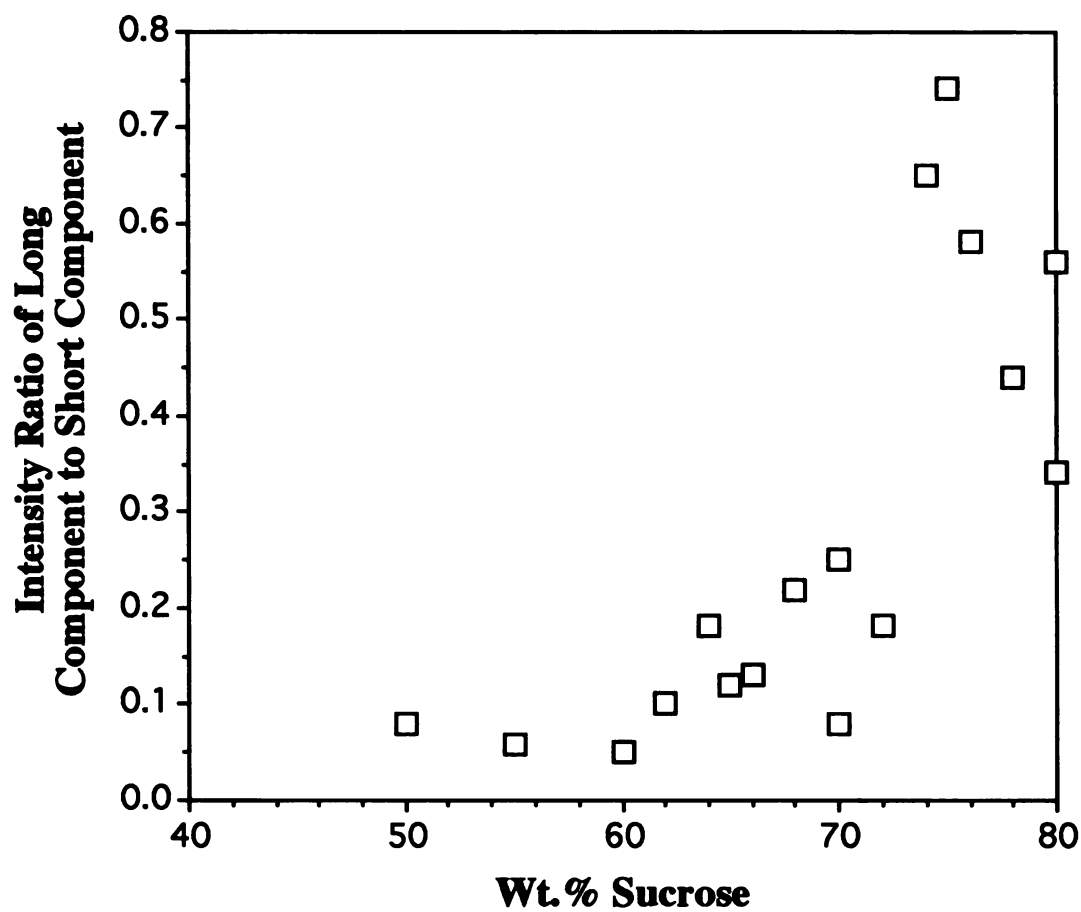


Figure 6.4. Ratio of the intensities of the long lifetime component to the short lifetime component of PBA at 380 nm.

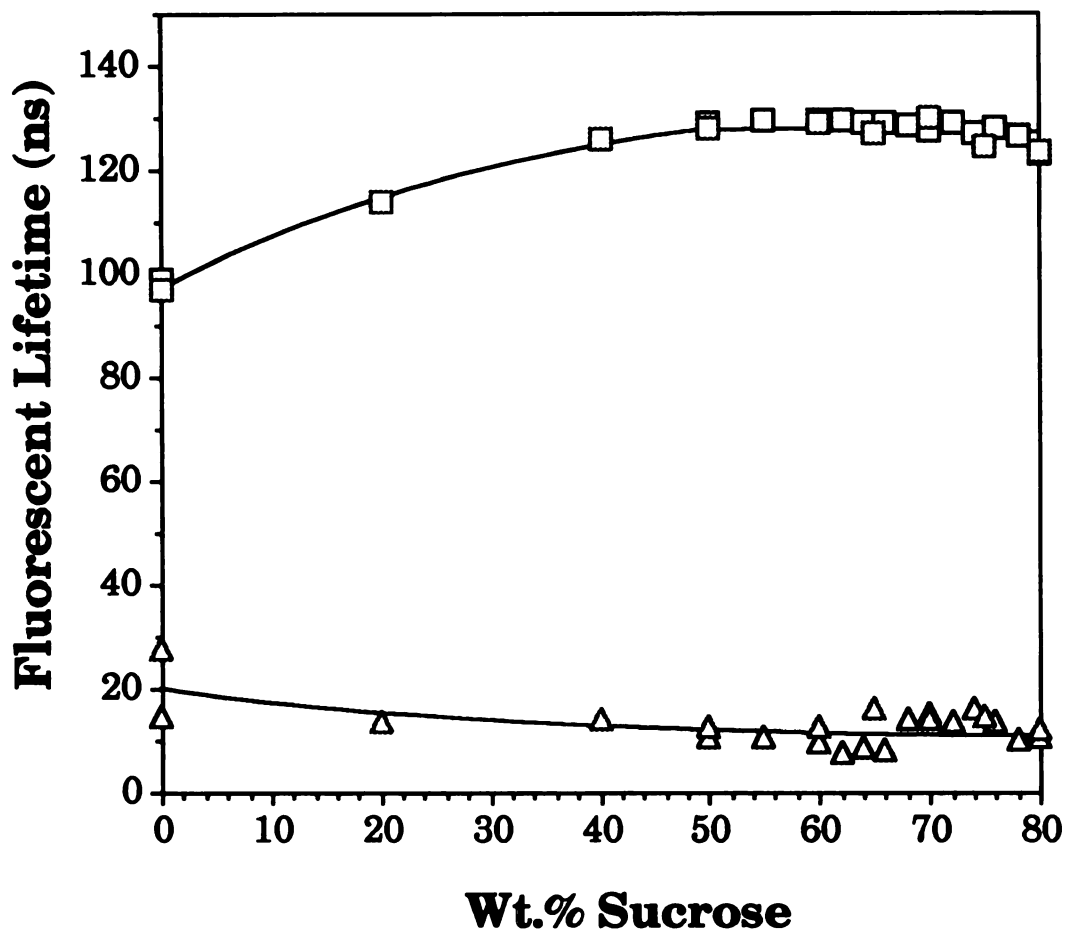


Figure 6.5. Fluorescent lifetimes of PBA in sucrose solutions observed at 400 nm and 293K as a function of sucrose concentration. Squares (□) represent the long lifetime component and triangles (Δ) represent the short lifetime component.

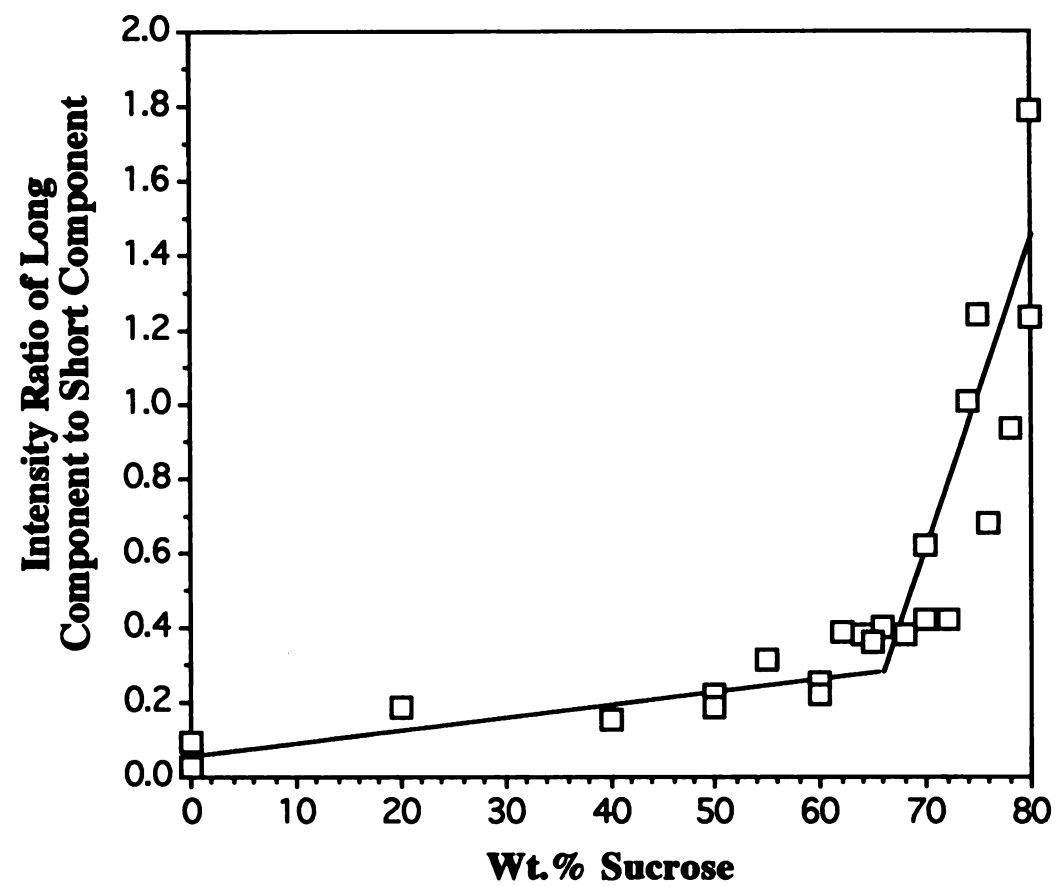


Figure 6.6. Ratio of the intensities of the long lifetime component to the short lifetime component of PBA at 400 nm.

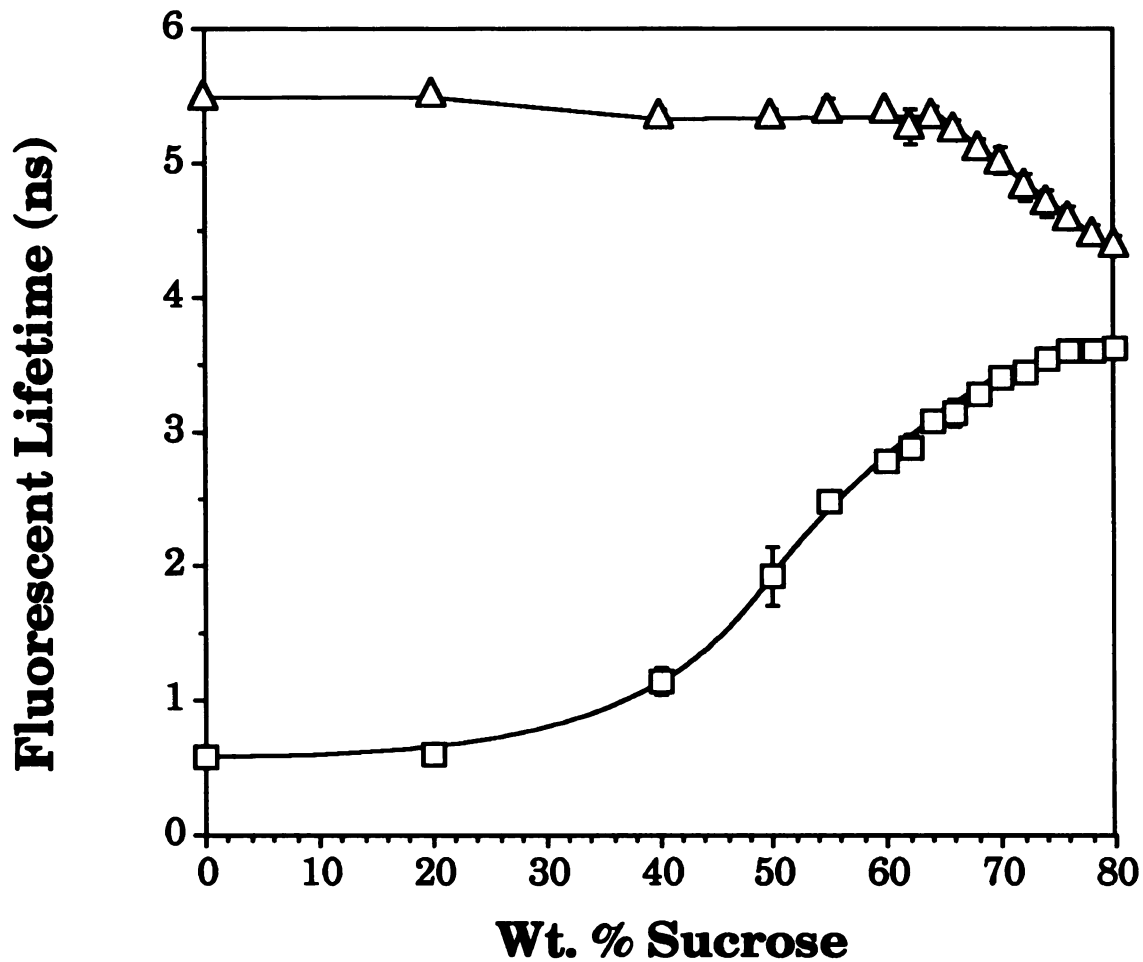


Figure 6.7. Fluorescent lifetimes of pyranine in sucrose solutions at 293 K. Squares (□) represent the emission at 440 nm and triangles (△) represent the emission at 511 nm. Error bars indicate the standard deviation of the measurements.

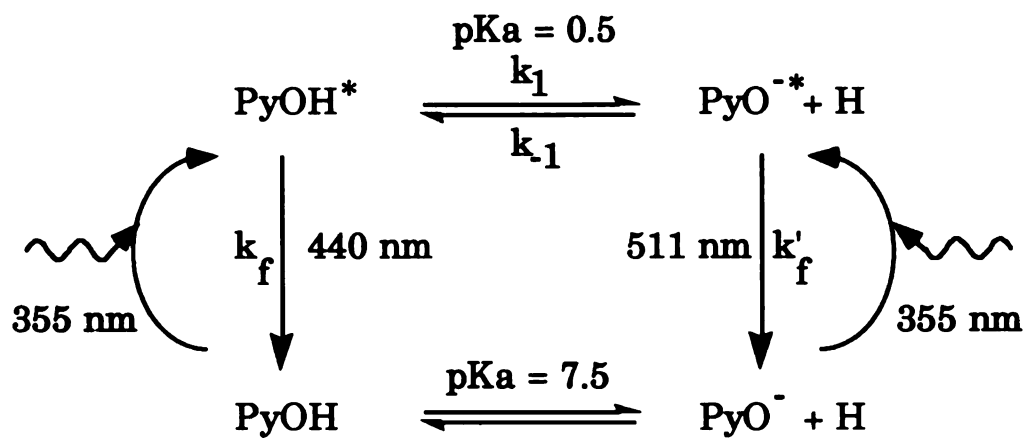


Figure 6.8. Kinetic Diagram for the two-state excited-state proton transfer of pyranine.

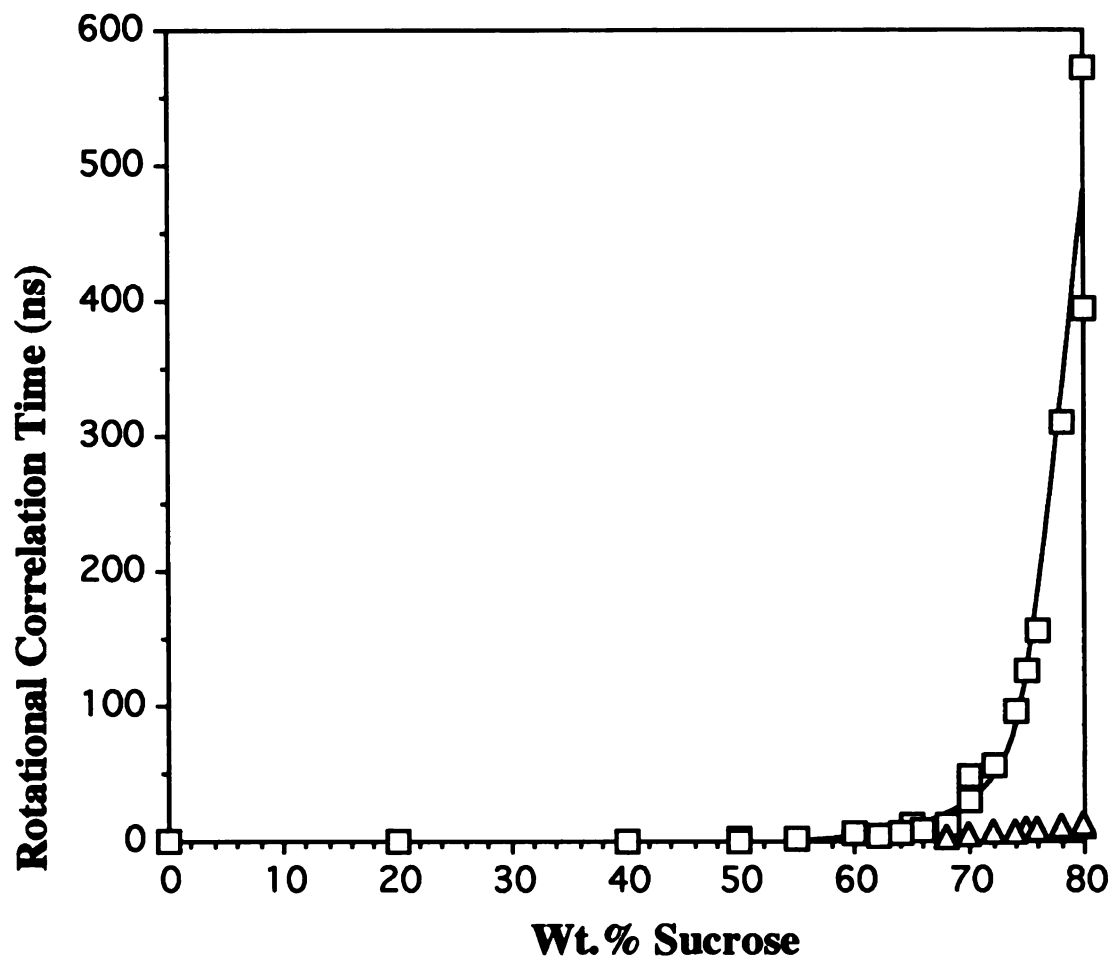


Figure 6.9. Dependence of the rotational correlation time of PBA on sucrose concentration. Squares (□) represent the rotational correlation time for the long lifetime component and triangles (Δ) represent the rotational correlation time for the short lifetime component.

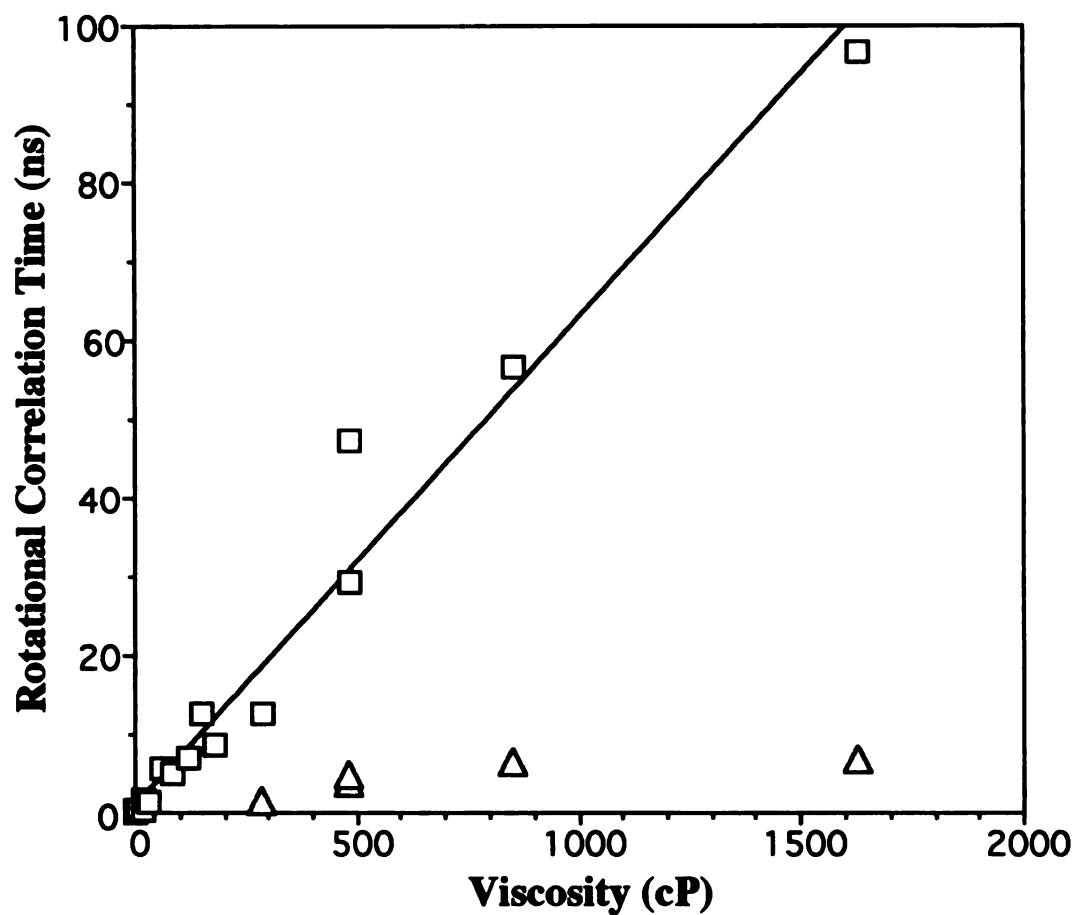


Figure 6.10. Dependence of the rotational correlation time of PBA on viscosity. Squares (□) represent the rotational correlation times for the long lifetime component and triangles (Δ) represent the rotational correlation times for the short lifetime component.

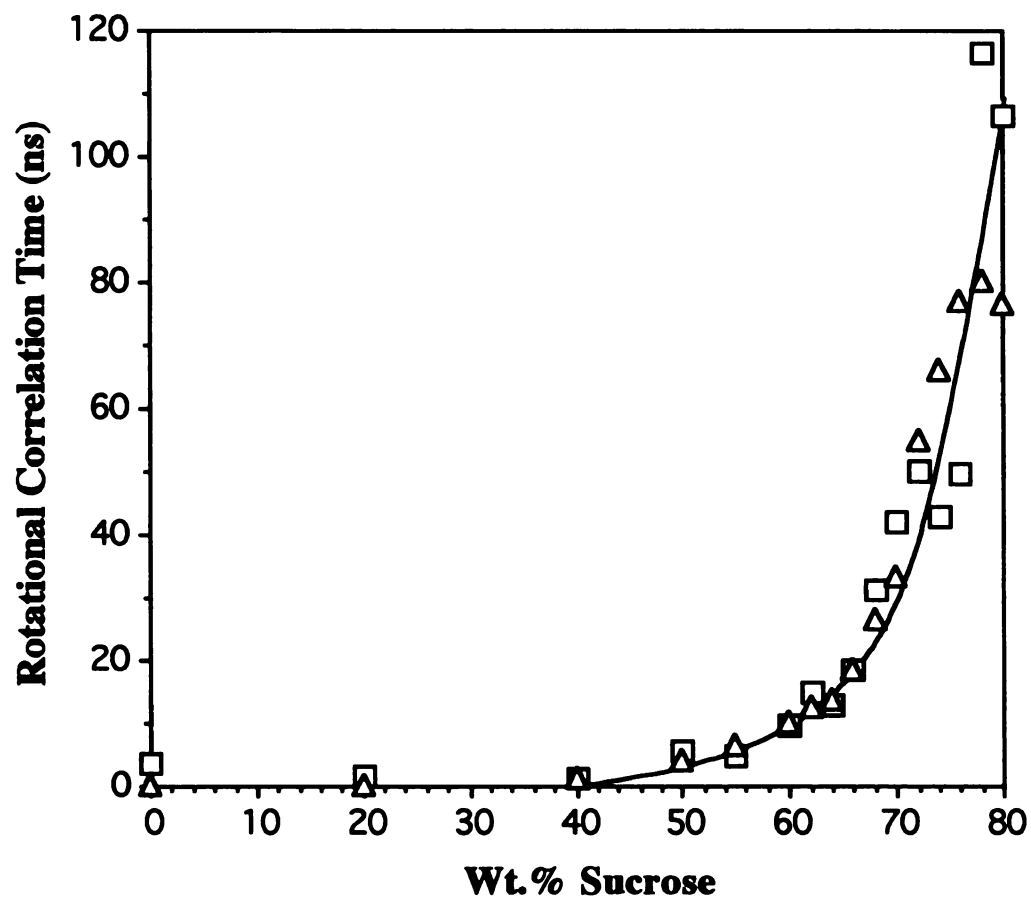


Figure 6.11. Dependence of the rotational correlation time of pyranine on sucrose concentration. Squares (□) represent the rotational correlation time observed at 440 nm and triangles (Δ) represent the rotational correlation time observed at 511 nm.

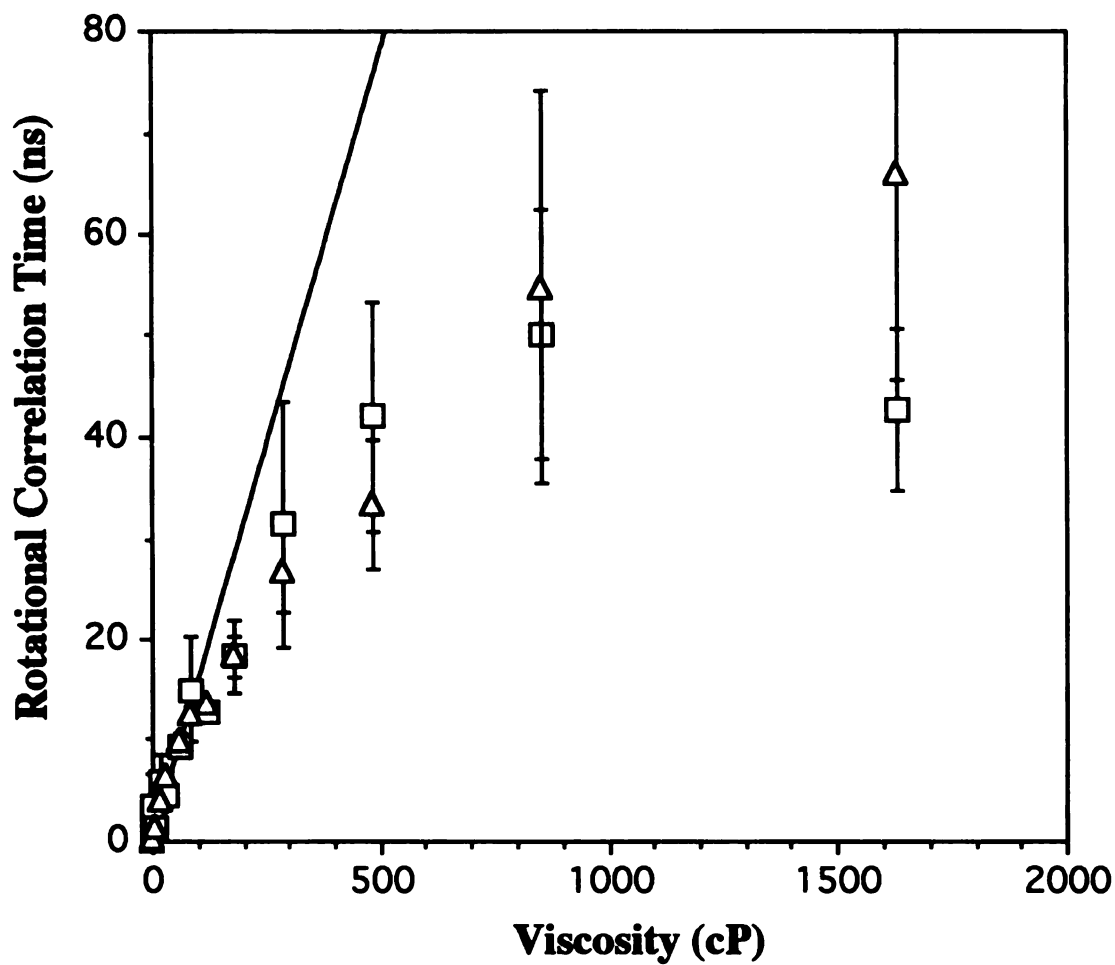


Figure 6.12. Dependence of the rotational correlation time of pyranine on viscosity. Squares (□) represent the rotational correlation times observed at 440 nm and triangles (△) represent the rotational correlation times observed at 511 nm. Error bars indicate the standard deviation of the measurements.

Chapter Seven

Solvent Imaging Studies of Supersaturated Sucrose Solutions in the Absence of Crystals and of the Near Interfacial Region of Growing and Dissolving Sucrose Crystals*

7.1 Background

The spatial distribution and transport characteristics of solvent and solute at or near the crystal-solution interface is a subject of much speculation. There is little experimental data related to the study of this region. Current speculations regarding structure at the crystal-solution interface propose the presence of solvent-exclusive solute aggregates, or solvated species that differ in degree of solvation from those found in bulk solution. Direct experimental verification of such structures has not been possible because of inherent difficulties associated with simultaneous measurement of concentration and interactions between each of the species in solution at various points along and near the interface. It is also difficult to correctly identify the moving interfacial boundary. Consequently, the few attempts to conduct measurements under such conditions have thus far yielded inconclusive, and sometimes contradictory, results.

The object of this work has been to develop new solvent sensitive experimental procedures that enable the study of solution structure. In previously reported work the steady state fluorescent behavior of pyranine was used for determination of solution supersaturation in various sugar solutions. This measurement was accomplished by relating the ratio of peak intensities due to the fluorescent states of pyranine to the amount of water present in the immediate vicinity

* Part of this work appeared as R. Chakraborty, M. H. Wade, & K. A. Berglund, "Imaging Concentration Gradients Near Growing and Dissolving Sucrose Crystals," pre-print, in Separations Conference Symposia, AIChE annual meeting, November 1992., Florida. Confocal images were provided by Dr. M. H. Wade of Meridian Instruments, Okemos.

of the hydroxyl moiety of the probe molecule and the exchange behavior of this water. It was convenient to describe water in the solution as solvation water, bulk water and non-bulk-non-solvation water (1,2). It became clear that the functional microphase distribution of the various species is an important indicator of solution structure. In subsequent work, time resolved fluorescence spectroscopy of pyrene butyric acid and pyranine indicated the absence of solvent exclusive aggregates in metastable solutions and also that the structure changed with increasing supersaturation. The issue of whether or not the probe is homogeneously distributed was unresolved (3).

7.2 Materials and Methods

Reagent grade sucrose from Sigma Chemicals, 8-hydroxy 1,3,6, pyrenetrisulfonate (pyranine) from Eastman Kodak, and 18 Mohm reverse osmosis water were used. Stock solutions of 100 ppm (1.9×10^{-4} M) pyranine were prepared using 18 Mohm reverse osmosis water. Solutions of the 10 ppm (1.9×10^{-5} M) pyranine and 1 ppm (1.9×10^{-6} M) pyranine were prepared by dilution.

The amount of sucrose and water required for 10 grams (0.01 kilogram) of each solution was calculated. Reagent grade sucrose samples were carefully measured out to +/- 1% of the required amount. Samples were prepared in 20 ml glass vials by adding the predetermined amount of stock pyranine solution to achieve the desired concentration. Samples varied in concentration between 60 and 80 wt.% sucrose. In undersaturated solutions samples were prepared at 5 wt.% intervals. Supersaturated solutions were prepared at 2 wt.% intervals for sucrose between 68 and 80 wt.%.. Supersaturated solutions were prepared by heating the vials in a water bath until the sugar dissolved. Spectra of the solutions were taken within 6 to 24 hours of preparation to ensure equilibration of the sucrose in solution [with respect to temperature] and prevent biological contamination of the sugar solutions.

Pyranine doped sugar solutions - with pyranine concentrations of 1 ppm (1.9×10^{-6} M), 10 ppm (1.9×10^{-5} M), and 100 ppm (1.9×10^{-4} M)- exhibited little variation in integrated half peak intensity ratio (IIR). The IIR is defined as the ratio of the integrated intensity of the peak observed at 440 nm from 370 nm to 445 nm to that of the peak at 511 nm from 485 nm to 507 nm when excited at 351 nm. This is not the same as the Peak Intensity Ratio or PIR defined as the ratio of the intensity of the peak at 440 nm to that of the peak at 511 nm (excited at 343 nm +/- 5 nm). The IIR may vary depending upon the set up of the ACAS and is obtained from a working curve obtained at the time the experiments are conducted. It was decided to work at 100 ppm (1.9×10^{-4} M) levels of pyranine to maximize the signal to noise ratio. Small changes in instrument settings did not affect the values obtained for the IIR. All experiments discussed in this paper were conducted at 20 °C.

The steady state technique can be easily adapted to an imaging system to study supersaturation in the presence of crystals. The ACAS-570 confocal system consists of a high quality optical light microscope with a confocal imaging system, a travelling stage, laser excitation using a 12 W Krypton laser and multi-line UV, and two 2-dimensional detectors which detect integrated fluorescence intensities at each "point" in solution, one from 400-445 nm, and one from 485-510 nm. The ACAS 570 interactive laser cytometer was used with an excitation of 351-360 nm, a laser power of 60 mW, 50% scan strength, 60% PMT on each detector, scan speed of 2 mm/s or less, and steps of 2 microns or .4 microns. A 10% neutral density filter, a 445 nm dichroic, and a 485 nm (22 nm band pass) filter were used. All spectra were obtained using an oil objective. The solution sample is placed in a sample holder which is then secured on the stage. When crystals are used, hot undersaturated solution is gently dropped on top of the crystal to dissolve crystal dust and also to ensure that the crystal adheres to the bottom of the sample holder. The scan area and resolution as well as the scan speed are specified. The half micron layer of solution nearest

the bottom of the sample holder is scanned. When high resolution (0.5 microns or less) is used it is necessary to focus on secondary nuclei or crystals formed therefrom.

Sucrose crystals were placed in a compartment of the sample holder. Five milliliters of solution were then gently introduced on top of the crystal. This, in effect, glued the crystal down. The solution was initially hot and slightly undersaturated. The sample holder was then placed in the slot on the moving stage and secured in place. An edge of an ink spot that had been placed on the bottom of the holder for the purpose of locating the plane corresponding to the bottom was then located and focused upon. The solutions were open to the atmosphere and nuclei were normally observed. Most of the data were obtained from observing well developed nuclei because it was most convenient and expedient to do so. The stage was moved at speeds of 2 mm/s or less to minimize motion in the solution. There was probably some agitation; however, the crystals appeared to remain stationary during the course of an experiment. The ratio analysis and dual detector data analysis routines on the Data Analysis System (DASY) were used to analyze the data.

7.3 Results

The data obtained from the detectors consists of two dimensional plots of integrated half-peak intensities. First a standard set of solutions of concentrations ranging from 60 wt.% sucrose to 76 wt.% sucrose were imaged in dual detector mode. Images for solutions of 60, 74 and 76 wt.% sucrose are presented in Figure 7.1. Data obtained from solutions in the absence of crystals indicate an isotropic distribution of pyranine in solution in both excited states. This is consistent with the time resolved experiments which also indicate an isotropic distribution of probe molecules. This data was used to generate a plot of IIR vs sucrose concentration (wt.% sucrose), Figure 7.2.

In the presence of small growing crystals, gradients in concentration and intensity were observed in the distributions of both the protonated and the deprotonated species of

the pyranine molecule. In each case the emission intensity of probe nearest the interface was lower than that observed in bulk solution. Our experiments with pyranine thus far indicate that the probe does not tend to incorporate itself into the sucrose crystal; this is supported by the fact that pyranine and sucrose are not likely to be attracted to each other. These observations together indicate the presence of less probe immediately near the interface than in bulk solution. Samples of crystals imaged in dual detector mode and the same crystals imaged in concentration ratio modes are presented in Figures 7.4, 7.5, and 7.6. A crystal in 68 wt.% sucrose solution is seen in Figure 7.3. Several different crystals observed growing in 71 wt.% sucrose solution are presented in Figure 7.4. A crystal observed growing in 76 wt.% sucrose solution is presented in Figure 7.5. The concentration ratio images indicate a 2-10 micron region immediately adjacent to the crystal surface that is more depleted of solvent than the rest of the boundary layer. Under the optical microscope as well as in the fluorescence image both the crystal and the interface appear to remain significantly stationary during the experiment. This data appears to lend credence to the existence of an "intermediate phase" as proposed by Powers (4), and supported by Clontz and McCabe (5), Mullin and Leci (6), and Berglund (7) among others. This data reinforces the idea that the 1-5 micron region near the crystal interface is solvent depleted, however, it does not suggest the existence of solvent exclusive clusters. This does not necessarily rule out the existence of solvent exclusive clusters because the structure in the less than one micron region is entirely unknown.

The extent of the boundary layer referred to here is determined by that distance from the crystal solution interface at which solution concentration is equal to the bulk solution concentration. The extent of the boundary layer was observed to be dependent on the size of the crystal rather than on the supersaturation. The smallest crystals observed were about a micron in size and had boundary layers that extended up to 10 microns into solution. Consequently the distance between data points was specified as 0.4 microns and smaller areas were scanned. Larger crystals that were 10-100 microns in length had larger

boundary layers extending several hundreds of microns into solution. As a result larger distances were specified between data points. In all cases the solution concentration reaches bulk solution value within about 10,000 microns from the crystal solution interface in a relatively quiescent solution. On the time scale of the experiment, prior experience led us to believe that the bulk concentration should not decrease by more than 0.5 wt.% due to crystal growth. This was observed to be true in each case.

Line scans taken in dual detector and concentration mode through the interfacial region indicate a fairly sharp transition in concentration in the 4 to 10 micron region, followed by a more gradual change in concentration out to the bulk solution, Figure 7.6. A great deal of noise can be observed in the data, particularly that in the blue (445 nm). This is probably because the ACAS-570 has detectors which are green and red biased. The ratio of bulk water to solvation water in the boundary layer differs significantly from that in bulk solution: proportionally more bulk water and less solvation water was observed than in bulk solution.

As expected, data taken in the presence of dissolving crystals indicate that the solute concentration near the interface is greater than that in the bulk, Figure 7.7. For dissolving crystals only concentration gradients were observed. We did not observe any gradients in probe intensity. Transport of solute seems to proceed down a concentration gradient from the interface out to the bulk.

Dual detector and concentration images can be obtained along vertical sections of the solutions to obtain three dimensional information related to concentration and solvent distribution. Figures 7.8 and 7.9 respectively present the dual detector and ratio images obtained by using confocal spectroscopy to observe a sucrose crystal in a 74 wt.% sucrose solution. Vertical sections are taken at 0.4 micron intervals and, the horizontal resolution is 0.2 micron x 0.2 micron.

7.4 Discussion

The data clearly indicates a marked difference between solvent distribution and, consequently, the structure of bulk solution, and solvent distribution and solution structure near the crystal-solution interface of growing crystals. Not only does the ratio of bulk water to free water differ on the average; it differs spatially across regions that differ in their size and extent. The total amount of water per molecule of solute appears to vary spatially in the presence of a growing crystal; there appear to be discrete spatial regions with water concentrations that indicate supersaturated solution separated by other discrete spatial regions with water concentrations indicative of undersaturated solution, so that on the average the solution concentration within the boundary layer is richer in solvent and poorer in solute than in bulk solution.

Initially we thought differences in the emission intensity of the probe from point to point in solution indicated less water: both solvation water and bulk water. Our observation of the behavior of water and how it distributes in supersaturated solutions in the absence of growing crystals indicates that the solvent distributes into the bulk phase only after all the solute has been solvated, even if this is accompanied by changes in the structure, composition, and dynamics of the bulk water phase. Such observations were not real time observations. While we can not rule out real time related differences we can say with certainty that lower emission density is indicative of fewer molecules of probe per unit volume of solution surrounding it. The local concentration is still accurately represented by the PIR (or the IIR in this case) because it is that quantity which is a measure of the nature of the solvation environment of the probe. Therefore a decrease in the emission intensity accompanied by an increase in the PIR or IIR indicates the presence of a greater number of solvated solute molecules. A decrease in the emission intensity accompanied by a corresponding decrease in the PIR or IIR indicates the presence of more bulk water in the solvation environment of the probe than in bulk solution.

On this basis our data suggests a "relatively" solute depleted region, extending 2-10 microns from the interface in which the solute is completely solvated. This region is adjacent to a "concentration boundary layer, the extent of which appears to depend on the size of the crystal, where there more bulk water is observed than in bulk solution. Bennema (8), Burton, Cabrera, and Frank (9), and Chernov (10) in their work on modelling crystal growth and the solution surrounding the growing crystal, each consider a boundary layer of unstirred solution between the supersaturated bulk solution and the solid-solution interface. Mullin (11) estimated the diffusion boundary layer to be about 10 microns away from the interface into solution. Since we define the extent of the boundary layer by the distance at which bulk solution concentration is observed, we measured larger layers. We should also point out that our layers are not completely unstirred. The "concentration boundary layer" is likely to occur as a direct result of crystal growth, and the release of solvation water. A supersaturation dependence on the extent of the boundary layer was not observed, this may be because we were unable to observe the full extent of the boundary layer in some cases. The diffusivity of the bulk supersaturated solution is low, and the viscosity is high; also, it is probable that water will self-associate and form bulk water like structures if it builds up because of transport resistance. Such build ups may lead to localized density differences and convection involving pockets of solution of slightly different concentrations. This would be consistent with the irregular "periodicity" observed in the near interface x-ray diffraction data of Mathlouthi (12) for sugars. It may also account for some of the patchiness observed in our images in concentration ratio mode which can't be explained entirely by system noise caused by the red and green bias of the detectors. At the same time we are unable to categorically rule out the possibility of existence of pre-crystalline clusters or other solute rich structures in the near interface region because we have thus far been able to investigate only a limited region. The structure of the less than 1 micron region near the interface is still completely unknown.

The issue of solution microstructure near the interface is still an open one. We see no evidence to suggest the presence of solvent exclusive clusters of a lifetime greater than the timescale of the experiment, or of a size greater than the resolution of the experiment. However, we are unable to conclusively rule out the existence of solvent exclusive structures at this juncture because we do not have reliable information regarding the spatial distribution of the solute molecules and their interactions.

7. 5 Crystal Growth

Partly as a result of observation and partly as a result of conjecture it is this author's suggestion that the growth of a crystal is best described in at least 2 stages: initial growth, and subsequent growth. The initial growth period follows some impact type catastrophic "local" event that affects the structure and organization of those solvatons which are in immediate contact with the event. Such an event may be due to a heterogeneous nucleus, the introduction of a seed, or mechanical or thermal disruption. It is possible that the mechanism of initial growth differs according to the origin of the nuclei or seed crystal. The introduction of a seed or heterogeneous nucleus puts a demand on solvent. Solvent is required for wetting or solvation of those moieties of the solid in contact with solution along the interface. Because the self diffusion coefficients are precipitously low, this solvent must necessarily be supplied from the solution in contact with the solid interface. As a result some of the solute is likely to be at least partially desolvated at least part of the time. Depending on the chemical nature of the substance some or all of this solute may crystallize quickly. During the initial growth period an abundant supply of solute is immediately available to the nucleus or seed and transport of solvatons from bulk solution is not likely to be a growth limiting factor. During initial growth the availability of water for wetting is a primary factor.

For some systems the primary source of resistance may be related to how fast the solvations can reach the interface or volume diffusion. For other systems like sucrose-water in which the chemical affinity of the solute for itself is not particularly high, the main resistance to growth may be related to how quickly the partially solvated solute leaves the solution. Once the solute is anchored to the crystal (to any extent) it may still be partially solvated at other points on the molecule but is no longer mobile, because unlike the water the solute crystal is immobile and the exchange rate is zero. Partially solvated solute in solution phase may be displaced due to contact or fluid shear or otherwise yield nuclei.

Once the initial growth period has ended, the crystal continues to grow. The water of solvation released from the crystallized solute at some point will be in excess of the water required to wet all the solute at the crystal-solution interface locally. Such water diffuses into the supersaturated solution and builds up a region of less concentrated solution adjacent to the crystal. Eventually bulk concentration gradients prevail and convection is likely to occur, bringing the surface of the crystal in contact with supersaturated solution of bulk concentration once again. It seems reasonable that the structure near the interface of the growing crystal changes with time, and the crystal grows in spurts.

7.6 Conclusion

The single most important conclusion that can be drawn as a result of this and related work regarding the study of solution structure in supersaturated sugar solutions is that in order to explain crystal growth and nucleation related phenomena it may not be sufficient to treat the solution as a continuum. How the solvent is spatially and functionally distributed and structured plays an important role in determining the properties and behavior of solution. A material balance treatment of crystal growth or dissolution is incomplete without an account of the solvent microphase distribution. The imaging of

pyranine in a sense allows us to determine the localized microphase distribution of water in solution. The role played by bulk water and solvation water, how the relative amounts change both globally and locally, and the significance of such phenomena in crystal growth and dissolution is not yet understood.

7.7 Acknowledgements

We would like to thank the Crop Bioprocessing Center/ Research Excellence Fund at Michigan State University for use of facilities and funding for R.C. We are grateful to Dr. Troscoe, of the Department of Pediatrics for use of the DASY, and to Dr. Asmina H. Jiwa for set-up and assistance on the confocal ACAS-570 at Meridian Instruments.

7.8 References

1. Chakraborty R. and K.A. Berglund, AIChE Symposium Series, no **284**, 113, (1991).
2. Chakraborty R. and K. A. Berglund, *Journal of Crystal Growth*, **125**, pp. 81-96 (1992).
3. Pan B., R. Chakraborty and K. A. Berglund, *Journal of Crystal Growth*, **130**, pp. 587-599, (1993).
4. Powers H.E. C., *Nature*, **178**, pp 139-140, (1956)
5. Clontz N.A. and W.L. McCabe, *Chem. Engg. Progress Symp. Ser.*, **67**(6), 6-17, (1971)
6. Mullin J.W. and C.L. Leci, *Phil. Mag.*, **19**, pp 1076-1077, (1969)
7. Berglund K.A., PhD. Dissertation, Iowa State University, (1981).
8. Bennema P., Theory and Experiment for Crystal Growth from Solutions, in J.W. Mullin ed. *Industrial Crystallization*, Plenum Press, New York, NY, (1976)
9. Burton, W.K., N. Cabrera, and F.C. Frank, *Phil Trans. Roy. Soc. London*, **243**, 299, (1951)
10. Chernov A.A., *Soviet Phys. USP*, **4**, 116, (1951)
11. Mullin J.W., *Crystallization*, Butterworths, London, (1972).
12. Mathlouthi M., *Carbohydrate Res.*, **91**, 113, (1981)

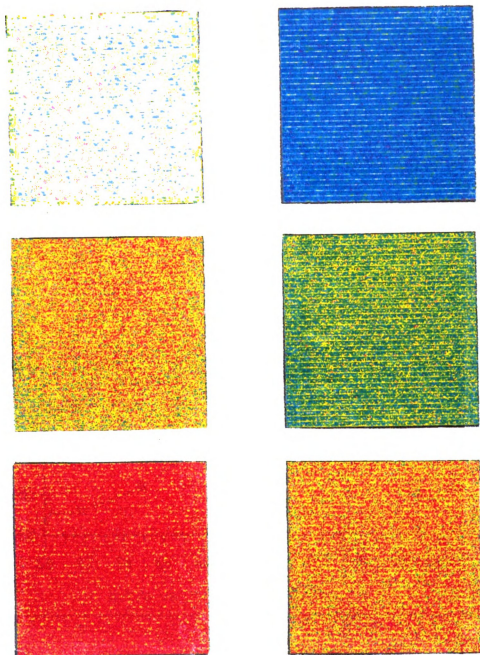


Figure 7.1. Dual detector images for aqueous sucrose solutions of 60, 74 and 76 wt. % at 293 K. Detector 1 images the half peak intensity of pyranine from 485 nm to 507 nm. Detector 2 images the half peak intensity of pyranine from 445 nm to 370 nm. One pixel represents an area of solution $0.4 \mu\text{m} \times 0.4 \mu\text{m}$.

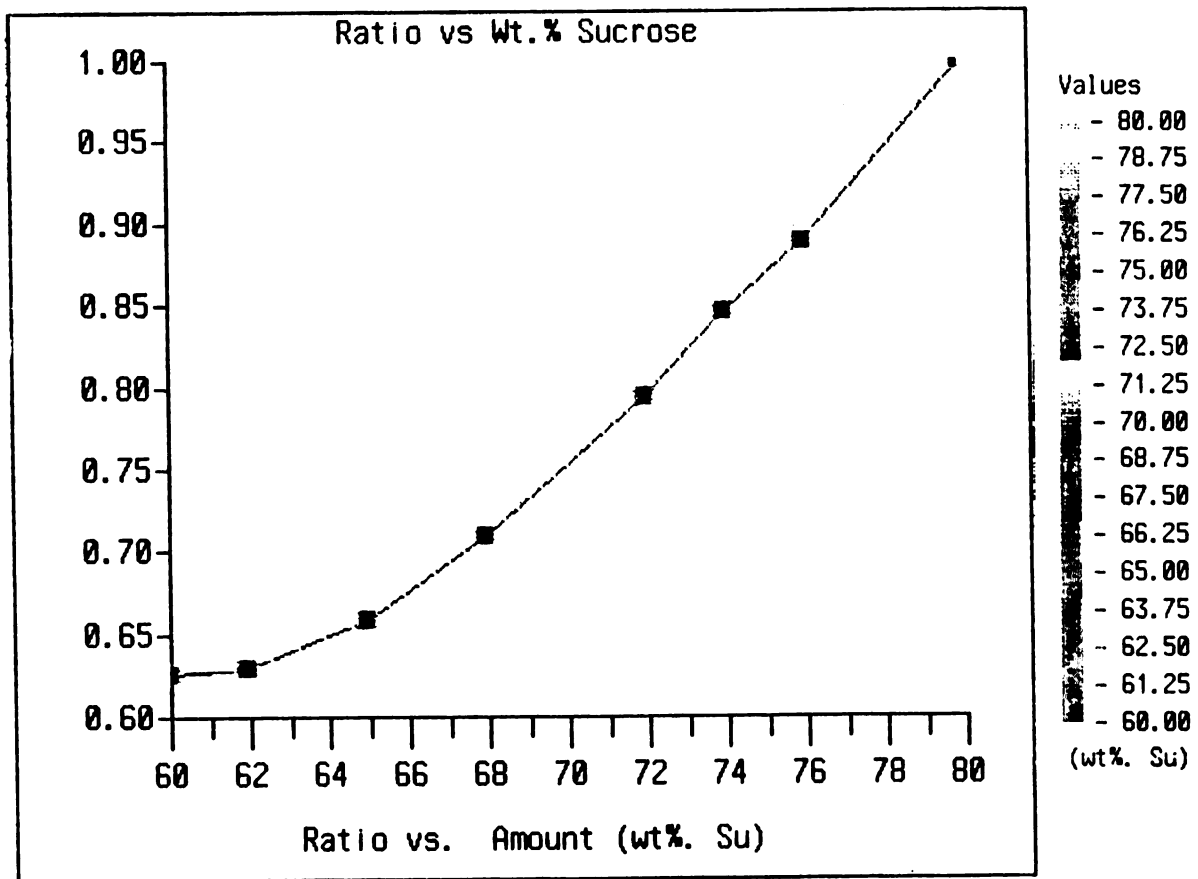


Figure 7.2. A plot of IIR (integrated emission intensity) of pyranine vs sucrose concentration (wt.% sucrose) at 293 K. Color values represent concentration in weight percent sucrose.

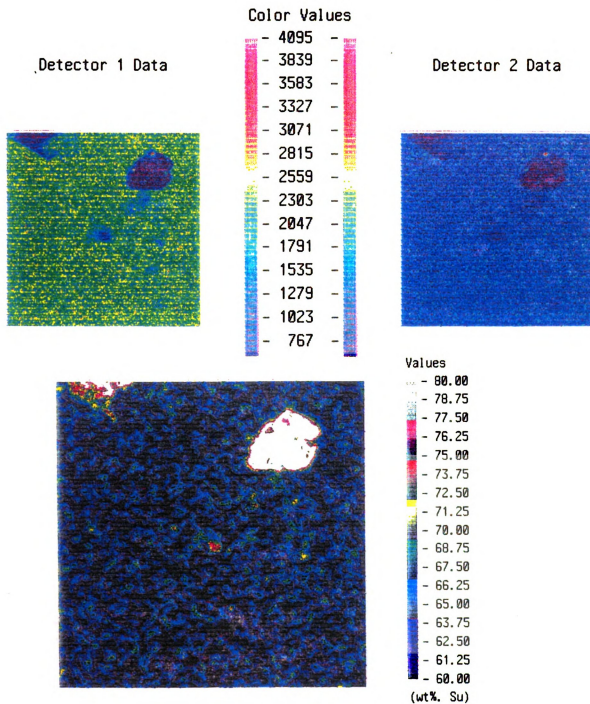


Figure 7.3 Dual detector (a) and concentration ratio mode (b) images of a sucrose crystal growing in 68 wt.% solution.

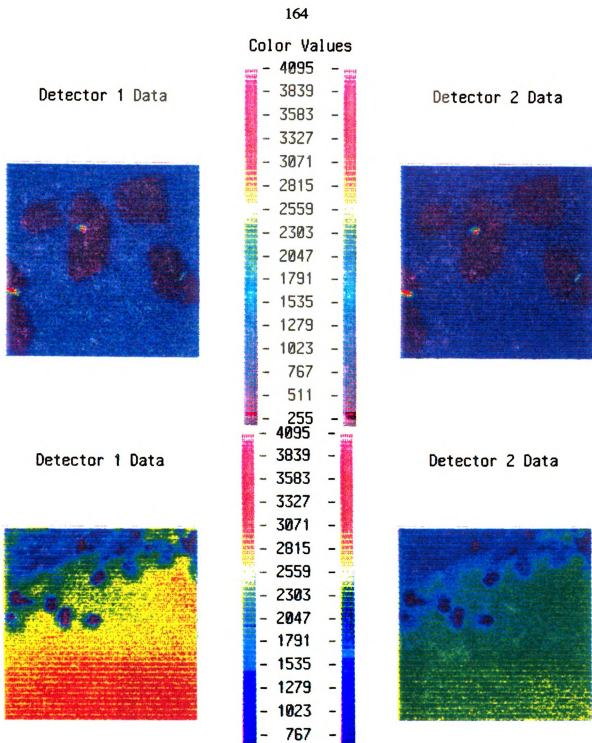


Figure 7.4 Dual detector mode images of several different sucrose crystals growing in 71 wt.% solution.

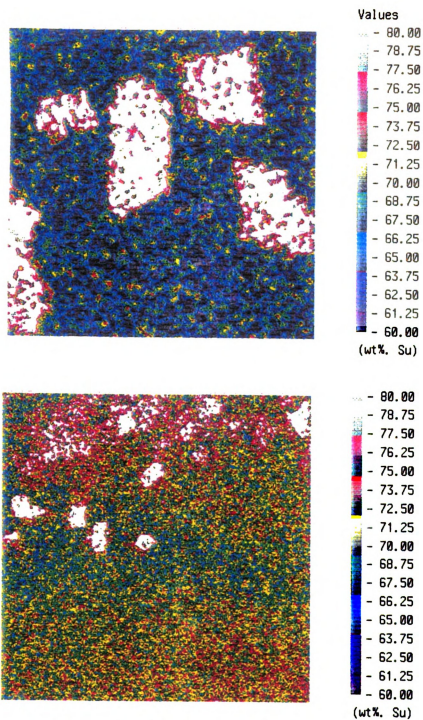


Figure 7.5 Concentration ratio mode images of several different sucrose crystals growing in 71 wt.% solution.

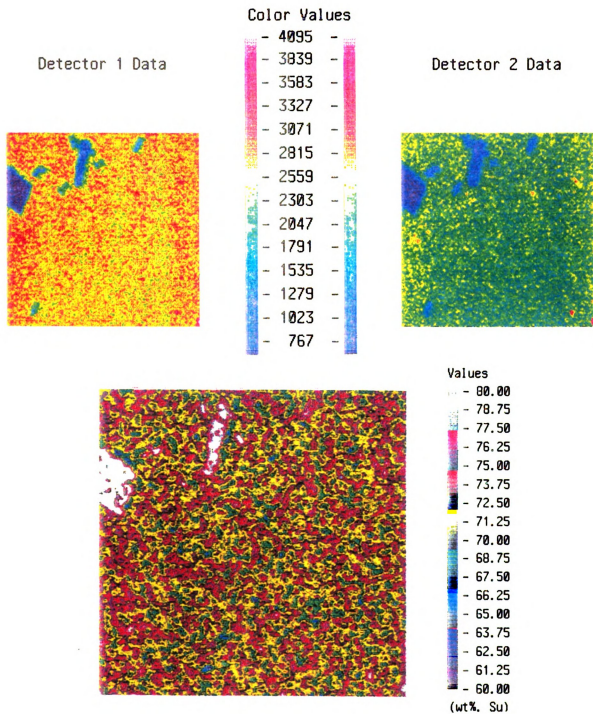


Figure 7.6 Dual detector (a) and concentration ratio mode (b) images of a sucrose crystal growing in 76 wt.% solution.

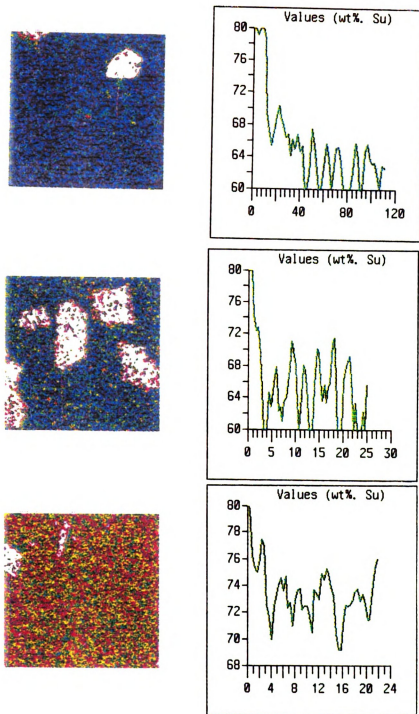


Figure 7.7. Samples of line scans in concentration ratio mode taken in the interfacial region of growing sucrose crystals at 293 K. The big dip in concentration indicates the interface of the crystal.

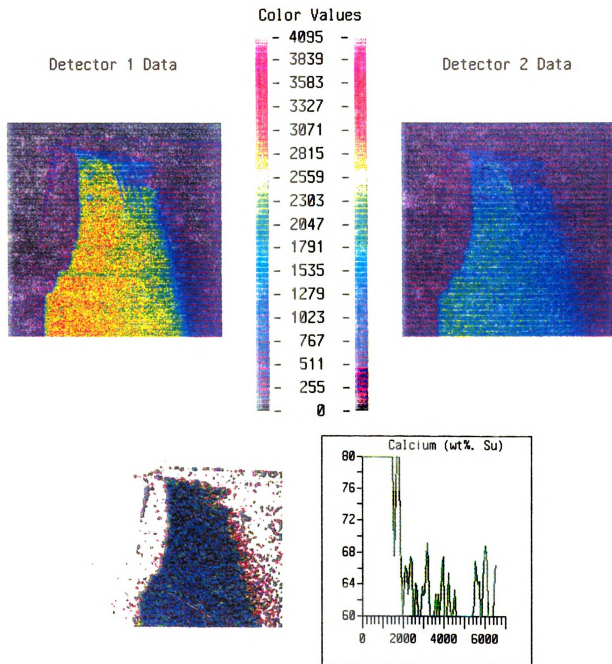


Figure 7.8 A sample of a line scan taken near the interface of a dissolving sucrose crystal in 60 wt% sucrose solution at 293 K. The big dip in concentration indicates the interface of the crystal.

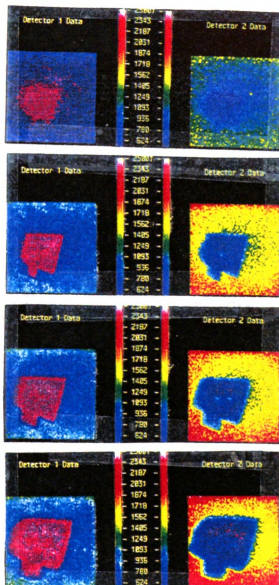


Figure 7.9 Dual detector images of a sucrose crystal in 74 wt. % solution at 293 K taken using confocal microscopy in 0.4 μm vertical steps, and 0.2 μm x 0.2 μm horizontal resolution. Instrument settings for this data differ from those of the rest of the data in this work.

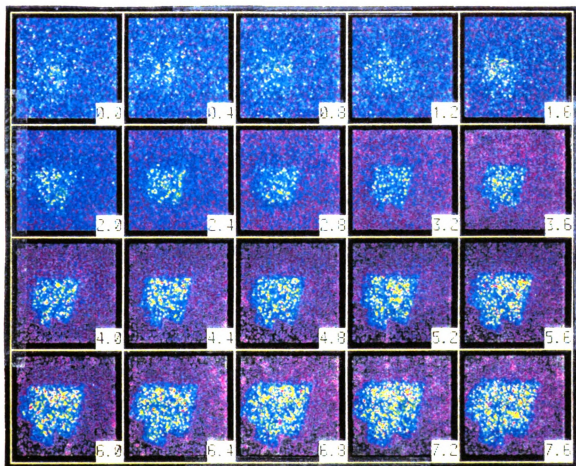


Figure 7.10. Concentration ratio images of the sucrose crystal imaged in Figure 7.9.

Chapter Eight

Summary, Conclusions, & Recommendations for Further Work

8.1 Summary

This work can be conveniently summarized in two parts for the purposes of discussion. The first part deals with issues related to the relationship between the solvent and solution structure in general and how this relationship changes with the solute and solvent concentration in solution in particular. The remainder deals with the attempt to extend these ideas and experimental techniques to the study of the solution structure in the near interface region of growing sucrose crystals.

8.1.1 Issues Related To Solution Structure

Short Range Order and Long Range Order

Solution structure is often described in literature in terms of short range order and long range order. Short range order, hence referred to as SRO, is the result of submolecular interactions which take place on relatively small space scales. In dilute solutions those interactions are in effect on time scales of the order of less than one picosecond and length scales of a few nanometers. In supersaturated solutions time scales are on the order of 100's of nanoseconds although length scales are still a few nanometers. SRO determines the dynamics of a system. System dynamics determine rates and mechanisms of physical transport properties and rates and mechanisms of chemical reactions.

Long range order, hence referred to as LRO, describes long-time and time-averaged structure which results from the organization of groups of molecules on the scale of tens of nanometers or more. Long range order is sometimes described to be a result of long range

or long term interactions between molecules. This is somewhat misleading because first of all the molecules themselves do not interact, it is the submolecular moieties on the molecules which are affected by forces of attraction and repulsion exerted by submolecular moieties of other molecules. The forces between atoms that make up these moieties can be expected to follow Heitler London behavior; all forces of interaction dying off within 2 atomic diameters. Such forces are inherently short range and short term. These short range forces acting on different parts of a molecule simultaneously can result in the formation of multi-molecular groups. In fact this is why the first multi-molecular groups thought to exist for water were dimers and trimers. These multi-molecular groups appear to exist for long periods of time when one views the time-averaged "snapshot" of spatial distribution of the components of the system. They may remain constant in composition in terms of the number and relative spatial orientation of molecules of each of the molecular species involved, even though different molecules of each species may occupy those same relative positions at different moments in time. There are short time periods, determined by SRO, when an exchange of molecule occurs at each of those positions, during which those positions may not be occupied by any molecule, and during which some other group may come into existence. In a mixture of two or more molecular species LRO describes all the different types of time-averaged structures, their composition, and relative spatial orientations. It is possible for a system to exhibit LRO on more than one spatial or temporal scale of order.

It is clear that LRO depends intimately on SRO, and that the description of the structure of a system is incomplete without an understanding of both. It is this author's hypothesis that there is a definite relationship for a system given a particular temperature and pressure and composition and number of macroscopic phases which defines the number of scales of order on which a system under consideration exhibits LRO of significance. The number of such scales is likely a function of the number of chemically distinct molecular species in the system; the number of distinct relaxation times for each of

those species, as determined by the chemical structure of each of those species, system temperature and pressure, and the SRO; the number of relaxation times of significance with respect to the mechanism of the phenomena being observed in that system; and the number of molecules of each species in the system.

8.1.2 SRO and LRO in The Aqueous Sucrose System

Let us examine the sucrose water system from this point of view. There are two chemically distinct molecular species, sucrose and water. Water has two distinct relaxation times of significance, hence two solvation states. There are three different types of possible interactions: solute-solute, solute-solvent, and solvent-solvent. Also the chemical affinity of water for water is greater than the chemical affinity of water for sucrose, which in turn is greater than the chemical affinity of sucrose for sucrose. Unless the solvent concentration is such that enough solvent is not available to solvate all solute molecules to the same extent that they are solvated in dilute solution, solute-solute interactions are unlikely. For the sucrose water system, data generated in this work indicates that such a situation is not observed below solution concentrations of about 76 % by weight sucrose.

LRO in Dilute Solutions

In dilute aqueous sucrose solutions there are four scales of LRO of significance. The first is related to the structure in bulk solvent, far from the solvated solute and corresponds to the length and time scales associated with flickering clusters. The second is related to the solvated solute and corresponds to the length and time scales related to the solvaton: a single solute molecule and the water of solvation most strongly associated with it. The third is related to the solvation environment of the solvaton and corresponds to the length and time scales associated with the structure of the bulk solvent immediately

surrounding the solvaton. And the fourth, to the structure of the solution on the scale of many solvated solvatons in bulk solvent and corresponds to the length and time scales associated with diffusion. A conceptual diagram of the dilute aqueous sucrose solution is presented in Figure 8.1.

Complexities that may arise in other systems due to other relaxation parameters

Dilute Aqueous Glucose solutions

For the sucrose water system the solvation environment of the solvaton in dilute solution is likely very similar to the structure of bulk water since the behavior of the solvent in the system is adequately described by two exchange rates for water. However in other systems, such as the glucose-water system, this environment is likely to be significantly different, due to the presence of significant amounts of non-bulk-non-solvation water per molecule of solute. The molecular dynamics simulations of Brady and the data analysis performed in this study both suggest that some water in the glucose water system is associated with the solute on time scales which are significantly faster than solvation water but significantly slower than bulk water. It is reasonable to assume that this water is associated with the solvation environment of the solvaton, and that it is more structured than bulk water. One possible reason could be that the solvent clusters are more tetrahedral and less flickering in nature.

Dilute Fructose and Lactose solutions

The description of relaxation states in dilute solution is more complex yet for aqueous fructose and lactose solutions. Whereas, dilute aqueous solutions of sucrose and glucose are fairly easy to characterize, in the absence of some working empirical correlation, these systems are not. Fructose, for example is known to exhibit rather

complex enantiomeric equilibrium in addition to the ability to adopt different conformations. Such complexities may require additional parameters for description, and hence increase the number of relaxation states needed to adequately characterize SRO. Subsequently the system is likely to exhibit LRO of significance on a greater number of spatial and temporal scales. Such a characterization is not possible using the experimental techniques or methods of analysis developed in this work, since the experiments indicate how water is distributed into one of two states with relaxation rates relative to the rate of proton exchange. However, data obtained using these methods may provide a bare framework against which to corroborate data obtained using other methods more inherently suited to the measurement of relaxation times. In any case, these limitations do not affect the characterization of structure or concentration measurements in supersaturated sucrose solutions: the focus of this work.

SRO and LRO in Concentrated Aqueous Sucrose Solutions

As the solution becomes more concentrated in solute, the bulk water per molecule of solute exponentially decreases. Many changes in properties are observed for sucrose solutions as the sucrose concentration approaches 40 wt.%. If one assumes that flickering clusters are on the average tetrahedral in structure and that a solvaton is on the average solvated by six such clusters, it is interesting to note that 40 wt% corresponds to the concentration where there is only enough water available to provide six tetrahedral water clusters (which still behave as bulk water) for every solvaton. This seems to indicate a change in SRO of the bulk water. At this point the solution is far from ideal, and no longer dilute. So, in terms of LRO for non-dilute solutions there appears to be one less scale of significance to consider. A conceptual representation of structure in concentrated sucrose solutions is presented in Figure 8.2.

Saturation described in terms of SRO, LRO and Phase Inversion Analogy

With the addition of more sucrose, the bulk water per molecule continues to exponentially decrease in availability until a concentration of 66.7 wt.% sucrose or saturation is reached. Near this point the number of bulk water per molecule of sucrose becomes equal to the number of solvation water, and at saturation the number of solvatons equals the number of tetrahedral clusters that could be formed by the bulk water available per molecule of sucrose (or per solvaton). Proceeding from dilute solutions to saturation, thus corresponds to a precipitous drop in bulk water, corresponding to a sharp change in the SRO of the bulk water, and duly evidenced by marked changes in transport properties. This is consistent with the fact that transport properties are governed by SRO.

In terms of LRO saturation is somewhat akin to a phase inversion point because at non-dilute concentrations less than saturation the solution can be viewed on some scale as solvatons being solvated by flickering clusters which are tetrahedral on the average (FC or TC), and for concentrations greater than saturation the solution can be viewed on the same scale as a solution of FC solvated by solvatons. A conceptual representation of structure in saturated aqueous sucrose solutions is presented in Figure 8.3.

Such an analogy holds true for aqueous glucose solutions, but not for aqueous fructose or lactose solutions. The PIR is still a steep function of solvent content, and hence indicator of solution concentration, and solvation water per molecule becomes equal to bulk water per molecule at or near the saturation point.

SRO and LRO in Supersaturated Solutions

The definitions of diffusion of solute through solvent, and other transport properties as envisioned for dilute solutions are not useful or of the same physical significance in supersaturated solutions. One view of transport which might be more

realistic is that transport and transport coefficients are governed by the SRO, structure, and availability (thus LRO), of the bulk solvent. It might be more useful to describe measures of resistance to transport in terms of the transport resistance experienced by some small but inert probe molecule through a solution of interest. Solutions which contain a significant amount of non-bulk-non-solvation water at saturation are likely to exhibit LRO on additional scales of significance and additional solution structure transition points

The bulk water per molecule of sucrose continues to decrease until at a concentration of about 76 wt. % sucrose the number of molecules of solvation water per molecule of sucrose changes significantly. At this point solute-solute interaction becomes more likely, even though in absolute terms there is still enough water available in the system to completely solvate every molecule of sucrose, although there would be no bulk water if this occurred. This may correspond to a glass transition point for the sucrose water system. A conceptual representation of structure in supersaturated aqueous sucrose solutions of concentrations less than 76 weight percent sucrose is presented in Figure 8.4. below.

8.1.3 Bulk Water and Solvation Water as indicators of SRO; Solvatons and Structure in Bulk Solvent as indicators of LRO

From a practical point of view it is unrealistic to deal with more than two or three different parameters to describe solution properties and behavior. Consequently the challenge is to identify a set of parameters that is small enough to be of practical use and at the same time of physical significance to the system and the changes taking place within it. Rather than identifying the parameters a-priori, we chose to investigate the the system and its behavior as crystallization proceeded, hoping that such a study would suggest scales of significance, and, consequently, such a set of parameters. We were searching in particular for scales significant to the crystal growth process, which led us to a related issue of significance: what these scales are and how they are identified. This is not a new problem

nor is it appropriate to attempt the solution in a generic manner. The approach we decided upon was to study several related systems in a comparative manner in the hope of determining a functional set of physically realistic parameters for the family of systems examined.

It appears from the analysis of the data obtained that the number of molecules of bulk water per molecule of solute, and the number of molecules of solvation water per molecule of solute are each indicators of the nature of the SRO associated with the solution. They are measures of the nature, extent, and time scales of short range interactions (relative to proton exchange) between solvent and solvent, and solvent and solute respectively. The non-bulk non-solvation water is an indicator of SRO and an indicator of LRO on additional scales of significance, but cannot be obtained by direct measurement. LRO in the sucrose water system may be described in terms of solvatons, consisting of a sucrose molecule and the number of water molecules of solvation measured at the concentration of the solution, and FC, which are determined by the number of tetrahedral clusters that can be formed by the bulk water per molecule of sucrose at the same concentration. Regimes of solution structure in aqueous sucrose systems are summarized in Figure 8.5.

In previous analyses the evidence indicating solvent solute interactions has sometimes been ignored. Micro and macroscopic transport properties are of the same order of magnitude in supersaturated sucrose solutions. In light of the previous analysis this makes sense. In supersaturated solutions the solvatons outnumber the bulk water structures, and in all likelihood it is the solvatons which solvate the bulk water structures or FC or TC. As a result there is not likely to be long range macroscopic transport in a supersaturated solution on the order of magnitude of diffusional time scales in dilute solutions.

In the particular case of supersaturated solutions, a study of the steady state fluorescence spectroscopy of pyranine (PYR) in sucrose solutions of various

concentrations indicates the molar ratio of solvation water to bulk water per mole solute is such that there is only enough water available on the average for one solvation shell or an incomplete solvation shell per molecule of solute (Chakraborty and Berglund 15 a). Also the data of Pan et. al., as well as viscosity data for supersaturated aqueous sucrose systems suggest that rotational as well as translational mobility of solvated solute is severely limited. For this reason, one would expect transport governing interactions in supersaturated solution to be dominated by short range non-equilibrium solvent-solute interactions. The absolute times required for these interactions to take place in supersaturated solutions may be tens, hundreds, or even thousands of times longer than in dilute solution (Pan and Berglund, 45); yet, in terms of distances involved, they are still short range, and in terms of time scales relative to diffusional transport, they are still fast.

One might object to the idea that bulk water moves faster (relative to diffusional time scales) in supersaturated solutions than in undersaturated ones because it seems contrary to intuition. However, when the energetics of the formation of a supersaturated solution are considered, this notion begins to make sense. It is impossible to make a phase transition from undersaturated to supersaturated solution without the addition of large amounts of external energy. This energy serves to increase the disorder of the solution and also increase the probability that enough bulk water molecules will be present in the vicinity of all the unsolvated solute molecules (one at a time) to solvate them (one at a time). The most common way of accomplishing this is to heat the solution until all the solute dissolves. Then as the solution cools, the solvated solute molecules transfer their kinetic energy to the surroundings in the form of heat, and become less mobile, (accounting for most of the cooling effect since these contain most of the mass) and the bulk water loses some kinetic energy as well. Under identical conditions of pressure and temperature, a supersaturated solution contains more energy per unit mass and volume than a saturated solution. In addition, the energy in a supersaturated solution is partitioned differently. In an undersaturated solution the bulk water structures form the immediate solvation environment

of the solvatons, in supersaturated solutions the solvatons form the immediate solvation environment of the bulk water structures. The saturated system retains energy of reorganization which is required to accomplish the transition from bulk water solvating the solvatons to the solvatons solvating the bulk water. The higher energy of a supersaturated solution when compared to the energy of a saturated system in equilibrium with solid at the same temperature may possibly be accounted for in terms of this energy of reorganization. Such a structural transition can also explain the long time structural stability of apparently metastable solutions. Such a restructuring may allow the system to achieve a new equilibrium between minimizing its total energy and maximizing the entropy of itself and its surroundings. Observations such as the fact that bulk water moves faster relative to solvated water in supersaturated solution than in a saturated solution (even though on an absolute basis, both bulk and solvation water are less mobile) could make more sense if this is true.

8.1.4 Other effects on structure and LRO

Temperature

Since SRO and LRO are both related to the Gibbs Free Energy of the system, there is an $e^{-(RT)}$ dependence on absolute temperature. At temperatures near 300 K, a ten percent variation in absolute temperature is not expected to significantly affect the magnitude of this term. Therefore we would expect relative spatial orientations of molecules to be a fairly weak function of temperature, and not expect to see major changes in solvent functional microphase distribution over the temperature range of interest. This is in fact, supported by our observations.

Absence of Significant Solute-Solute Interactions

Large (>10 molecule) solvent exclusive solute clusters are unlikely to exist in supersaturated solutions of sucrose and glucose in water. All spectroscopic evidence for highly supersaturated sucrose solutions indicates some molecular interaction between solute molecules. Such associated groups likely consist of no more than two or three partially solvated solute molecules. Spectroscopic evidence for solute association in supersaturated glucose-water system is more doubtful, particularly when the large amounts of non-bulk-non-solvation water in a system are taken into account. Structure in the aqueous glucose system is summarized in Figure 8.6.

Likelihood of Significant Solute-Solute Interaction

Data for other systems such as the citric acid water system and the fructose water system indicate that solute-solute association is probable and likely in those supersaturated solutions because there is simply not enough water to maintain the solvation structure indicated in under-saturated solutions. In the aqueous fructose system there is clearly not enough water per molecule of fructose to completely solvate it. Also the assumption that bulk water tends to associate in tetrahedral clusters when time and space averaged may no longer be a good assumption. Perhaps the appropriate structural module of bulk water is a single molecule under these conditions. If this is so, calculating the number of solvatons per bulk water and number of bulk water per solvaton, shows that the number of bulk water molecules equals the number of solvatons at 72 wt.% fructose. While this does not give an exact value of 78 wt% fructose as reported by Bates, enantiomeric and conformational effects were not considered, nor were the presence of difructose dianhydrides any or all of which may significantly affect the LRO of the system. This is summarized in Figure 8.7.

Weakly Dissociated Species with Partial Ionic Character

Saturation in the citric acid water system occurs near the point where the number of water of solvation per molecule of citric acid equals the number of bulk water per molecule of citric acid. At this concentration the citric acid molecule is still weakly dissociated. There are 2 FC or TC per solvaton. One way to explain this behavior might be to say that some of the bulk water solvates the dissociated protons so that on the average the presence of an extra four molecules of bulk water is required per molecule of citric acid. Such water might be involved in solvation of protons but would exhibit the exchange rate

of bulk water (since bulk water is water able to participate in proton exchange). This is summarized in Figure 8.8.

8.1.5 Issues related to structure near growing sucrose crystals.

With the introduction of a crystal or nucleus a new phase is introduced into the system and therefore the number of scales on which the system exhibits LRO must increase. It is interesting to interpret the "patches" observed in the ratioed and time averaged fluorescence density images obtained in dual detector mode using laser induced optical fluorescence microscopy in this light. Most of these patches vary in extent from a few square microns to a few hundred square microns. They appear to represent areas of solution with sucrose concentrations comparable to bulk concentration separated by areas of solution with considerably lower sucrose concentrations. None of the regions appear to be solvent exclusive (except for regions clearly corresponding to the crystal itself). The very near interface region of the crystal has a structure which is completely unknown, however the water of solvation released due to crystallization to collect in relatively large patches. The sucrose concentration in these patches corresponds to undersaturated but concentrated solution.

Solvatons likely diffuse into the solvent rich regions while bulk-solvent counter-diffuses into the solvaton rich region. Bulk solvent structure is likely different in each region, and transport is much slower in the solvaton rich region than in the solvent rich region. When one considers the energetics of saturation it becomes evident that there is not enough energy available in the system for the undersaturated patches to become supersaturated and thus the "phase inversion" from the solvatons being solvated by the bulk water to the bulk water being solvated by the solvatons to occur. In a like manner because the chemical affinity of sucrose for water is greater than the chemical affinity of sucrose for sucrose it is unlikely that there is enough energy available for the supersaturated

regions of solution to ever attain undersaturation. This may be a way to conceptualize in spatial terms or on the level of LRO, why crystallization stops when the concentration of bulk solution reaches saturation. Even though one might be tempted to apply the term clusters to these regions, it is important to note that these are not solvent exclusive aggregates and they are no more "pre-crystalline" than the supersaturated solution itself prior to nucleation or seeding.

The crystallization itself (at bulk solution concentrations of less than 76%) is likely initially driven by interfacial competition for water of solvation between the sucrose molecules on the solution side and the sucrose molecules on the solid side on the one hand and the fact that the affinity of water molecules for other water molecules is greater than the affinity of water molecules for sucrose on the other. Some water molecules are likely to associate with other water molecules in the neighborhood instead of making themselves available for solvating sucrose.

The boundary layer which extends to the point that bulk solution concentration is observed, likely constitutes the next scale of LRO of significance. This research suggests that the spatial descriptor of LRO in the boundary layer must be relative to the size of the crystal but not to the degree of supersaturation of the bulk solution. This work does not provide information related to the temporal descriptor.

8.2 Conclusions

Steady state fluorescence spectroscopy of pyranine as a solvent probe can be used to determine concentration in supersaturated solutions of sugars such as sucrose, glucose, fructose and lactose. The PIR determined by this method may also be related to the measurement of activity. In this sense, pyranine can be used as a simultaneous probe of activity and concentration in such systems.

Steady state emission spectroscopy of pyranine is not a good indicator of solute concentration in dilute solution. Water appears to have more than one function in solution, some of the molecules at any given time are unavailable for participation in solvent exchange and constitute the solvation water microphase, and other water molecules are available for participation in solvent exchange to differing degrees and constitute the bulk water microphase. The solvation water microphase for most substances studied remains fairly constant until high degrees of supersaturation are reached. Steady state fluorescence spectroscopy of pyranine can only directly measure solvent exchange rates relative to the rate of proton exchange on two time scales. Such information is not enough to completely describe the behavior of systems such as glucose-water where large amounts of non-bulk-non-solvation water are present, or fructose-water where a some solute association is likely, or citric acid water where partial dissociation occurs.

Combined with other techniques such as time-resolved-fluorescence-spectroscopy or NMR, useful information related to structure, can be obtained on more than one scale. An analysis of all information available in literature combined with the information generated for the sucrose-water, glucose-water, fructose-water, and citric acid water systems indicates that at or near the saturation point structural changes occur in terms of both short range and long range order. The structure of the bulk water phase may also change although the steady state fluorescence method by itself does not provide evidence on the correct scale of long range order. The transport resistances in a system appear to be related to the structure and quantity of bulk water present.

The steady state fluorescence method can be modified for use in laser excited optical fluorescence spectroscopy to yield information related to the solvent distribution in a 2-dimensional area of solution. Such images collected in supersaturated solution, in the presence and absence of growing crystals, and in concentrated solutions in the presence of dissolving crystals, indicate that structure in each case is different. The extent of the boundary layer appears to be related to the size of the crystal and have no

supersaturation dependence. The structure of the near interface region is completely unknown.

8.3 Recommendations for Further Work

Information related to the structure of the bulk water phase in supersaturated solution is critical to the understanding of crystal growth. The NMR data of Richardson and Lang should be a good starting point with which to corroborate data obtained by other methods. This author is unable to suggest any existing method which might be of use.

Two dimensional laser induced optical fluorescence microscopy and confocal techniques have the capability of providing three dimensional concentration profiles of solvent in supersaturated solution. Studies of growing crystals in different systems may provide useful information regarding crystal growth mechanisms and the role of solution structure in crystal growth.

Investigations of crystallization from non-aqueous solvents may provide further information regarding the general role of solution structure in crystal growth from solution.

Two dimensional imaging techniques may prove to be the best candidates for developing on-line particle imaging and control instrumentation. The effects of noise, detector response, movement of particles, and appearance of new nuclei need to be characterized first.

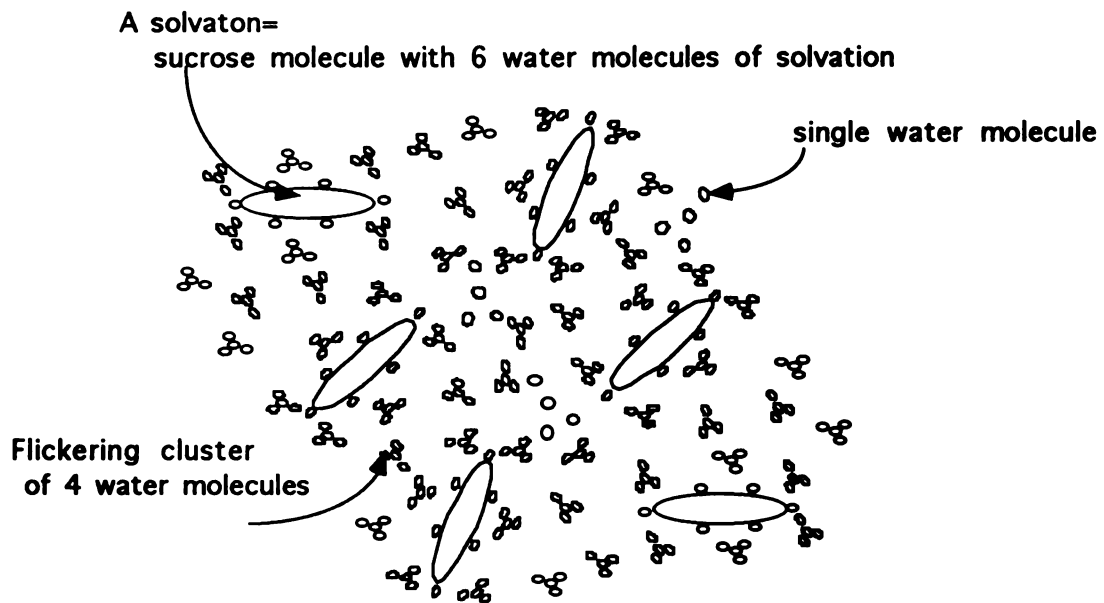


Figure 8.1 Conceptual diagram of structure in dilute aqueous sucrose solution.

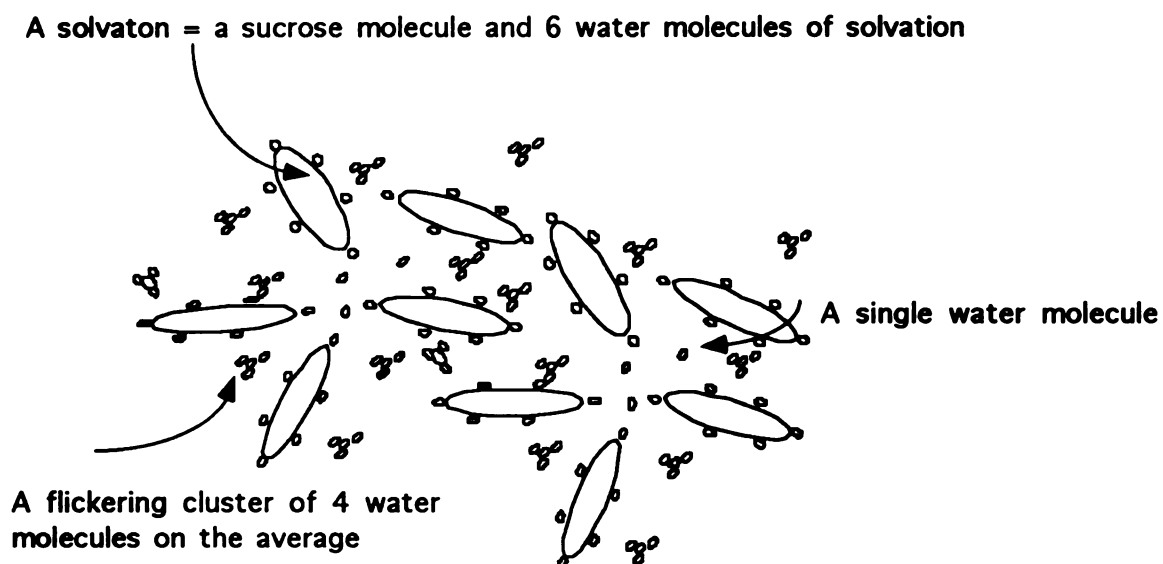


Figure 8.2. A conceptual representation of structure in concentrated aqueous sucrose solutions.

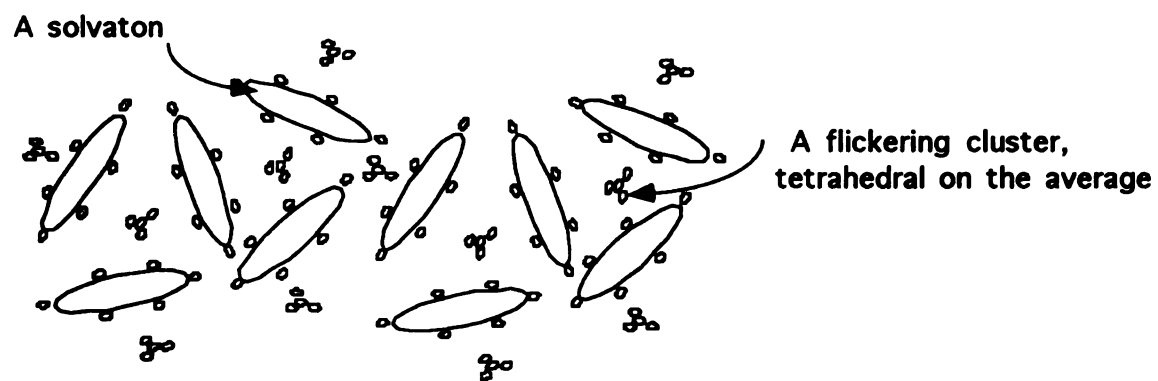


Figure 8.3. A conceptual representation of structure in saturated aqueous sucrose solution.

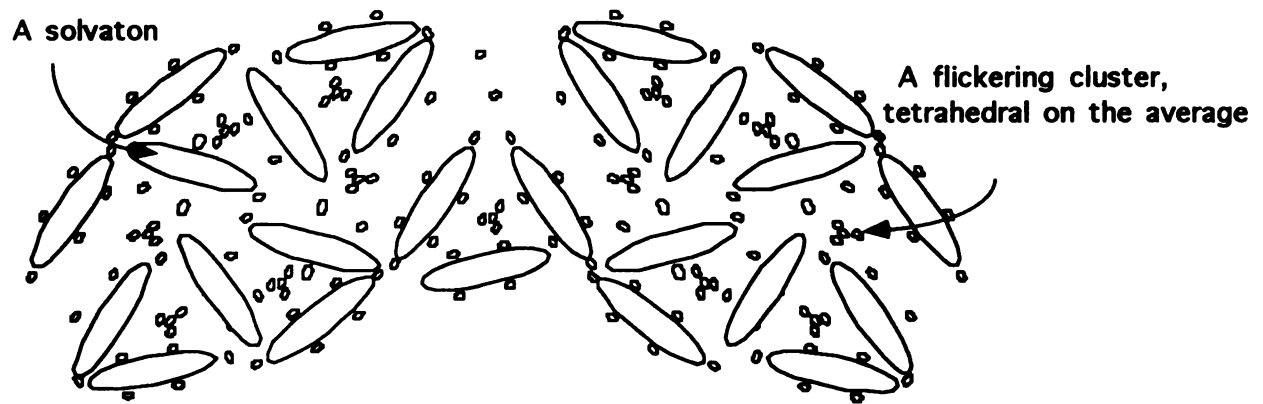


Figure 8.4. A conceptual representation of structure in supersaturated aqueous sucrose solutions of less than 76% by weight sucrose.

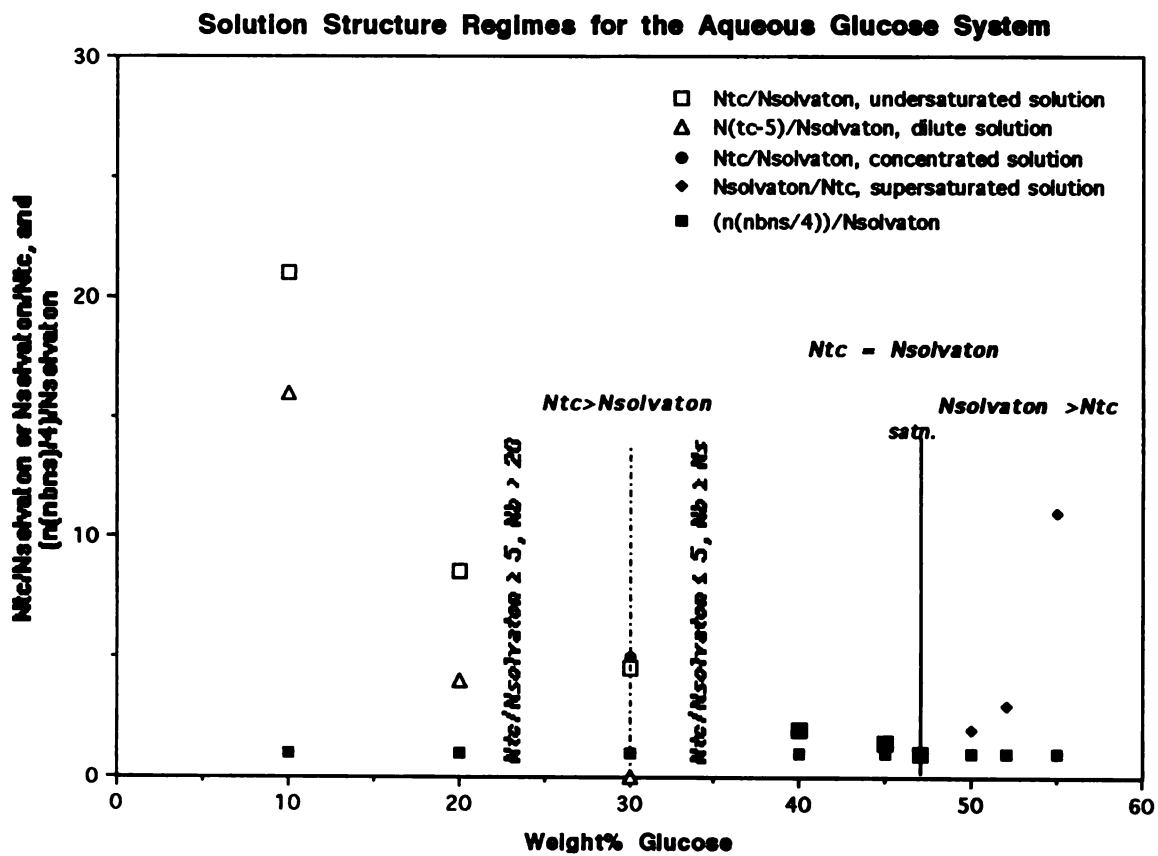


Figure 8.5. Structure in the aqueous glucose system.

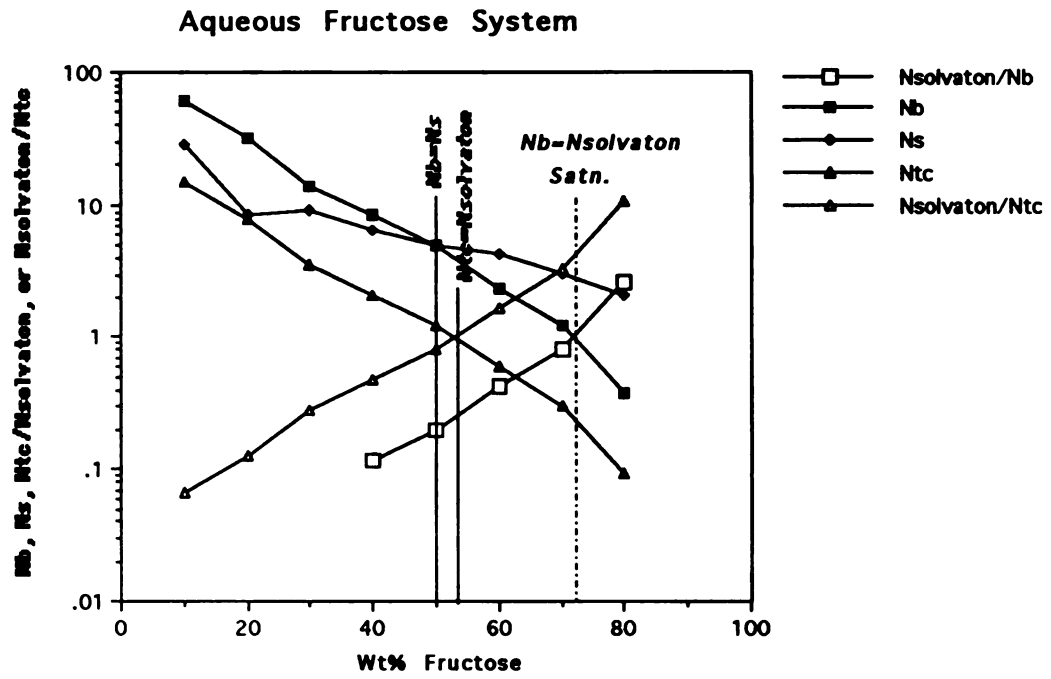


Figure 8.6. Solution structure in aqueous fructose systems.

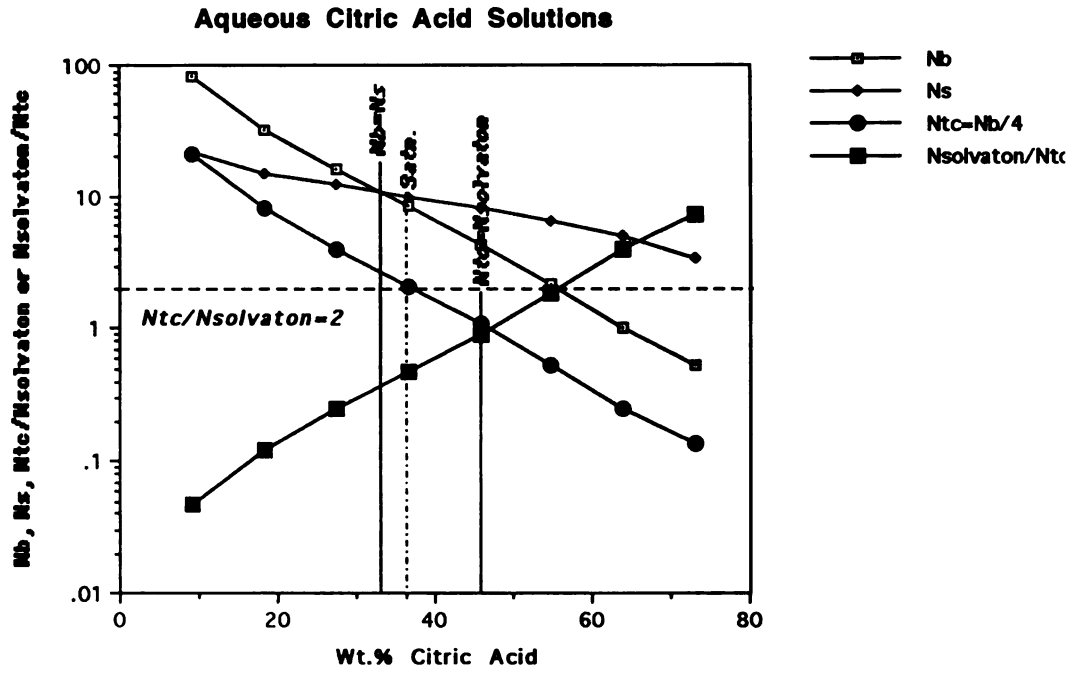


Figure 8.7. Summary of structure in aqueous citric acid systems.

Solution Structure Regimes in Aqueous Sucrose Solutions

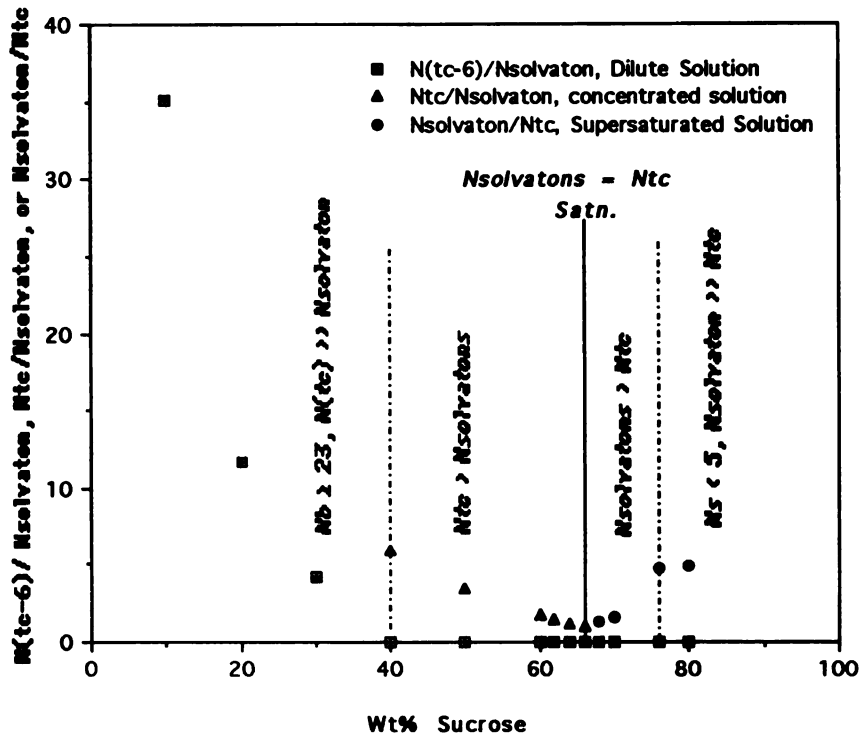


Figure 8.8. Regimes of solution structure in aqueous sucrose solutions.

MICHIGAN STATE UNIV. LIBRARIES



31293015660784